Air quality and climate change in the greater Cape Town area

Masters dissertation of Evangelia-Anna Kalognomou

Submitted to the Department of Environmental & Geographical Science, Faculty of Science, University of Cape Town, in partial fulfilment of an MSc by coursework and dissertation.

June 2009

University of Cape Town

Declaration:

1. I know that plagiarism is wrong. Plagiarism is to use another's work and pretend it is one's own.
2. This submission is my own work.
3. I have not allowed, and will not allow, anyone to copy my work with the intention of passing it off as their own work.
4. I acknowledge that copying someone else's assignment or essay, or part of it, is wrong, and declare that this is my own work.

First Name and Surname:	*Student number:*
Evangelia-Anna Kalognomou	*KLGEVA001*
Signature:	*Date:*

To my daughter Anastasia and my husband Vangeli for the love, patience, dedication and trust that he has shown me all these years.

Abstract

The work presented in this dissertation stems from the link that exists between meteorological conditions and the significant accumulation of air pollutants in large urban agglomerations. The research focuses on the Greater Cape Town Area (GCTA), where temperature inversions lead to high air pollutant concentrations and episodes of air pollution. As local meteorological conditions are often manifestations of larger weather producing phenomena (e.g. anticyclones), the work presented studies the changes that may occur in the synoptic conditions associated with temperature inversions, which will consequently affect the rate of occurrence of air pollution episodes.

After a brief introduction of the topic, background information on the relevant legislation and the actions taken towards an air pollution abatement strategy and a detailed literature review, the high levels of air pollution in the GCTA during winter and especially during the morning peak hour traffic and their link to temperature inversions are studied in detail for the year 2002. The large scale circulation and its link to temperature inversions are studied through the application of the Self-Organizing Maps technique using NCEP-DOE Reanalysis 2 data and making use of the findings for the year 2002. The synoptic states most associated with temperature inversions are found to be the anticyclonic conditions caused by the South Atlantic High Pressure (SAHP) system and the west coast trough associated with berg winds bringing dry continental air towards the GCTA. The 2002 data also show that more air pollution episode days are associated with west coast troughs than with the SAHP system and the average strength of the temperature inversions associated with west coast troughs is found to be approximately 50 % higher than that associated with the SAHP system.

The Global Circulation Models (GCMs) ECHAM5, CNRM- CM3 and CSIRO- MK3.5 are used to study the potential changes in the future climate of the area under the IPCC A2 emissions scenario. ECHAM5 shows a small increase in the synoptic states associated with anticyclonic influence over the south western part of South Africa and CNRM- CM3 shows a small increase in both the synoptic states associated with anticyclonic influence and those associated with a west coast trough. Both models show a small decrease in the synoptic states associated with cold fronts. CSIRO-MK3.5 was not found to adequately reflect the current climatology in the domain, making it difficult to distinguish between model bias and future climate trends.

Acknowledgments

I would like to thank my supervisors Prof. Bruce Hewitson and Dr. Mark Tadross for their inspiration, continuous support and useful comments throughout this project as well as my colleagues Lisa Coop, Chris Lennard, Chris Jack, Nana Browne and Suzanne Carter for the fruitful discussions, support and recommendations. The Air Quality Monitoring Laboratory of the Scientific Services Department (City of Cape Town) and especially Fazlin Waggie, and the South African Weather Service are especially thanked for providing the data necessary to complete this study. I would also like to thank my family and especially my father for his continuous encouragement and support.

Table of Contents

List of Tables

List of Figures

1. Introduction

1.1 Air pollution in Cape Town

Cape Town is a large urban agglomeration, within which the increased level of human activities related to the emission of air pollutants leads to a deterioration of ambient air quality. As outlined in the Brown Haze II study (Piketh et al, 2004), the main anthropogenic activities that contribute to the emission of air pollutants in the Greater Cape Town Area (GCTA) are:

- Motor vehicle emissions (PM in particular emitted from diesel vehicles).
- Industrial emissions (refineries, steel mills, smelters, cement manufacturing, paper manufacturing, brickworks etc.) and burning of industrial waste.
- Domestic activities in residential areas (cooking, heating and burning of household waste).

These emission sources lead to high air pollution levels, which are continuously monitored through an air quality network operated by the City of Cape Town. The network currently monitors the concentration of the main pollutants carbon monoxide (CO), nitric oxide (NO), nitrogen dioxide (NO_2), nitrogen oxides (NO_x), sulphur dioxide (SO_2), particulate matter (PM_{10}) and ozone (O_3), which are directly or indirectly linked to the combustion of fossil fuels, as well as the pollutants hydrogen sulfide (H_2S) and total reduced sulphur compounds (TRS), which are related to certain types of industrial activity and sewage treatment facilities.

1.1.1 Impacts of air pollution on health

Air pollution has a number of impacts ranging from increased corrosion of buildings to reduced agricultural yield and effects on ecosystems, but most importantly it has significant negative impacts on human health. A number of epidemiological studies have been conducted worldwide aiming to quantify the increased morbidity and mortality associated with exposure to ambient air pollutant levels (WHO, 2003; Pope et al, 2002). It is widely recognised that a single pollutant-based approach is in many ways limited, as in reality the population is exposed to a mixture of pollutants and it is the combined effect of this exposure that leads to the observed health effects. It is however extremely difficult to determine the

synergistic effect of combinations of pollutants (Katsouyanni, 2003) and this remains the subject of ongoing research (e.g. Mauderly & Samet, 2009).

In 2000 a study was conducted in South Africa which focused on the quantification of the impacts of urban population exposure to elevated levels of PM. A number of diseases can be attributed to air pollution and in the study of Norman et al (2007) cardiopulmonary diseases, cancers of the respiratory system (trachea, bronchus and lung) as well as acute respiratory infections in children of young age (0-4 years) were considered. The results showed that the number of deaths in urban areas in South Africa which can be attributed to air pollution are about 0.9 % of the total number of deaths from all causes in 2000 (uncertainty interval 0.3-1.5%), which is approximately 4650 deaths. The uncertainty interval is certainly significant, however as the study only considers exposure to PM, the number of deaths are most likely underestimated. The consideration of the accumulative effect from exposure to all known pollutants would certainly lead to larger estimates. The study also points out that a detailed local research has not yet been conducted about the numbers of people who get sick and lose their quality of life because of air pollution, which would also increase the number of people significantly affected by air pollution. According to the study, fossil fuel combustion and traffic-related air pollution are the main sources of PM related air pollution in South Africa.

1.2 Synoptic climatology, temperature inversions and air pollution episodes

Apart from the emission of air pollutants, prevailing meteorology and the consequent dispersion of pollutants in the atmosphere also plays a significant role in the concentrations monitored and during stable atmospheric conditions air quality becomes significantly worst. This leads to air pollution episodes, when the concentration of air pollutants is found to be above health and environmental standards. In the GCTA, stable atmospheric conditions are observed mainly during the winter period (between cold fronts) when the associated weak land/sea temperature and pressure differences result in stagnant conditions during which temperature inversions are pronounced and lead to the trapping of air pollutants close to the surface (Jury et al, 1990; Wicking-Baird et al, 1997). In the GCTA these air pollution episodes are widely known as brown haze episodes due to the reduced visibility associated with the elevated concentrations.

Temperature inversions are a weather pattern in which as one moves from the surface to higher altitudes, the temperature increases rather than following the normal pattern of

decreasing temperature, i.e. the normal lapse rate. The vertical distance in which the temperature inversion occurs is the inversion layer, which may start at the surface or it may be an elevated condition such that there is a surface layer that exhibits normal temperature conditions before the inversion base is reached. Temperature inversions can thus be broadly categorised into two types, elevated and surface inversions as shown in Figure 1-1.

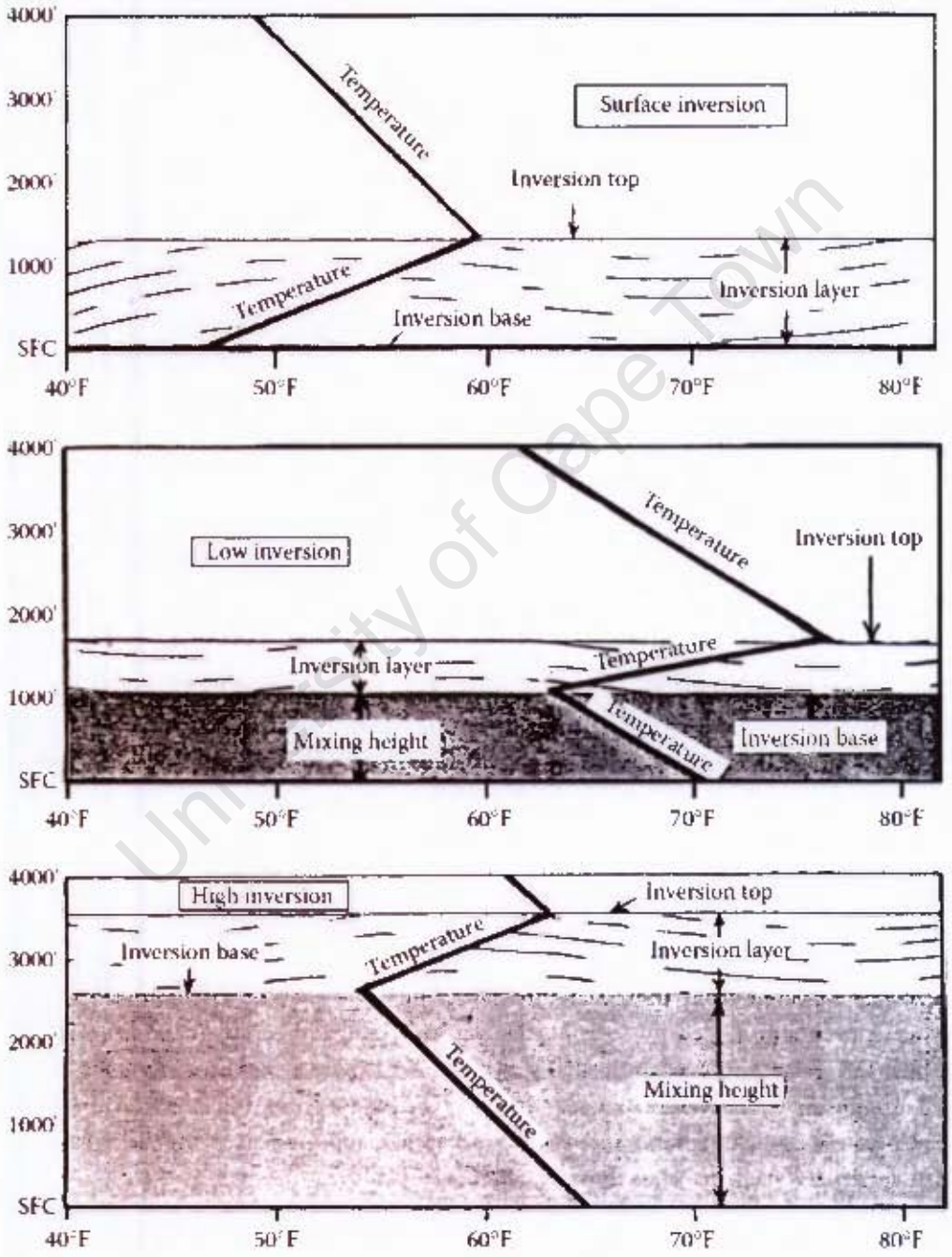

Figure 1-1: Typical temperature inversions (Griffin, 2007).

Perhaps the most common cause of elevated temperature inversions is the subsidence of air mass associated with high-pressure areas. The descending air is compressed and undergoes adiabatic heating. As a result, in the lower regions of a high-pressure system the air has a higher temperature than the cooler air parcels directly in contact with the earth's surface and this form of temperature inversion is termed a *subsidence inversion* (e.g. Griffin, 2007).

In addition to the subsidence inversion, Griffin (2007) distinguishes three types of inversions depending on the way these are formed. A *frontal inversion* in which a rapidly moving warm or cold air masse advances on a more stationary mass of a significantly different temperature, an *advective inversion* which may be formed when warm air moves over a colder surface and a *radiation inversion*, the most common form of surface-based inversion, which occurs during nightime when the surface of the earth has become cooler as a result of the loss of radiant energy.

This project studies the relationship between the large-scale atmospheric circulation and the stable atmospheric conditions observed at local or regional scale, which lead to air pollution episodes in the GCTA. It will thus make use of the principles of Synoptic Climatology, which according to Barry and Perry (1973) can be defined as "obtaining insight into local or regional climates by examining the relationship of weather elements, individually or collectively, to atmospheric circulation". The approach most commonly used to link the two scales (regional and large scale) is to categorise the atmospheric state into broad categories (classes) and then relate these synoptic categories to a dependent variable (Hewitson & Crane, 2002), which in this study is local temperature inversion. The technique that is applied in this study to classify the synoptic states is called Self Organising Maps (SOMs) and its usefulness in recognising important links between the synoptic-scale patterns and weather conditions at the surface has been noted in a number of studies (e.g. Michaelides et al, 2007; Hewitson & Crane, 2002; Cavazos, 2000; Cavazos, 1999).

In addition to studying the link between atmospheric circulation and the stable atmospheric conditions observed at local scale, the current study investigates the changes that may occur in the synoptic conditions, under a particular climate change scenario. As a consequence, temperature inversions and the potential for the build up of air pollution may be different. Climate change scenarios are primarily studied using Global Circulation Models (GCMs) and the results of three GCMs applied in the context of the Intergovernmental Panel on Climate

Change (IPCC) Fourth Assessment Report (AR4) (IPCC, 2007a) are used to investigate changes in the synoptic circulation.

1.3 Previous Studies- Literature review

Temperature inversions and their link to air pollution episodes has been the subject of much research. Weather conditions resulting in temperature inversions are a frequently observed phenomenon that leads to high concentrations of air pollutants in big cities such as Mumbai, Los Angeles, Mexico City, Sao Paulo, Santiago, Tehran and also smaller cities like Oslo, Salt Lake City, Boise. One of the most serious air pollution episodes related to a temperature inversion was the Great Smog which occurred in London in 1952 and claimed the life of ~4,000 people (e.g. Bell & Davis, 2001). Such air pollution episodes are often associated with reduced visibility due to the formation of a brown haze.

The occurrence of brown haze in the GCTA has lead to two studies, the Brown Haze projects, which aimed at (a) determining the major sources of the brown haze (Wicking-Baird et al, 1997) and (b) characterising the physical and chemical properties of brown haze and quantifying the concentrations (lateral and vertical extent) for the evaluation of potential health effects and the design of air pollution abatement strategies (Piketh et al, 2004). The first study focused on source apportionment and was based on ground measurements. In the second study the vertical structure of the atmosphere during the brown haze episodes was also studied. It was confirmed that the meteorology of the GCTA during winter is conducive to the establishment of highly stable atmospheric conditions close to the surface as well as between 1-3 km above sea level. Episodes were found to occur on days when inversion layers formed close to the surface, particularly under the influence of anticyclonic circulation. Such conditions occur between the passage of cold fronts, when atmospheric subsidence is driven by the South Atlantic High Pressure (SAHP) system which ridges in eastwards over the south-western tip of Africa. Subsidence inversions are generally present in the eastern regions of the semi-permanent oceanic high-pressure systems found in the Southern Hemisphere at about 30^0S and in these locations they are quasi-permanent and reasonably stationary systems (Keen, 1979). Both Cape Town and Los Angeles are in such latitudes, the latter experiencing subsidence inversions due to the Eastern Pacific High (NRC, 1991; Griffin, 2007), but combined with the high levels of emissions experiences especially strong air pollution episodes which have been the subject of research over many years (e.g. Magill, 1949) and

have necessitated the design of serious air pollution abatement strategies (e.g. Schwartz & Hayward, 2004).

Keen (1979) associates both subsidence inversions and surface based radiation inversions with high-pressure systems, as the surface based temperature inversion is predominantly a nocturnal phenomenon (especially during long winter nights) associated with clear night-time skies and light winds, also a characteristic of anticyclonic circulation. Radiative inversion persists into the morning hours (when the rate of air pollutant emissions is also high) until the heating from the earth's surface causes an erosion of this inversion layer, enabling diffusion and vertical motion. Both subsidence and radiation inversions may be widespread phenomena and could on occasions co-exist at different levels (Keen, 1979).

The climate in South Africa and the domain of interest is described in detail in Tyson and Preston-Whyte (2000). Dracoulides (1994) distinguishes the meteorology in the GCTA according to four typical synoptic maps, shown in Figure 1-2.

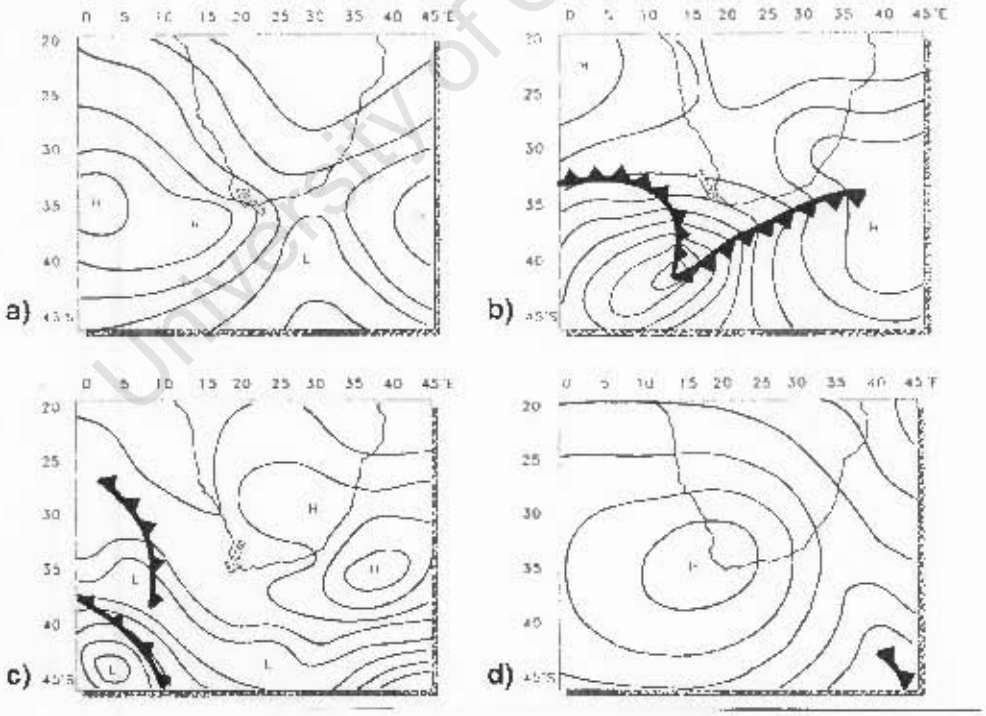

Figure 1-2: Typical synoptic maps for the Southern African subcontinent (Dracoulides, 1994) which are associated primarily with (a) the summer period (b) the winter period (c) early spring and late winter and (d) anticyclonic circulation.

During the summer period, a high south-easterly air flow dominates (Figure 1-2a), which is caused by a ridging anticyclone over the south Atlantic (SAWB, 1996). This leads to high wind velocities and high atmospheric turbulence which efficiently dilute and disperse air pollutants. In the winter months the wind is generally from the north-west (Figure 1-2b). This flow is caused by a pre-frontal system, which also brings overcast conditions and low temperatures (SAWB, 1996). The high wind velocities also effectively disperse pollutants during these conditions. The synoptic conditions displayed in Figure 1-2c occur mainly in early spring and late winter.The formation of a high pressure system over the western Cape, in association with another high over Natal and a cold front over the west coast, result in berg wind recirculations over the western coast area. Berg winds and coastal lows tend to occur together. The term coastal low describes a unique, shallow (does not normally extend above the 800 hPa level) low pressure system which develops along the coast. Depending on whether the pressure rises or falls to the south of the system, the low may move northwards or southwards along the coast, though more often in migrates to the south coast. Coastal lows produce warm offshore airflow (berg winds) ahead of the system and cool onshore airflow behind it. Strong overnight temperature inversions are associated with the light berg wind conditions ahead of migrating coastal lows (SAWB, 1996). In their study of winter air pollution episodes over Cape Town, Jury et al (1990) associated these conditions with the occurrence of brown haze episodes. Finally, in Figure 1-2d the stagnant conditions associated with anticyclonic circulation are shown. These lead to light variable winds and elevated temperature inversions and have the potential to result in air pollution episodes, as there is insufficient air flow to dilute pollutants (Jury et al, 1990). The synoptic meteorological aspects of brown haze episodes in Cape Town have also been described in Jury et al (1989), Ngeleza (1989) and Jury and Barclay (1992).

The use of GCM results to study the changes that may occur in the synoptic conditions under various climate change (CC) scenarios and their impact on air pollution build-up potential, has been the subject of recent research. Numerous studies have used GCM results to drive the application of regional models and study the impact of changing meteorological conditions on air pollutant transport and transformation. Mickley et al (2004) examined the impact of future climate change on regional air pollution meteorology in the US using the Goddard Institute of Space Studies (GISS) model. They found an increase in summertime regional pollution episodes in the midwestern and northeastern US, which appear to be driven by a decline in the frequency of mid-latitude cyclones tracking across southern Canada, as the cold

fronts associated with these cyclones provide the main mechanism for ventilation of the midwestern and northeastern US. Anderson et al (2001) used the HadCM3 model results for a single grid point in the British Isles, [52.5°N, 0°W], corresponding to the location of central England, to study the changing frequency of episodes of cold still winter weather and of episodes of hot sunny summer days, based on the IPCC IS92a (business as usual) scenario. They found that the number of days with both low windspeeds and low minimum temperatures (combining to create poor dispersion) declined through the 21st Century as winters become milder and windier. The summer findings showed that the occurrence of elevated temperatures and low windspeed condition, conducive to photochemical episodes, became significantly more common in the second half of the 21st Century. It should however be noted that care needs to be taken when using model results for a single grid cell for any given assessment. The same model can produce different results for an identical region and period, if different initial conditions and/or parameterisation schemes are applied. Moreover, despite substantial progress in understanding inter-model differences (IPCC, 2007a: 591), the internal variability between GCMs can lead to results that differ greatly over the same region. Depending on the application, instead of single grid cell model results different aggregation techniques and other methods can be employed (e.g. Hewitson, 2003).

For the area of Cape Town, Shannon and Hewitson (1996) used the GENESIS (developed by the National Centre for Atmospheric Research) and the GISS models to study changes in the frequency of temperature inversions. Normalised sea level pressure, expressed by four statistical terms, was found to best characterise the impact of the larger circulation on local temperature inversions. This study made use of a type of Artificial Neural Network (ANN) which was trained using data from the National Meteorological Centre (NMC). The GCM model results were presented to the ANN and for the control simulation it was found that both models compared favourably with each other, predicting on average 20 boundary layer inversions per year. For a doubling of CO_2 scenario, the results showed an increase in the frequency of temperature inversions by 25 % according to GISS and 33 % according to GENESIS.

The current study extends the work of Shannon and Hewitson (1996). Radiosonde data is used to determine the strength and extent of boundary layer temperature inversions and is then further combined with air pollution data to link temperature inversion to air pollution episodes in the GCTA. Focusing on the winter period, when air pollution episodes in the

GCTA are most pronounced, the Self-Organising Maps (SOMs) technique, a different type of ANN than that used by Shannon and Hewitson (1996), is applied to classify the synoptic states observed in current climatology and relate particular synoptic states to temperature inversions. Finally, making further use of SOMs, three GCM results are used to study the implication of future CC on air pollution episodes.

2. State of air quality in Cape Town

2.1 Definition of air pollution, legislation and actions

The *official definition of air pollution in South African law*, is "any change in the environment caused by any substance emitted into the atmosphere from any activity, where that change has an adverse effect on human health or well-being or on the composition, resilience and productivity of natural or managed eco-systems, or on materials useful to people, or will have such an effect in the future" (City of Cape Town, 2001).

To protect the effects on human health and the environment, a number of laws and regulations relating to the emission of air pollutants and ambient air quality levels have been set. These can be distinguished between laws that are applicable at national scale and regulations, additional by-laws as well as other policies that are set by the local authorities.

Firstly, the right to clean air is ensured through section 24 of the South African Constitution. In 2004, the South African government passed the National Environmental Management: Air Quality Act (NEM-AQA, 2004). The purpose of the act is to improve air quality through laws and regulations; to set standards for monitoring, managing and controlling ambient air quality; and to set out fines and penalties for where non-compliance is noted (the "polluter pays principle" applies).

At the local government scale, appropriate action is taken in the form of air quality management plans, by-laws and other policies. In Cape Town, the City of Cape Town is the authority responsible for Air Quality Management. The City has enacted a by-law that aims to control air pollution, and to remedy the damage caused by any air pollution that does occur. This Air Pollution Control By-law (City of Cape Town, 2001) is in line with the South African Constitution and makes rulings about: how much smoke may be emitted from non-

residential premises, residences and vehicles; who may install, alter, replace or operate fuel-burning equipment; when and where any open burning may take place (such as waste) and which emissions are regarded a nuisance. The City of Cape Town can also make any number of new laws which prohibit or restrict the emission of air pollutants from certain premises, the combustion of certain types of fuel etc.

In 2005, the final "Air Quality Management Plan for the City of Cape Town" (AQMP) was released (City Health Department, 2005) aiming to establish Cape Town as "the city with the cleanest air in Africa". It can be viewed as a first step towards designing an overall strategy to improve air quality and reduce the sources of air pollution. The AQMP places particular emphasis in the reduction of the health effects related to air quality, especially during brown haze episodes. It comprises of 11 key objectives, which are further broken down into strategies and action plans.

The City of Cape Town has also collaborated with research groups in order to further study the nature of brown haze episodes. During the Brown Haze (Wicking-Baird et al, 1997) and Brown Haze II (Piketh et al, 2004) projects, the causes of brown haze were studied in detail, the physical and chemical characteristics were determined and the potential health effects were examined.

Finally, to improve air quality in informal areas of Cape Town, where due to specific emission sources the concentration of certain air pollutants has been found to be especially high, pilot projects such as the Khayelitsha Air Pollution Strategy (CapeTown, 2008a) have been set up. In Khayelitsha the problem mainly resides in the smoke emitted from wood and tyre burning, as well as the strong winds that contribute to the resuspension of dust from unpaved roads and pavements. Systematic air quality measurements are being performed and the project is expected to identify the main sources and educate households as to the measures that can be taken to reduce air pollution.

2.2 Air pollution monitoring network in Cape Town

2.2.1 Station location and measurements

The City of Cape Town monitoring network currently comprises of 12 stations spread around the greater area of the city as shown in Figure 2-1.

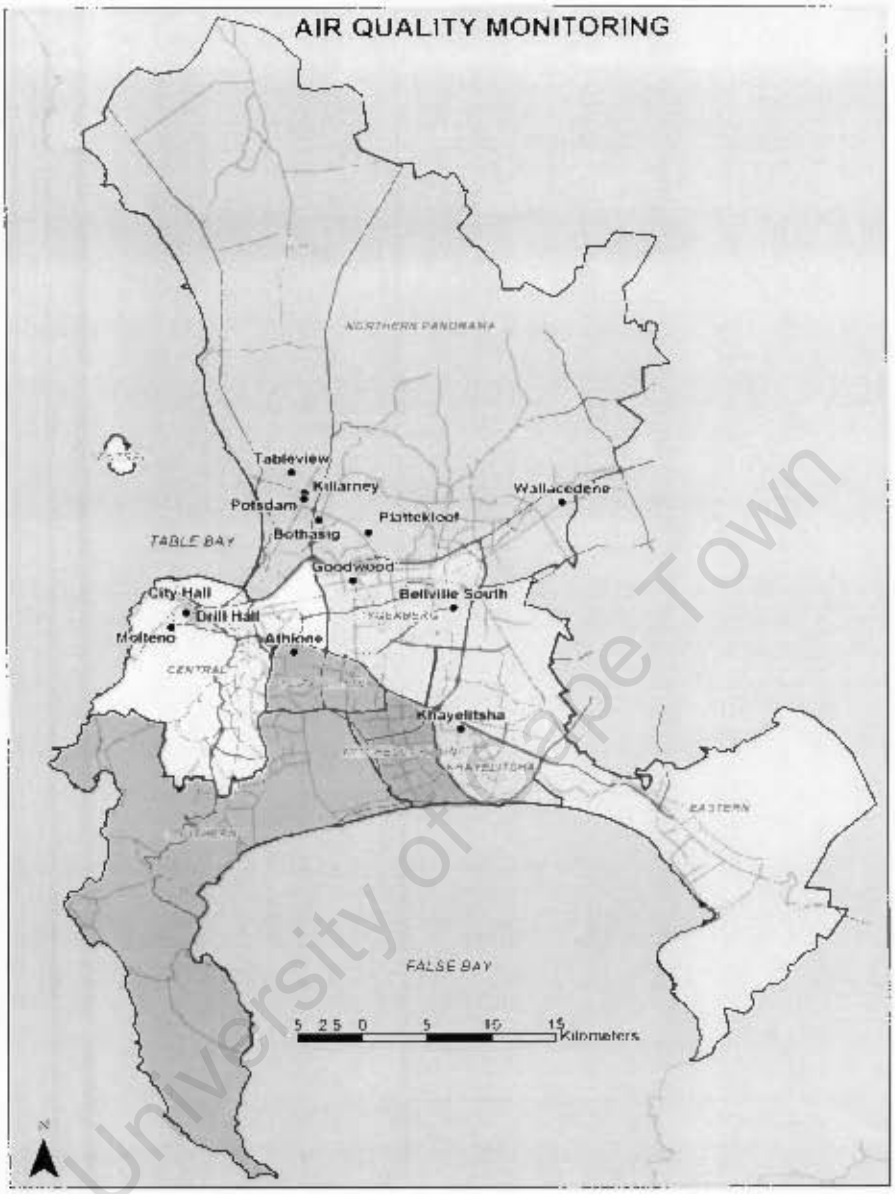

Figure 2-1: Location of the air quality monitoring stations (CapeTown, 2008b).

Near-to-real time information concerning daily air pollutant levels is available through CapeTown (2008b). For the purposes of this study, hourly meteorological and air pollutant concentration data from certain stations was made available by the City of Cape Town, Air Quality Monitoring Laboratory of the Scientific Services Department (Waggie, 2008) following a specific formal request. An overview of the data considered in this study as well as the characterisation of each station type according to information from CapeTown (2008b) and Waggie (2008) can be found in Table 2-1. The time period and the pollutants measured

differ from station to station. From the full details presented in Annex I (year and data completeness) the hourly data availability for certain periods of time is poor, necessitating a careful selection of the time period and stations that will be used further on in the analysis, so that the most comprehensive data set is chosen.

Table 2-1: Overview of the data made available for this study and characterisation of each station type.

Station name	Abbreviated station name	Station code	Type of station	PM_{10}	NO_2	NO_x	SO_2	CO	O_3	Wind speed	Wind direction	Time period
Athlone	ATHL	CC3	Urban background	x	x	x	x					1998-2003
Bothasig	BOTH	BM3	Urban background	x	x	x	x					1998-2007
City Hall	CH	CC1	Traffic		x	x	x	x				1998-2003
Drill Hall	DH	CC6	Urban background	x								1998-2007
Goodwood	GOOD	DD7	Urban background	x	x	x	x	x	x	x	x	1998-2004
Khayelitsha	KHAY	CC4	Urban background	x								1999-2007
Killarney	KILL	ZD7	Industrial (located 0.6 km from Caltex refinery)	x	x		x					2002
Molteno	MOLT	CC2	Urban background						x			1998-2003
Plattekloof	PLAT	DD8	N/A	x	x	x	x					2000-2003
Table View	TBLV	TM1	Urban background	x	x	x	x			x	x	1998-2003

2.2.2 Limit and Target values

The Department of Environmental Affairs and Tourism (DEAT) has established national ambient air quality standards (SANS, 2005) for the protection of human health, setting in this way the permissible concentration of various pollutants in ambient air. These standards are termed air pollution limit or target values and have been set in accordance with international standards, which are in turn based on the findings of international scientific groups active in this field. The specific dates by which these values must be met are to be determined in accordance with SANS (2004), which is the framework for setting and implementing the national ambient air quality standards. Furthermore, in SANS (2004) the definitions of "limit" and "target" are provided, the main difference being that the limit values are "not to be exceeded once attained", whereas the target values are "to be attained where possible". Target values are frequently termed "long term acceptable thresholds" and at these values pollutants are either harmless to health and the environment or unlikely to be reduced through

expending further reasonable cost on abatement due to background sources or other factors. As an example, from the pollutants which are considered in this study only for O_3 target rather than limit values have been set, due to "the potential which exists for transboundary transportation of this pollutant" (SANS, 2005).

Table 2-2: Limit and target values for the protection of human health in $\mu g/m^3$, as defined in SANS (2005).

Pollutant	10 min limit value for the protection of human health (10-min running average)	Hourly limit value for the protection of human health (1h average)	8-hourly running average for the protection of human health (calculated on 1-hourly averages)	Daily limit value for the protection of human health (24-hour average)	Annual limit value for the protection of human health (calendar year average)
Sulphur dioxide (SO_2)	500	350		125	50
Nitrogen dioxide (NO_2)		200			40
Carbon Monoxide (CO)		30	10		
Particulate matter (PM_{10})				75	40
Ozone (O_3)*		200	120		

* The values refer to target values as only these have been defined in SANS (2005).

Note: All concentrations are measured at a standard temperature (25°C) and pressure (101.3 kPa).

2.3 Sources of emissions

According to the Cape Town emission inventory which was compiled in 1995 and was used and reported in detail in the Cape Town Brown Haze Study (Wicking-Baird et al, 1997), emissions from road transport are the single largest source of primary NO_x, PM_{10}, $PM_{2.5}$ and Volatile Organic Compound (VOC) emissions comprising 65.7 %, 52.6 %, 42.5 % and 69.2 % of the total emissions respectively. The Caltex oil refinery, heavy fuel oil boilers and the use of coal for industrial and commercial purposes are the largest contributors to the total SO_2 emissions with a contribution of 72.4 %.

The detailed contribution of each emission source to the concentrations measured at the various monitoring stations spread across the city will be different depending on the location and the particular meteorological conditions that occur during the measurements. A detailed source apportionment study for the city of Cape Town has been performed for $PM_{2.5}$ during brown haze episodes which occurred between July 1995 and June 1996 and the results can be found in Wicking-Baird et al (1997).

2.4 *Concentration of air pollutants*

2.4.1 Inter-annual variation

In order to provide an overview of the state of air quality in the GCTA, the inter-annual variation of the concentration of main air pollutants is presented in Figures 2-2 to 2-4.

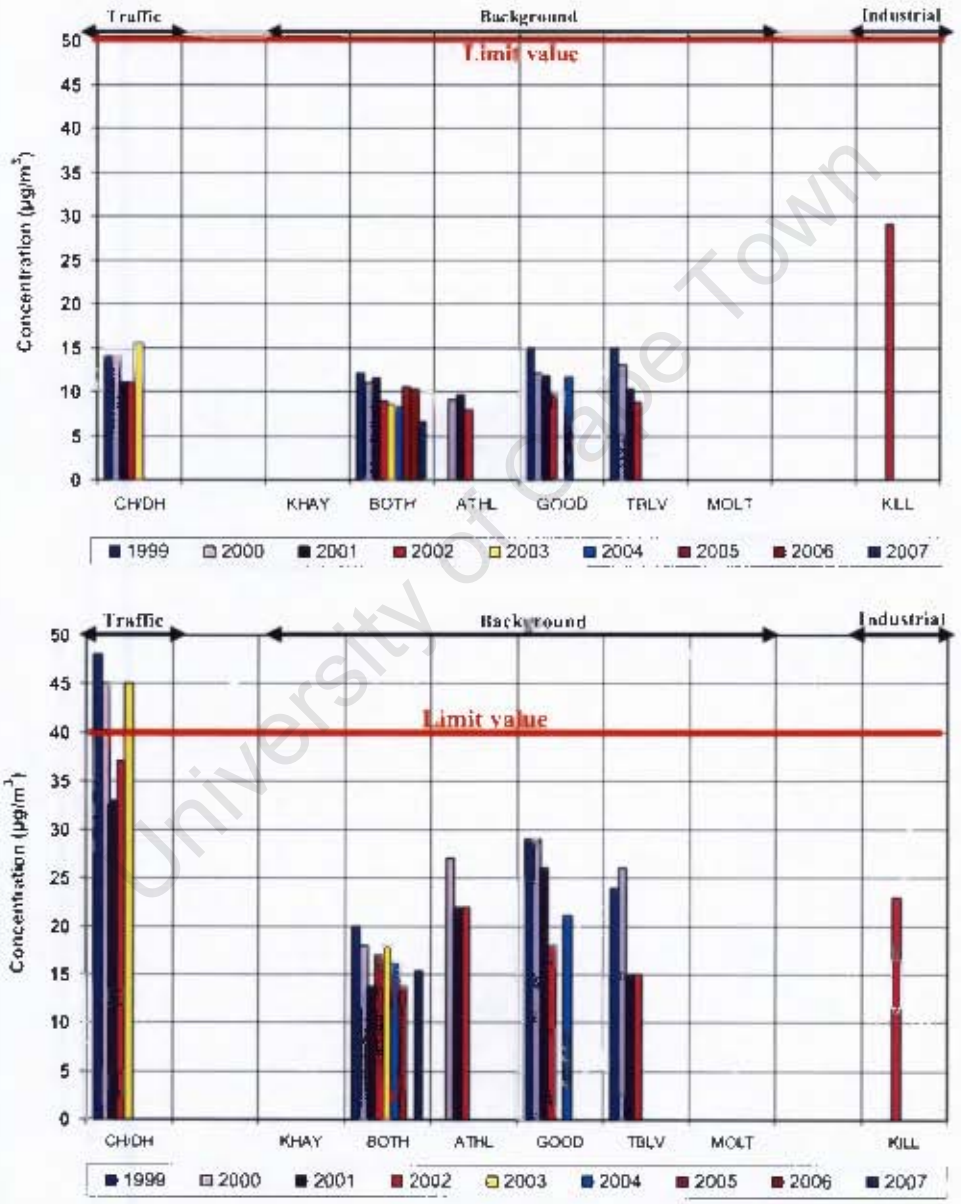

Figure 2-2: Annual mean SO_2 (top) and NO_2 (bottom) concentrations across various types of monitoring stations in the GCTA.

Figure 2-2 shows the inter-annual variation of the mean SO_2 and NO_2 concentrations. Although data for recent years is lacking for most stations, for SO_2 it is clear that the

industrial station at Killarney measures the highest concentrations, though these were still below the annual limit value of 50 $\mu g/m^3$ in 2002. At Bothasig station, for which the most complete data set is available, the concentrations appear to remain relatively stable, though a significant decrease in 2007 is noted. The monitoring station in the city centre (City Hall station) shows an increase of SO_2 concentrations in 2003, most probably due to the increase in vehicle traffic observed in recent years. Overall, the concentrations observed are similar to the concentrations observed in large cities in Europe which do not yet make wide use of zero sulphur fuels for diesel and petrol vehicles, such as Athens, Bratislava and Krakow (EEA, 2008a; EEA, 2008b).

For NO_2, concentrations at the industrial and the urban background stations are low. However, measurements at the City Hall traffic station are significantly elevated and in most years the annual mean concentration is above the limit value of 40 $\mu g/m^3$. From the data available a clear upward or downward trend cannot be deduced and data for more recent years are needed to draw robust conclusions. Clearly vehicle traffic is a significant source of emissions contributing to the NO_2 concentrations measured at this site. For comparison it is mentioned that higher NO_2 concentrations at traffic stations are also systematically observed in large European cities, where very high concentrations of around 100 $\mu g/m^3$ are measured at traffic stations in e.g. London, Rome and Bucurest (EEA, 2008a).

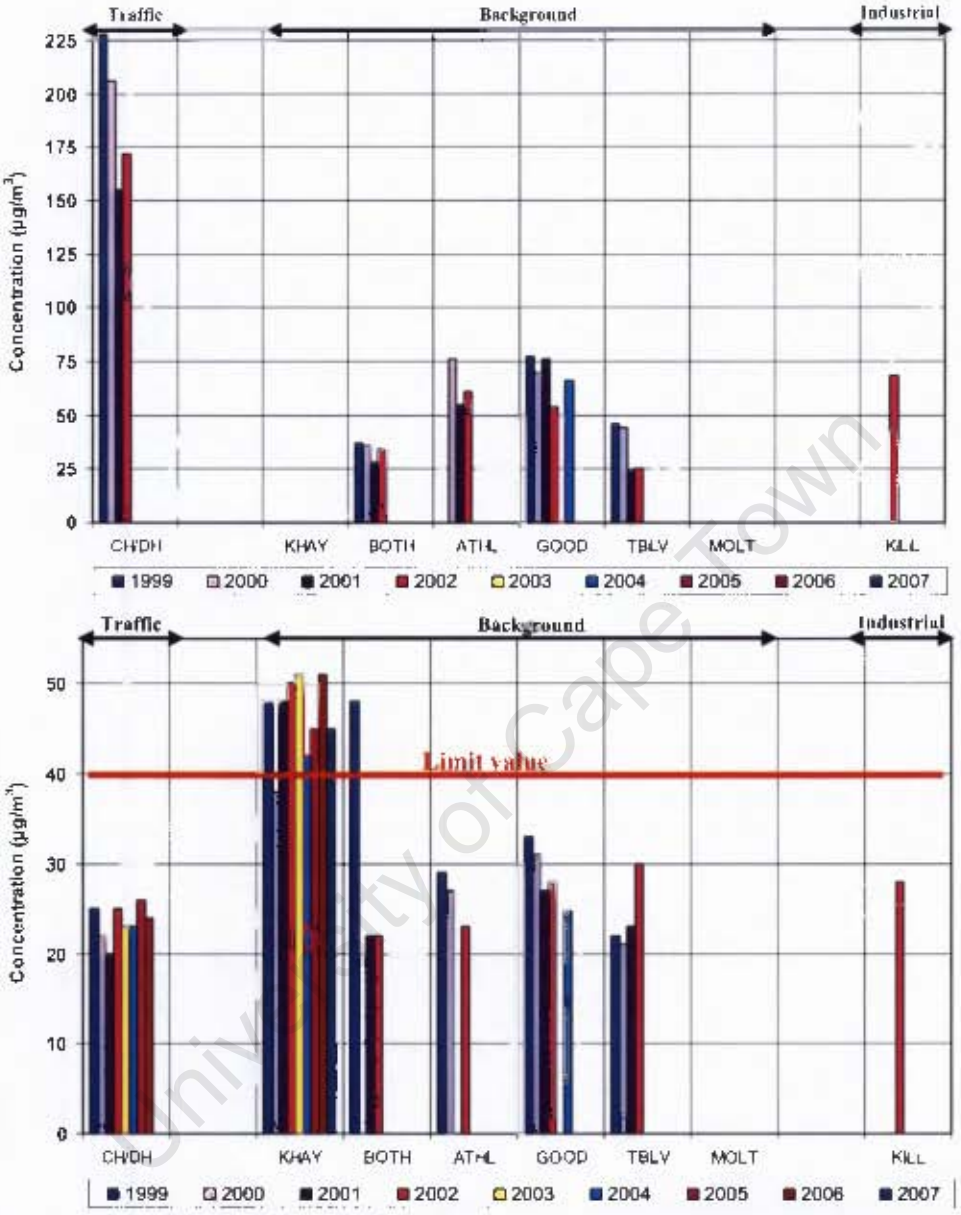

Figure 2-3: Annual mean NO_x (top) and PM_{10} (bottom) concentrations across various types of monitoring stations in the GCTA.

In Figure 2-3 the inter-annual variation of the mean NO_x and PM_{10} concentrations are presented. As concerns NO_x, the measurements are in line with those for NO_2 and by far the highest NO_x concentrations are recorded at the City Hall traffic station. NO_x are produced by combustion processes and the primary pollutant, directly emitted, is NO together with a small proportion of NO_2. NO is oxidised by O_3 in the atmosphere on a time scale of tens of minutes to give NO_2. NO and NO_2 are collectively known as NO_x because they are rapidly inter-converted during the day. NO_2 is split up by UV light to give NO and an O atom, which

combines with molecular oxygen (O_2) to give O_3. Therefore, although a limit value for NO_x concentrations is not set by legislation, it is convenient to study the sum of NO and NO_2 to acquire an overview of the contribution of fossil fuel combustion to the ambient concentrations (in the case of City Hall station the main source of emissions being fossil fuel use by road vehicles).

For PM_{10} systematic exceedances of the annual limit value of 40 $\mu g/m^3$ are recorded at the background station of Khayelitsha, though concentrations are not significantly elevated at any other traffic, industrial or background station. As has been mentioned in section 2.1, a dedicated project (the "Khayelitsha Air Pollution Strategy") has been set up to study and improve air quality in this area. The local emission sources contributing to the elevated concentrations are mainly smoke emitted from tyre and wood burning, though there is also considerable contribution from natural PM_{10} sources due to the strong winds that cause e.g. road dust resuspension. As discussed in chapter 1.1.1, the impacts of PM air pollution on health are significant and it necessary to take up specific measures to reduce the anthropogenic sources as far as possible. For comparison it is mentioned that the concentrations observed in Khayelitsha are high even compared to background concentrations in European cities, where values of around 50 $\mu g/m^3$ are observed in very few cities, e.g. Bucurest and Krakow (EEA, 2008a).

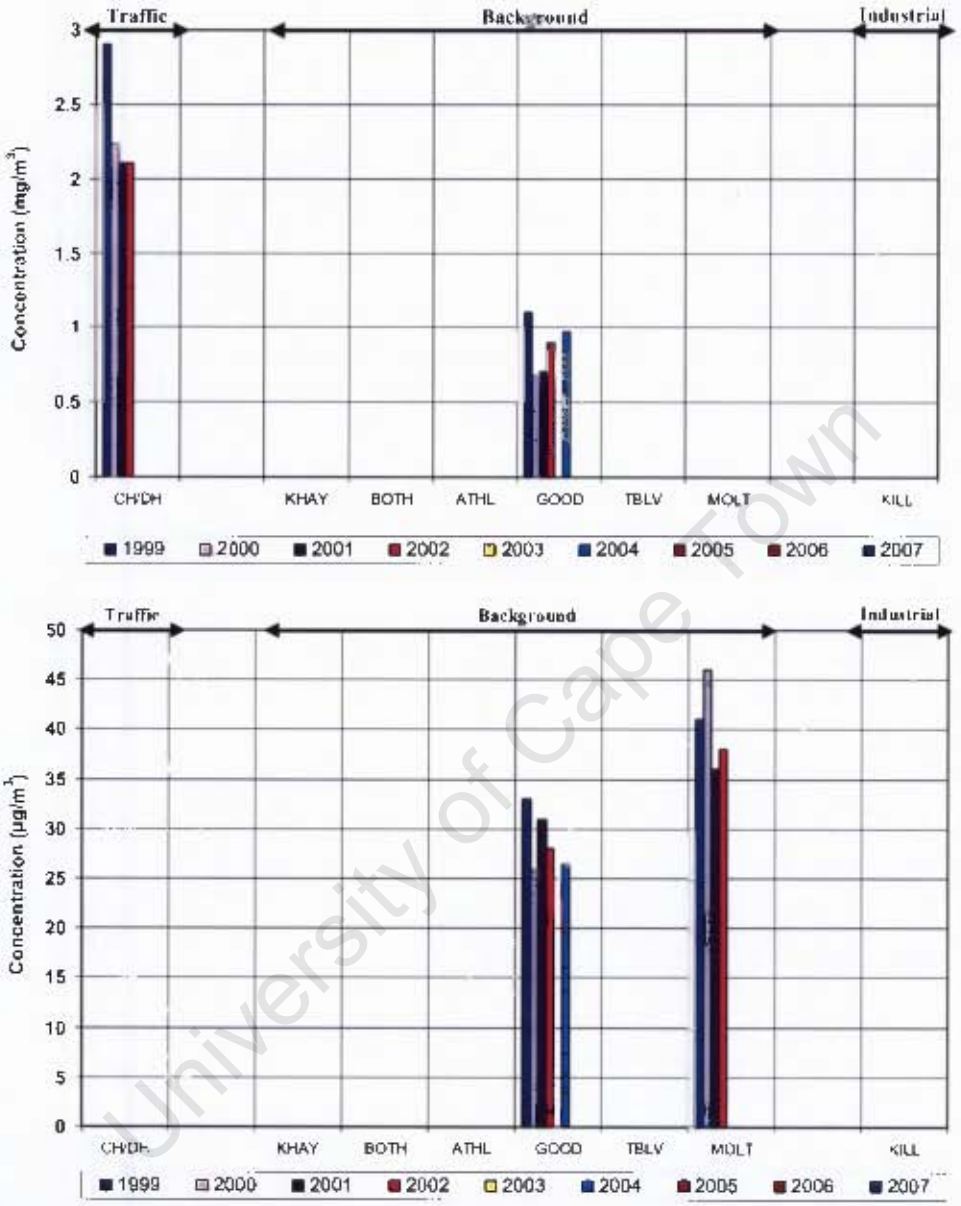

Figure 2-4: Annual mean CO (top, in mg/m^3) and O_3 (bottom, in $\mu g/m^3$) concentrations across various types of monitoring stations in the GCTA.

Inter-annual variation of mean CO and O_3 concentrations are shown in Figure 2-4. Measurements of CO are only available for the City Hall traffic station and the Goodwood background station. The elevated concentrations at the City Hall station confirm once again that traffic is a significant source of emissions in the city centre, though as the limit value only applies to hourly concentrations these are not further analysed in this section. For comparison it is mentioned that due to the wide use of catalytic vehicles, CO concentrations

in large European cities are generally low and the annual mean concentrations measured in recent years at traffic stations are ~1.5 mg/m^3 or lower (EEA, 2008a).

Ozone measurements are only available for two background stations. The concentrations measured are comparable but generally lower than those observed in Europe, where a number of large cities are found to have annual mean concentrations of around 45-50 μg/m^3. However, as the limit value only applies to hourly concentrations, these are not further analysed in this section.

2.4.2 Daily, weekly and monthly patterns

In order to analyse hourly, daily, weekly and monthly patterns of air pollutant concentrations, the most complete year, considering both temporal and spatial (across stations) data availability, was chosen. The detailed tables in Annex I concern hourly data capture and the year 2002 was found to provide the most comprehensive data set. The daily, weekly and monthly averages that follow were all computed based on the hourly data. Furthermore, the daily monthly, weekly averages were calculated using both the fully hourly data set and the data set that resulted if the daily averages were computed only when the hourly data availability was greater than 13 times per day. It is common practice to establish such a data availability threshold (e.g. Medina et al, 2002) and the data capture percentage used in this study is in line with the guidelines provided by the European Commission for the exchange of data and information from air pollution networks (European Commission, 2001) and followed by e.g. AIRBASE (2008). Nevertheless, it should be noted that the changes in the monthly and weekly values were found to be minimal and it is not the focus of this study to analyse this issue further. A more important source of uncertainty in certain cases is the lack of sufficient daily averages (due to the complete lack of hourly data for those days) for the calculation of monthly averages and the determination of an air pollution episode. Where data availability is low, this is mentioned in the analysis. The weekly variation of the concentration of main air pollutants is presented in Figures 2-5 to 2-7.

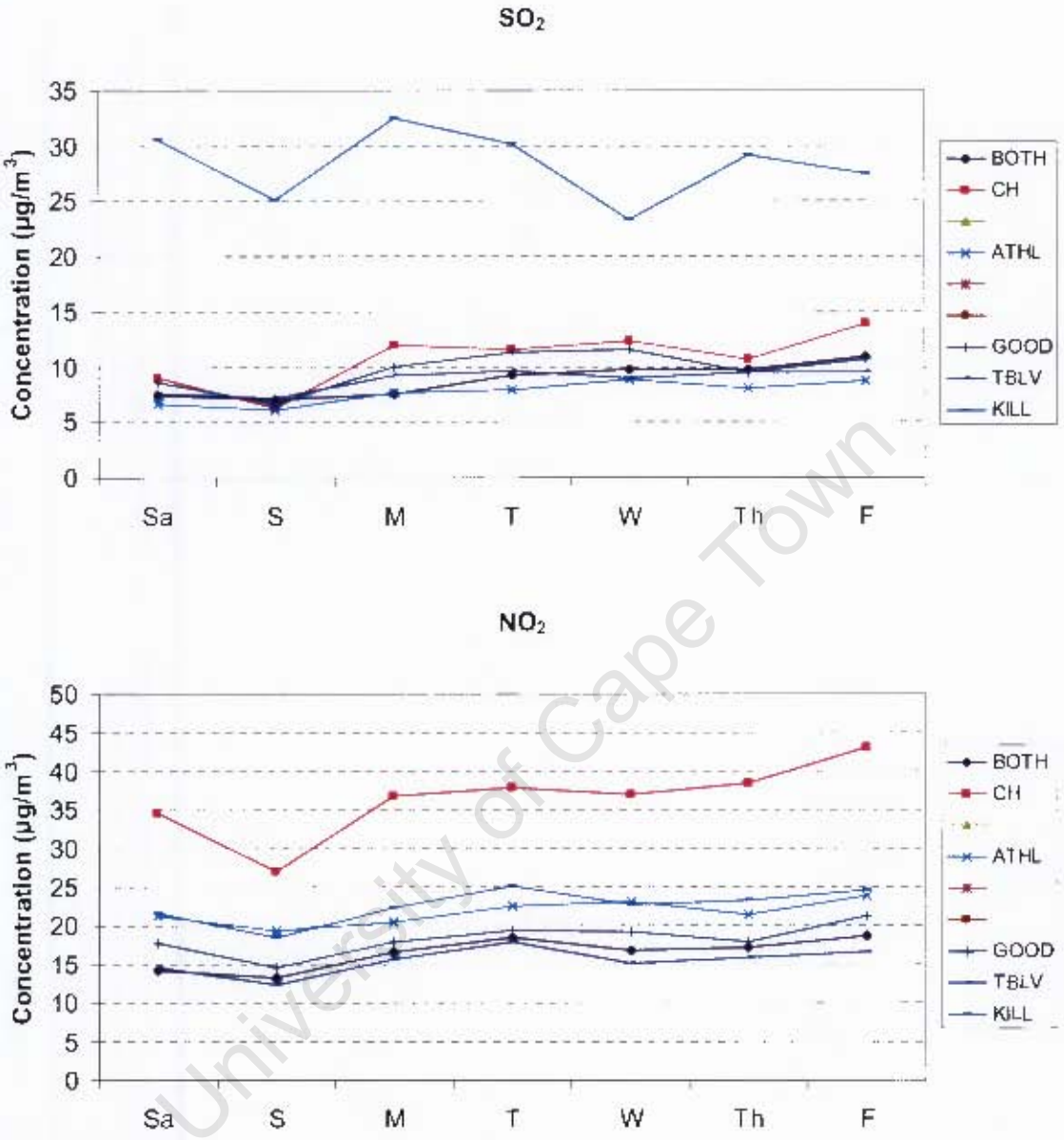

Figure 2-5: Average weekly variation of SO_2 (top) and NO_2 (bottom) concentrations in 2002 across various types of monitoring stations in the GCTA.

From the weekly variation in Figure 2-5 it is noted that the SO_2 concentrations appear lower on Sundays at all stations, with the exception of Killarney industrial station. This is due to the fact that the SO_2 concentrations measured at background stations are influenced by industrial activity and vehicle traffic which is significantly lower on Sundays. This is the reason why the reduction of SO_2 concentrations on Sunday is all the more pronounced in the measurements from City Hall traffic station. The concentrations at Killarney industrial station

are related to the industrial activity, the precise pattern of which is not known and hence cannot be analysed further.

The weekly variation of NO_2 concentrations also shows a reduction on Sundays and this is observed for all stations. Again this effect is due to the reduced industrial activity but mostly the reduced traffic on Sundays and the effect is most pronounced at City Hall traffic station.

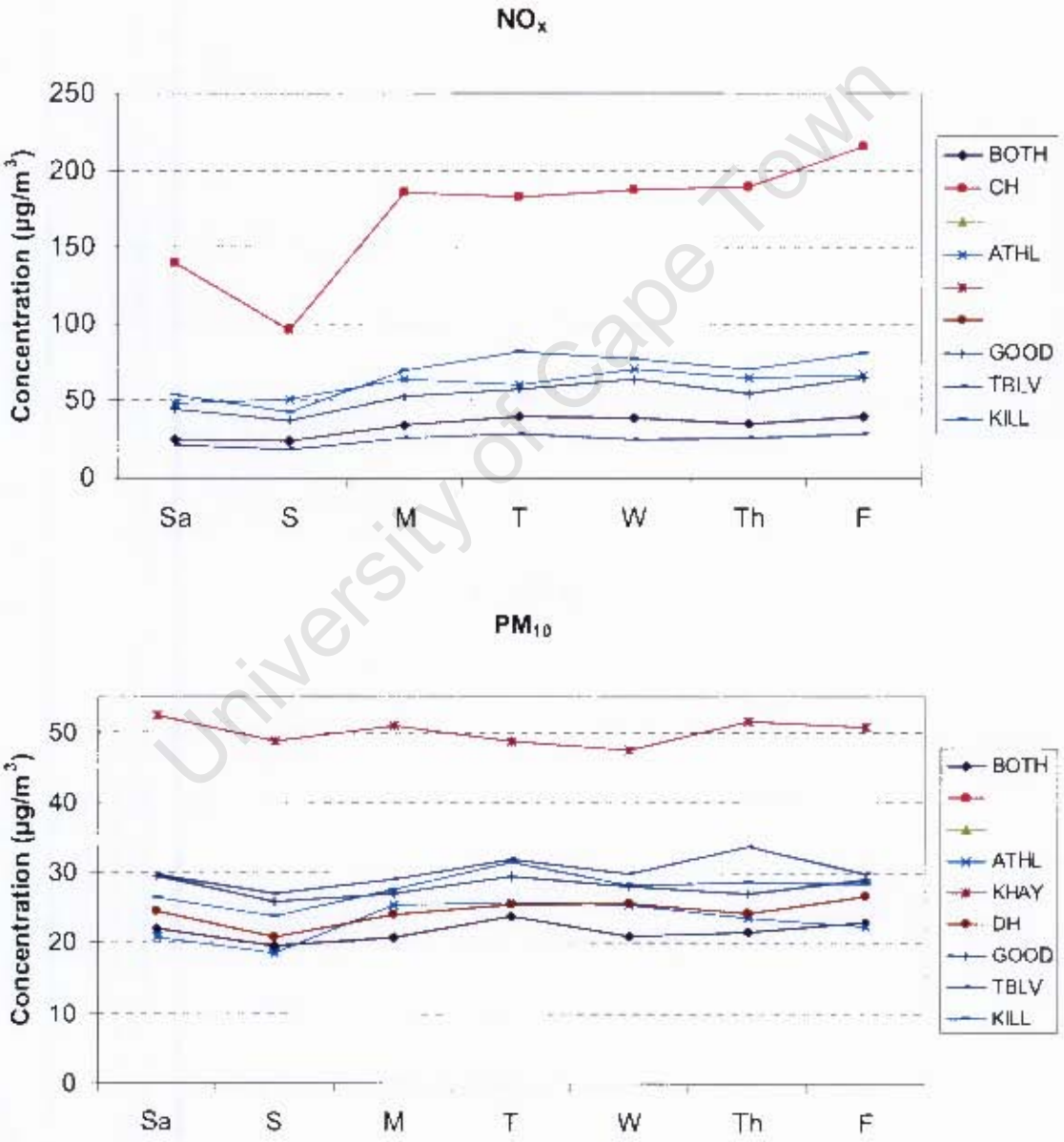

Figure 2-6: Average weekly variation of NO_x (top) and PM_{10} (bottom) concentrations in 2002 across various types of monitoring stations in the GCTA.

In Figure 2-6, the weekly variation of NO_x and PM_{10} is shown. For NO_x lower concentrations over the weekend (mainly Sunday) are noted for all stations. As for SO_2 and NO_2 this is mainly due to the reduction in vehicle traffic volumes, the effect of which is most pronounced at City Hall traffic station.

The weekly pattern for PM_{10} is quite different depending on the station. In Khayelitsha the significant contribution of natural sources (wind blown dust) and road dust resuspension as well as the anthopogenic emissions linked to cooking and heating, also mentioned in chapter 2.4.1, cause high concentrations to be observed throughout the week. In other cases (stations), industrial activity and traffic contribute significantly to PM_{10} concentrations through both coarse and fine PM emissions (PM_{10} and $PM_{2.5}$ respectively) and reduced PM_{10} concentrations are observed on Sunday. As in the case of SO_2, the pattern at Killarney station is expected to be influenced by the industrial activity, which however is not known and therefore not further analysed.

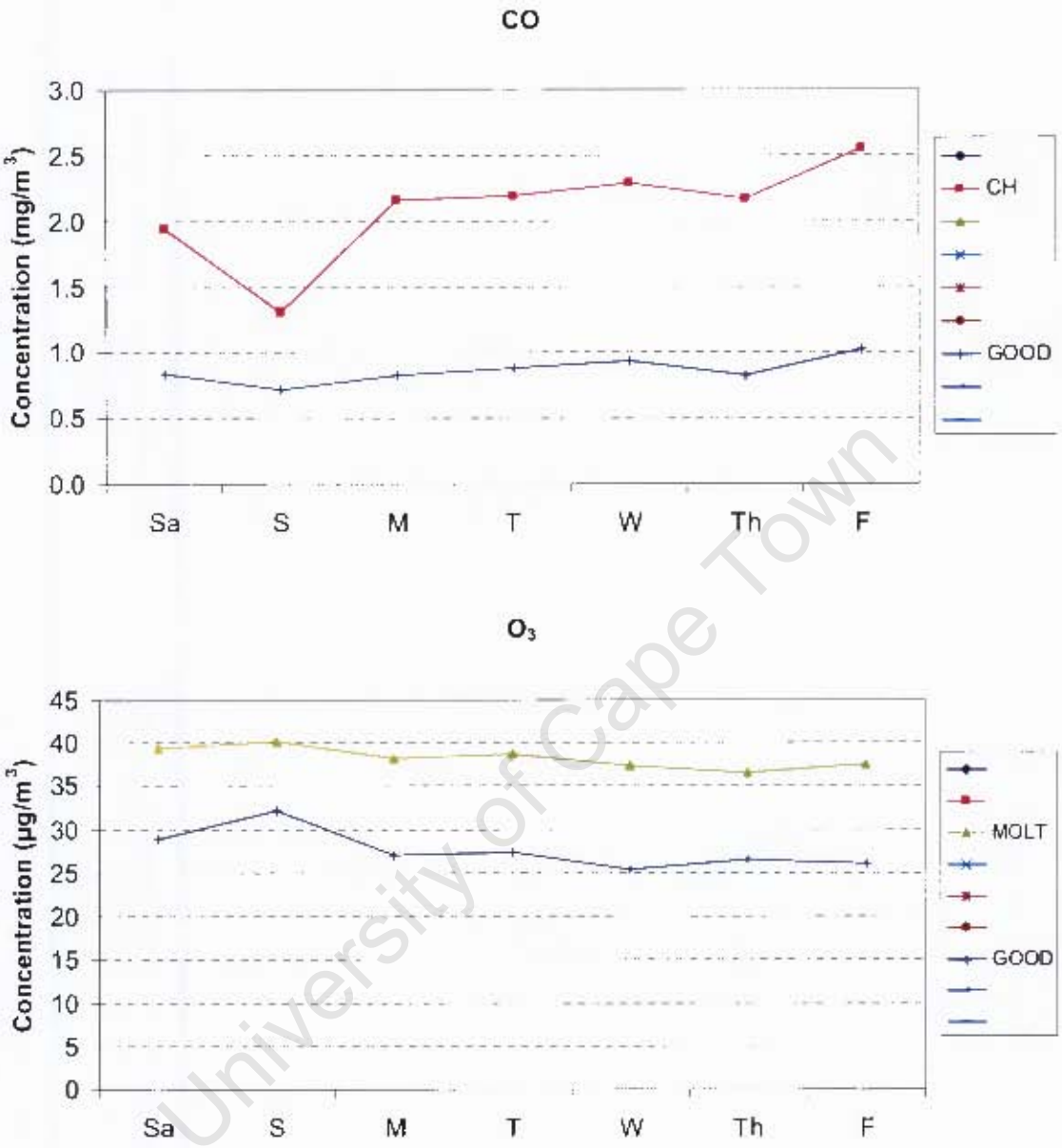

Figure 2-7: Average weekly variation of CO (top) and O_3 (bottom) concentrations in 2002 across various types of monitoring stations in the GCTA.

In Figure 2-7 the weekly variation of CO and O_3 is shown. As CO measured at City Hall traffic station is directly related to CO emissions from vehicles, the reduction in CO concentrations measured on Sunday is very much pronounced due to reduced traffic volumes. Goodwood station is a background station therefore this reduction is not as pronounced, but it is still observed.

For O_3, higher concentrations are observed over the weekend and especially on Sunday. The complex formation and destruction mechanisms for O_3 have been the subject of much research and especially in urban areas O_3 reduction strategies rely on the balanced reduction of NO_x and VOC emissions (e.g. Moussiopoulos et al, 2000). The higher O_3 concentrations observed over the weekend in Figure 2-7 are most probably caused by the reduction in NO_x emissions attributed to the reduction in the number of vehicles, without the simultaneous reduction in VOC emissions.

For the evaluation of the monthly patterns, meteorological data was also considered in the analysis. The data was partly obtained from the measurements performed by the City of Cape Town network (see Table 2-1) and partly from data provided by the South African Weather Service following a specific formal request (Linnow, 2008). The location of the SAWS stations used in the analysis can be seen in Figure 2-8 and station details can be found in Table 2-3.

Figure 2-8: Location of the meteorological stations which are operated by the South African Weather Service and which were used in this study.

Table 2-3: Characteristics of the South African Weather Service stations used in this study (Linnow, 2008).

Full station name	Station abbreviation	LAT	LON	Height from sea level
CAPE TOWN - PORTNET	PORT	-33.913	18.453	6 m
CAPE TOWN WO	AIR (WO-AIR)	-33.970	18.600	42 m
MOLTENO RESERVOIR	RES	-33.937	18.410	97 m

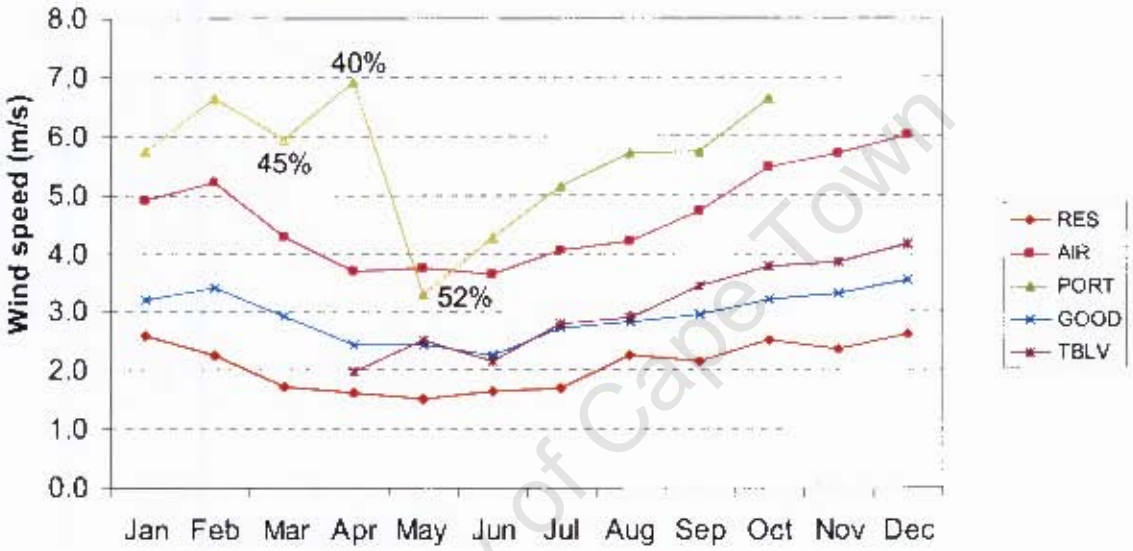

Figure 2-9: Average monthly variation of wind speed in 2002 across a number of monitoring stations in the GCTA. The percentages indicate where the availability of daily averages for the calculation of the monthly means was low.

The monthly variation of wind speed in 2002 at various locations around Cape Town is shown in Figure 2-9. A clear seasonal pattern of higher wind speeds during the summer months emerges, the intensity of which depends on the location. This pattern corresponds closely to the seasonal pattern observed using longer time series records (Kruger, 2002). Higher wind speeds are expected at the Port station, as the site experiences very laminar flow during the two dominant wind regimes (south easterly and north westerly). However, the monthly means recorded at the Port station during March, April and May are based on low data availability and are considered unreliable. It is expected that full data capture would show an overall pattern similar to that observed for other stations.

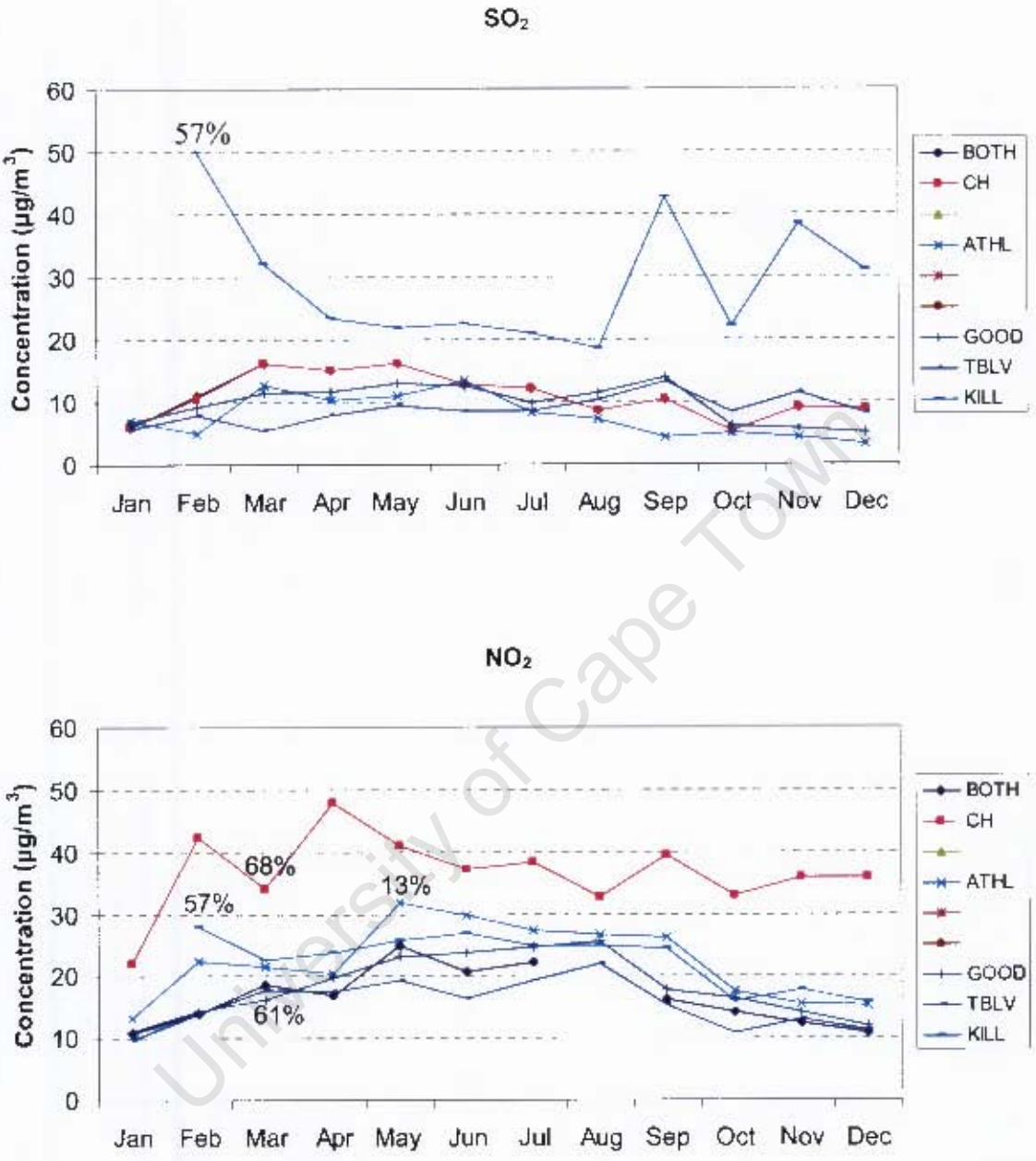

Figure 2-10: Average monthly variation of SO_2 (top) and NO_2 (bottom) concentrations ($\mu g/m^3$) in 2002 across various types of monitoring stations in the GCTA.

The monthly variation of SO_2 and NO_2 concentrations is shown in Figure 2-10. Apart from the concentrations at Killarney industrial station, where pronounced peaks are observed, the SO_2 concentrations at all stations are generally found to be relatively stable all year round. A clear seasonal cycle is not observed, a finding which is confirmed by previous studies (Jury et al, 1990). The low data capture for Killarney station in February (57 %) is noted and this

value is not considered to be as reliable as for other months. As in the case of the weekly variation of SO_2 at Killarney station, the monthly variation will also be related to the monthly industrial activity pattern. The peaks observed in September, November and December are attributed to the emissions from the Caltex refinery, which during the prevalent south-easterly conditions are transported downwind towards the Killarney station (see monthly and episode reports in CapeTown (2008b)). Overall, the meteorological conditions will have an important influence on the build up of concentrations and the lower SO_2 concentrations observed during the summer months across most stations are influenced by the stronger winds recorded in Cape Town during that period of the year (see Figure 2-9). A comparison of the monthly concentrations observed in 2002 against those of previous years can be found in the Milnerton Air Quality project and the CMC Administration monthly reports available in CapeTown (2008b).

The monthly variation of NO_2 generally shows higher concentrations during the winter months for all stations, except for City Hall. The low data capture for Killarney station in February (57 %), for City Hall and Table View in March (68 % and 61 % respectively) and for Athlone in May (13 %) is noted and these values are not considered to be as reliable as for other months. As has already been discussed in chapter 2.4.1, NO and NO_2 are rapidly inter-converted during the day depending on the availability of O_3 and sunlight. Therefore, it is expected that high NO_2 concentrations observed in February at City Hall are linked to the balance of O_3 concentrations and the high insolation and temperatures during that time of the year. The peak observed in April at City Hall is attributed to the overall lower than usual wind speeds during that time of the year, but also the air pollution episodes attributed to temperature inversions and stable atmospheric conditions which occurred between the 10^{th}-12^{th} and 15^{th}-19^{th} (see monthly and episode reports in CapeTown (2008b)).

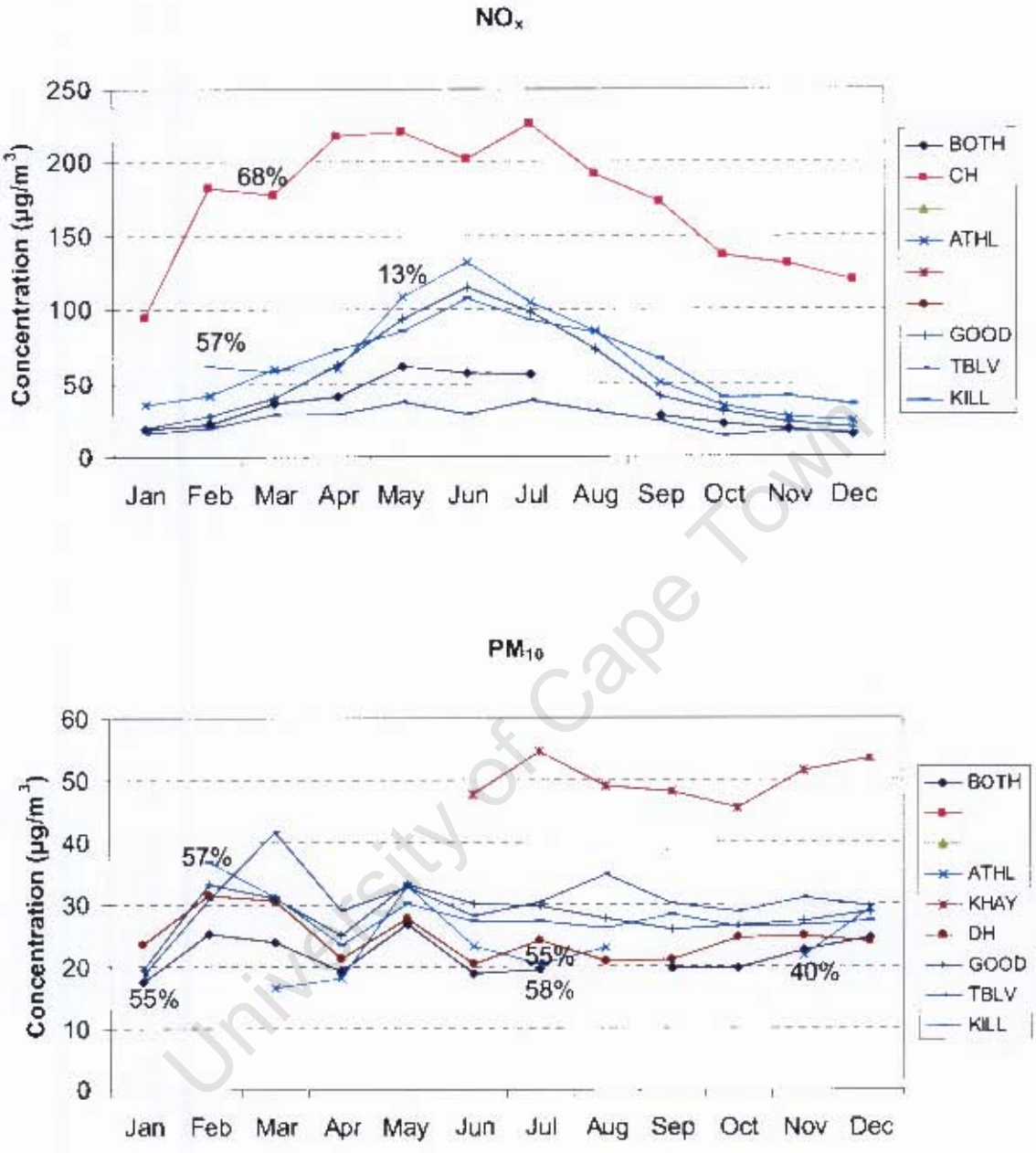

Figure 2-11: Average monthly variation of NO_x (top) and PM_{10} (bottom) concentrations ($\mu g/m^3$) in 2002 across various types of monitoring stations in the GCTA.

The monthly variation of NO_x and PM_{10} concentrations are shown in Figure 2-11. The low NO_x data capture for Killarney station in February (57 %), for City Hall in March (68 %) and for Athlone in May (13 %) is noted and these values is not considered to be as reliable as for other months. Overall, higher NO_x concentrations are clearly observed during the winter months across all stations. NO_x (the sum of NO and NO_2) can be considered an inert gas and

the higher concentrations during the winter months are attributed to the unfavourable dispersion conditions which occur during that period of the year (Tyson et al, 1976), also confirmed in Loewenheim (1988) and Ngleza (1989).

PM_{10} concentrations across all stations are generally found to be relatively stable all year round (Figure 2-11). Concentrations at Khayelitsha station are systematically higher than all other stations, though the seasonal variability follows that of the other stations. The higher concentrations observed are the result of local emissions sources (smoke) related to wood and tyre burning. As already mentioned in section 2.1, specific actions are planned to reduce these emissions. The low data capture for Bothasig station in January and July (55 % and 58 %), for Killarney in February (57 %) and for Athlone in July and November (55 % and 40 %) is noted and these values are not considered to be as reliable as for other months. The higher concentrations observed in February are attributed to slightly lower wind speeds compared to other years. For Table View in particular, building operations taking place close to the site also contributed to the elevated concentrations. The peak observed at Table View station in March is again attributed to the ongoing building operations taking place close to the site throughout the month. The peak observed in the month of May for all stations is attributed to the lower wind speeds compared to other years and the prolonged air pollutant episode that lasted between 18-22 May and was caused by stable atmospheric conditions and the re-circulation of air pollutants (see monthly and episode reports in CapeTown (2008b)). Apart from the anthropogenic emission sources, it is expected that natural sources such as windblown dust and sea salts also contribute significantly to the measured concentrations and the seasonal variation of these sources would need to be investigated to analyse the monthly patterns any further.

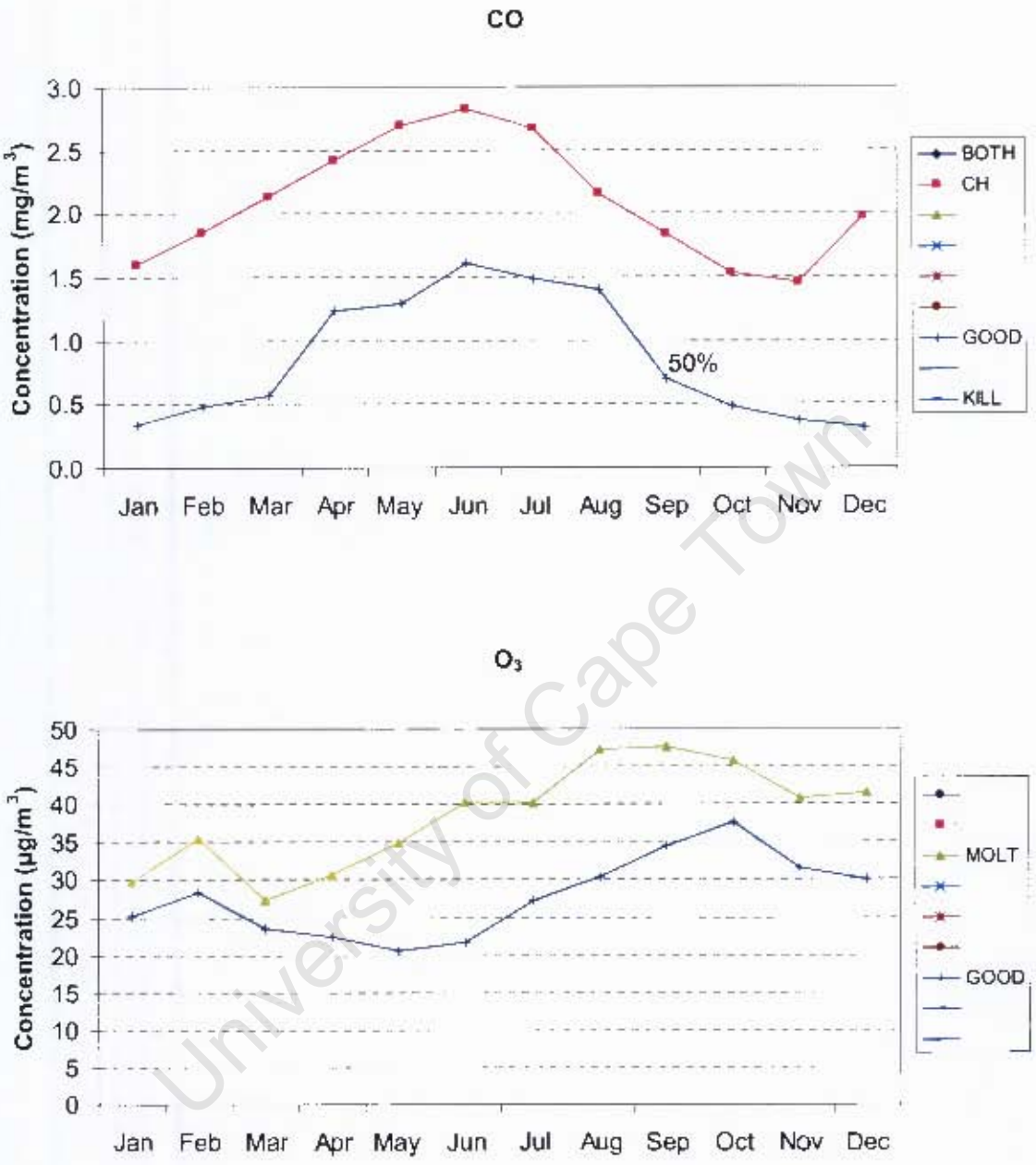

Figure 2-12: Average monthly variation of CO (top) and O_3 (bottom) concentrations ($\mu g/m^3$) in 2002 across various types of monitoring stations in the GCTA.

The monthly variation of CO and O_3 concentrations are shown in Figure 2-12. The low data capture for CO concentrations measured at Goodwood station in September (50 %) is noted. CO concentrations across both stations are clearly found to be higher during the winter months. As has already been discussed in the analysis of weekly CO variation (Figure 2-7), the concentrations at City Hall are primarily due to traffic emissions and the peak observed in

December could be due to higher traffic volumes associated with tourism activity during the holiday period. Traffic counts would be needed to further validate this point.

The monthly variation of O_3 concentrations does not reveal higher values during the summer months, as is most commonly found to be the case in e.g. Europe (EEA, 2008c). This is primarily due to the high wind speeds and favourable dispersion conditions which occur during the summer months (see Figure 2-9) which inhibit the build up of O_3 precursor gases. Similarly, high concentrations are found to occur in late winter and early spring, when stagnant meteorological conditions which most commonly occur during that time of the year (Tyson et al, 1976) combine with high insolation and higher ambient temperatures.

Figure 2-13: Average diurnal variation of wind speed in 2002 across a number of monitoring stations in the GCTA.

The average diurnal variation of wind speed at various locations around Cape Town is shown in Figure 2-13. A clear tendency towards higher wind speeds during the afternoon hours is observed, which is in agreement with the pattern from longer time series records (Kruger, 2002).

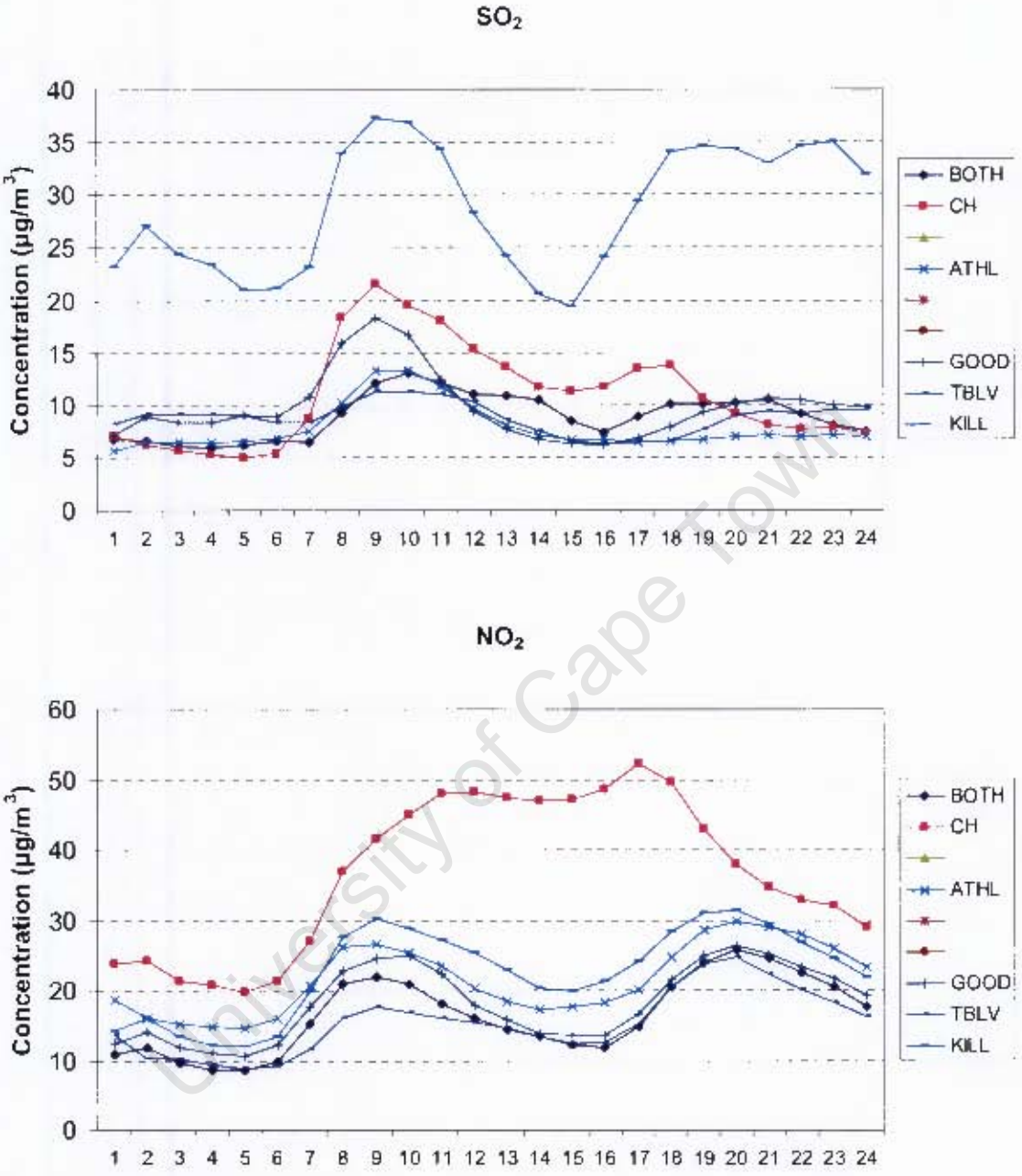

Figure 2-14: Diurnal variation of SO_2 (top) and NO_2 (bottom) concentrations ($\mu g/m^3$) in 2002 across various types of monitoring stations in the GCTA.

The average diurnal variation of SO_2 and NO_2 concentrations in 2002 are shown in Figure 2-14. The SO_2 pattern observed for Killarney industrial station will be directly related to the industrial activity pattern, the detailed form of which is not known. The diurnal pattern at background stations will also be influenced by industrial activity, but mostly by traffic emissions and two peaks are observed during the morning and afternoon hours. Morning and

afternoon peaks are most pronounced at the City Hall traffic station and are related to the business working hours. It is important to note that the morning peak is much more pronounced than the afternoon peak, which is mainly due to the increased wind speeds which are systematically observed during the afternoon hours, as can be seen in Figure 2-13. Another contributing factor is most probably the higher traffic volumes expected in the morning hours, since these include school related transport which is temporally much more dispersed in the afternoon. The higher traffic volumes in the morning hours also coincide with the nocturnal radiative temperature inversions which persist into the morning hours until the heating from the earth's surface causes an erosion of this inversion layer (see also chapter 1.3). This leads to increased levels of air pollution between 8:00-10:00 am.

The diurnal pattern for NO_2 concentrations at most stations reveals similar peaks to those observed for SO_2, related to the increased vehicle traffic during the start and finish of business working hours. The diurnal pattern at City Hall is slightly different, showing elevated NO_2 concentrations throughout the day. This is due to the complex balance between O_3 availability, insolation and NO emissions from vehicles which are rapidly converted to NO_2. The city centre, being the centre of main economic activity, is also expected to have high traffic volumes throughout the day, leading to increased NO and NO_2 emissions and thus increased NO_2 concentrations. However, detailed traffic counts are not available to confirm this hypothesis.

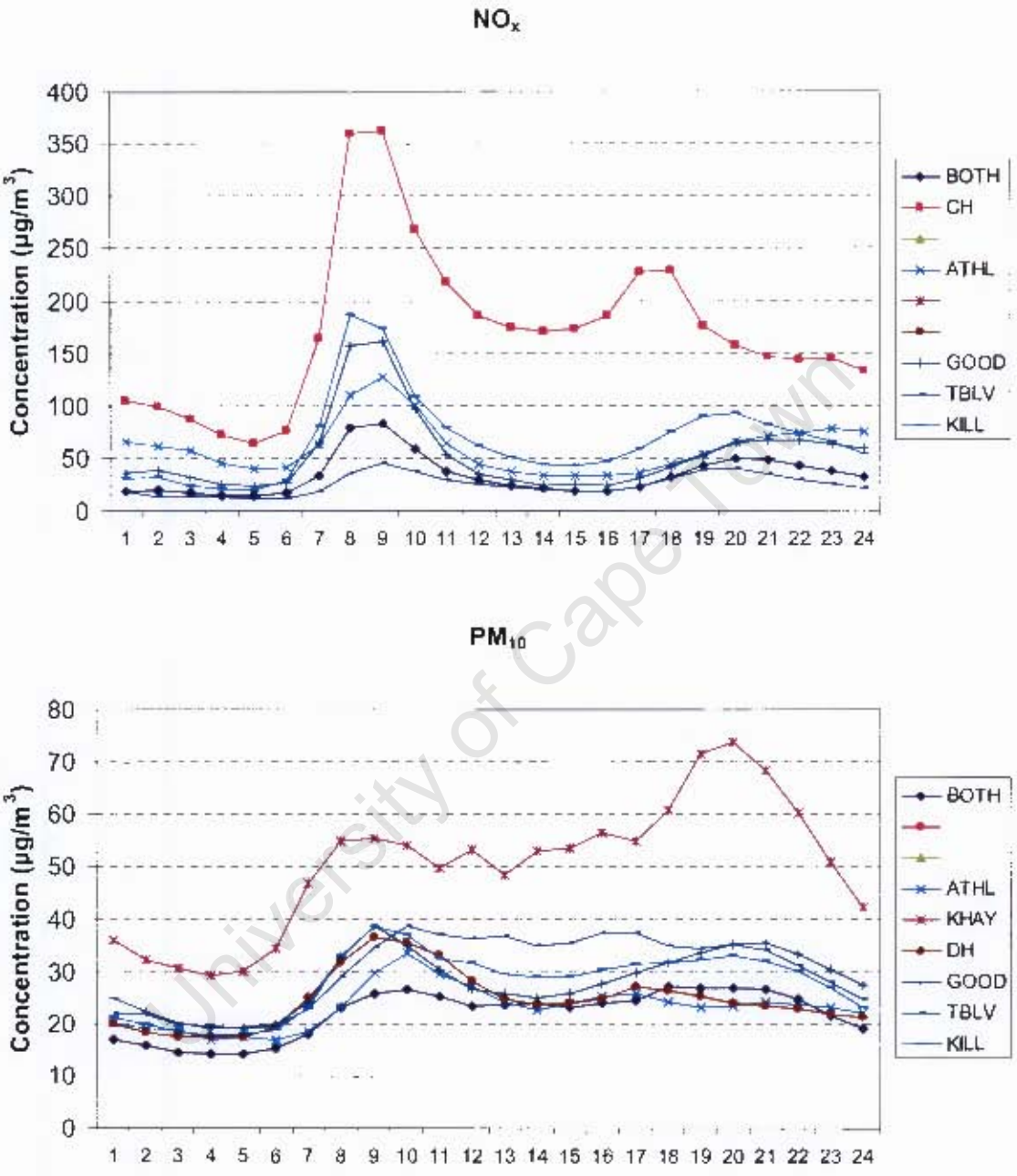

Figure 2-15: Diurnal variation of NO_x (top) and PM_{10} (bottom) concentrations ($\mu g/m^3$) in 2002 across various types of monitoring stations in the GCTA.

The average diurnal variation of NO_x and PM_{10} concentrations in 2002 are shown in Figure 2-15. For NO_x concentrations, two distinct peaks are observed across all stations during the morning and afternoon peak traffic hours. As in the case of SO_2, the NO_x morning peak is especially pronounced, most probably related to the reduced wind speeds observed in the

morning hours compared to the afternoon throughout the area of study (Figure 2-13). The close correspondence of SO_2 and NO_x peaks on a daily basis has also been noted in previous studies (Jury et al, 1990). As has been mentioned in the SO_2 analysis, the higher traffic volumes in the morning hours coincide with the nocturnal radiative temperature inversions which persist into the morning hours leading to increased levels of air pollution between 8:00-10:00 am.

The diurnal variation of PM_{10} also shows two peaks for most stations. These are primarily related to the proportion of PM_{10} attributed to $PM_{2.5}$ emissions from traffic. At Khayelitsha station, a pronounced evening peak is observed and is related to the increased anthropogenic activities in the evenings such as cooking and heating (burning of wood, coal and paraffin).

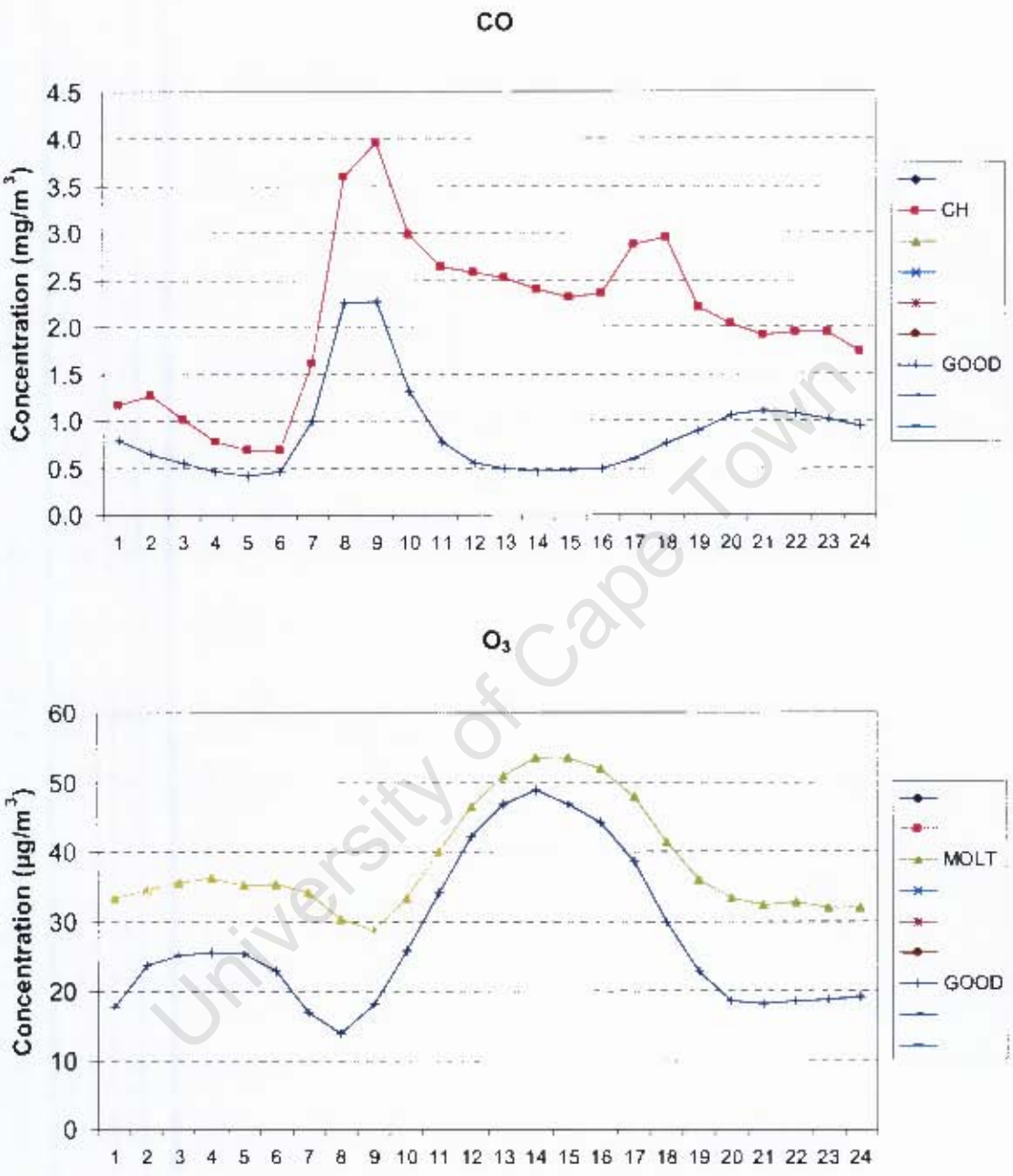

Figure 2-16: Diurnal variation of CO (top) and O_3 (bottom) concentrations ($\mu g/m^3$) in 2002 across various types of monitoring stations in the GCTA.

The average diurnal variation of CO and O_3 in 2002 are shown in Figure 2-16. As the CO concentrations for both stations are primarily attributed to CO emissions from traffic, the peaks observed are in line with the peak traffic hours, as has been the case for NO_x, NO_2 and

SO_2. The higher morning peak is attributed to the lower dispersion conditions observed in the morning, in comparison to the afternoon hours (Figure 2-13).

The diurnal pattern for O_3 is similar to that observed in most urban areas (e.g. EEA 2008a), and the higher concentrations observed after midday are attributed to the high insolation during that time of the day.

2.4.3 Air pollution episodes

In this study, NO_x concentrations are selected to characterise air pollutions episodes. The selection was made for a number of reasons. Firstly, NO_x can be considered an inert gas and hence can be directly linked to dispersion conditions, unlike NO_2 which is a photochemical air pollutant and its concentration levels change during the day with the changing solar isolation levels and its participation in a number of chemical reactions. SO_2 can also be considered inert, but from the analysis in section 2.4.2 it was found that SO_2 levels are closely linked to industrial activity levels, a local emission source compared to traffic, which can significantly influence the concentrations measured at certain stations under certain meteorological conditions. This study aims at linking air pollution episodes to the large circulation patterns which cause stagnant meteorological conditions across most of the GCTA and a pollutant with high background concentrations levels is required. A similar problem exists with PM_{10}, for which local emission sources are also found to have a significant impact on the concentrations measured, masking in certain cases the link to widespread meteorological conditions. Finally, a very important reason for selecting NO_x concentrations is the temporal and spatial data availability, since e.g. CO concentrations are only measured at two stations, whereas NO_x data are available for six. For the above reasons, the high NO_x concentrations observed in the GCTA are found to be most appropriate for the characterisation of air pollution episode days in this study. This is in line with previous studies focusing on meteorological aspects and air pollution episodes in the GCTA (Jury et al, 1989; Ngeleza, 1989; Jury et al, 1990; Jury & Barclay, 1992).

For each station in the GCTA, the variation of average daily NO_x concentrations in 2002 and the maximum hourly value recorded per day are shown in Figures 2-17 to 2-19. As was also pointed out in the analysis of Figure 2-11, for all stations higher concentrations are observed during the winter period. The analysis will therefore focus on the six month period April-September. The highest concentrations are observed at the City Hall traffic station, which is

located close to the monitoring site used in Jury et al (1990) and is the only station in 2002 that measures concentrations close to the magnitude reported in Jury et al (1990).

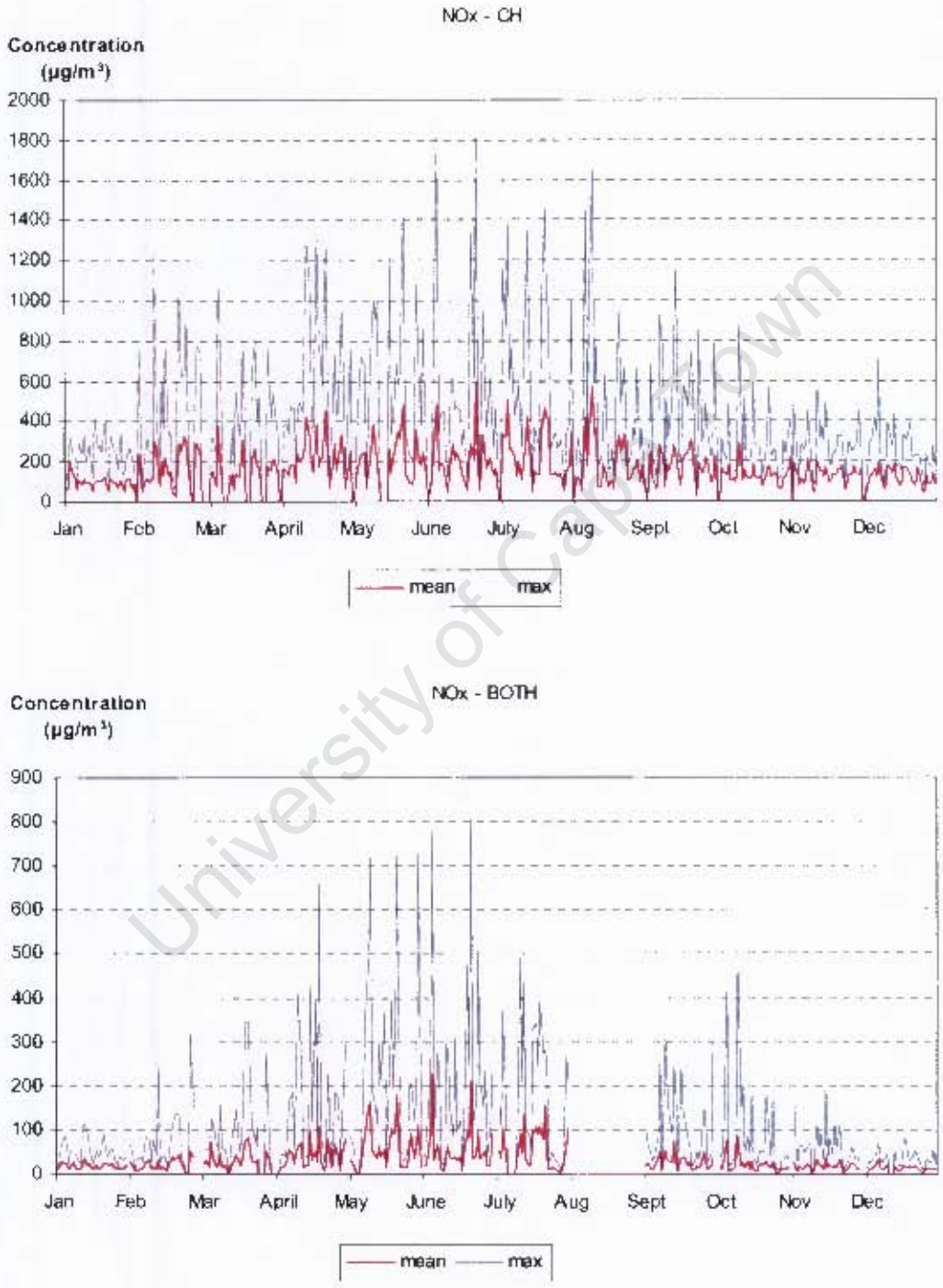

Figure 2-17: Daily average and maximum hourly NO_x concentrations ($\mu g/m^3$) in 2002 measured at City Hall (top) and Bothasig (bottom) stations.

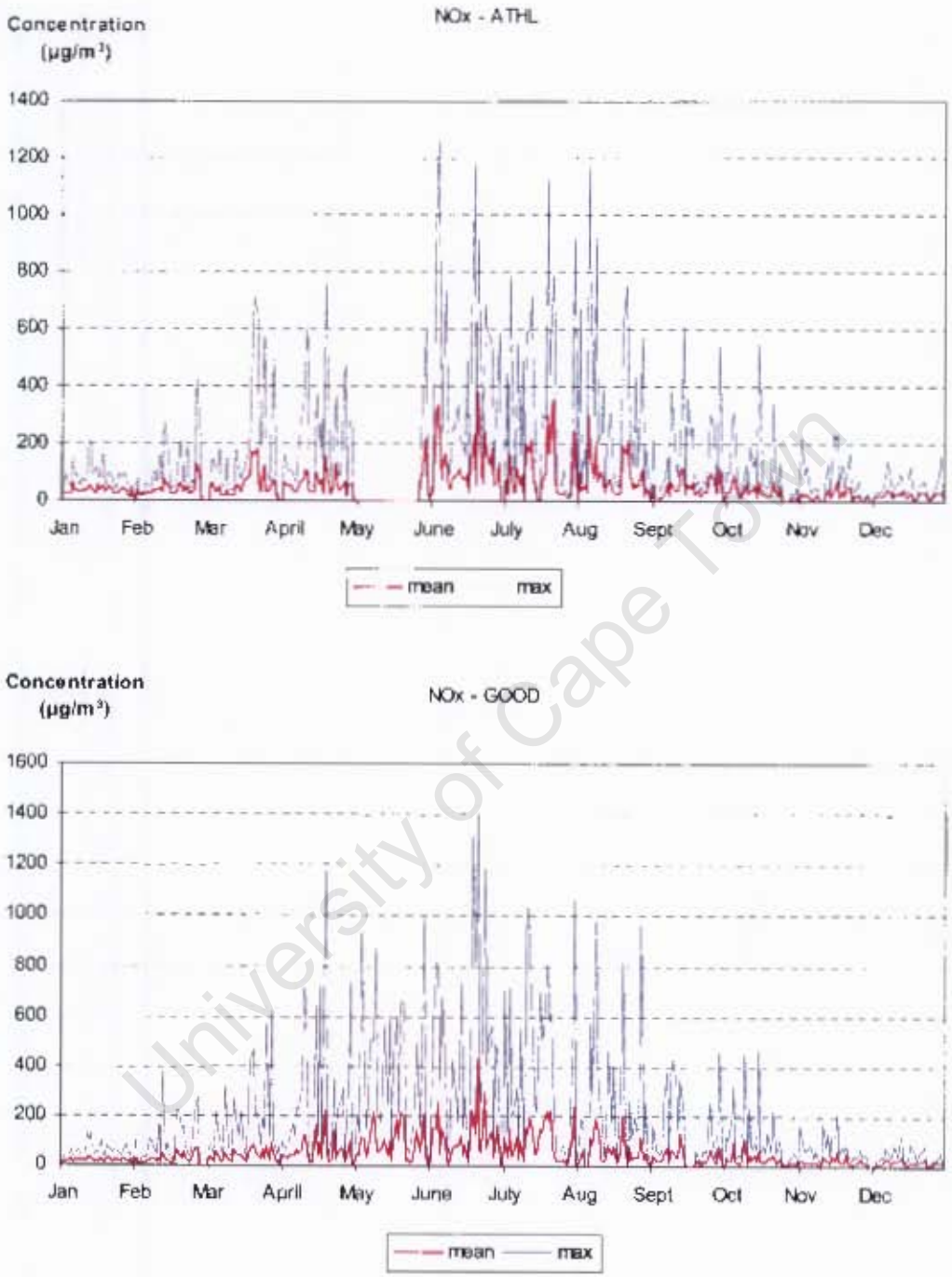

Figure 2-18: Daily average and maximum hourly NO_x concentrations ($\mu g/m^3$) in 2002 measured at Athlone (top) and Goodwood (bottom) stations.

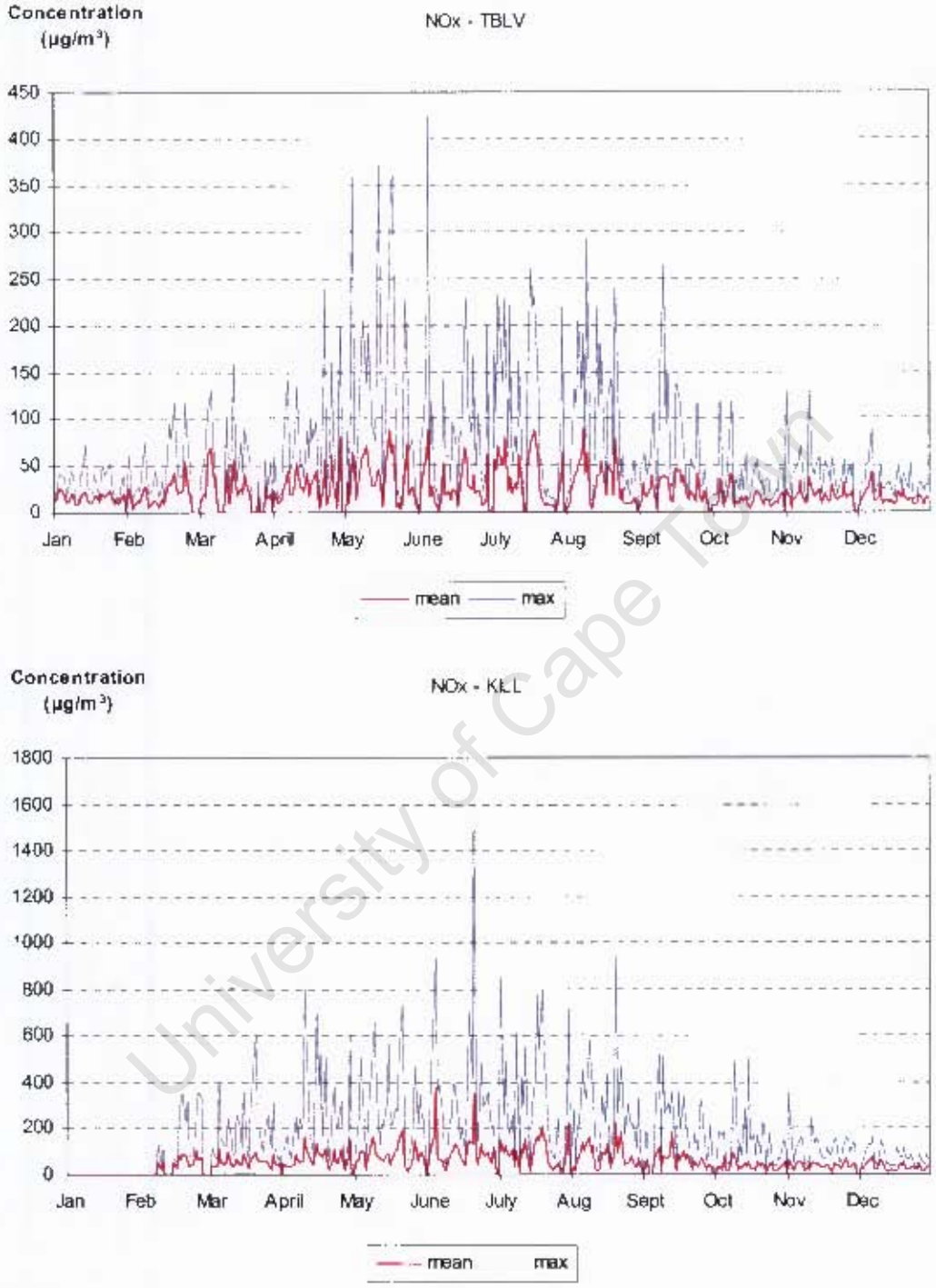

Figure 2-19: Daily average and maximum hourly NO_x concentrations ($\mu g/m^3$) in 2002 measured at Table View (top) and Killarney (bottom) stations.

In order to study the link between air pollution episodes, temperature inversion and the larger synoptic circulation, it is necessary to establish an "episode day" criterion. Studies that focus on the analysis of air pollution impacts on health usually define such a criterion as the

exceedance of air quality objectives. These can be exceedances of the World Health Organisation (WHO) guidelines or those indicated in national standards set by legislation. For the reporting of air pollution episodes in the GCTA performed for compliance purposes, the Air Quality Monitoring Section of the Scientific Services Department of the City of Cape Town uses the air quality standards set by DEAT (defined in SANS (2005)), but also the UK and WHO guidelines.

This study does not aim at checking compliance, but at determining days with higher than average air pollution which can then be linked to specific meteorological conditions and larger scale weather producing systems. Along the lines of the work of Jury et al (1990), two criteria are set:

1. The daily average should be at least 1.5 times the monthly average.
2. The above criterion should be met across more than two stations.

The second criterion aims at ensuring that the high air pollution observed on the particular day is linked to the meteorological conditions that occur in the greater area and not just a phenomenon caused by local topography or a local emission source. Using both these criteria, 49 episodes days are found to occur between April and September 2002 and of these 12 occur in just two stations, 8 in three stations, 12 in four stations, 11 in five stations and 6 in all six stations (see Annex II for a complete list of days). The episode days resulting from the application of both these criteria to the whole 2002 time series (January-December) leads to 87 episode days, i.e. 38 occur in the summer period between January-March and October-December. However, the intensity of the episodes is much reduced in the summer months, since from the top 37 episode days only 8 are in the summer months and of these one is in late March and the other beginning of October (hence almost in the winter period). The above results were obtained by categorising the episode days firstly according to the number of stations that the episodes occur in (i.e. episodes across all 6 stations are at the top of the list) and secondly according to the magnitude of the episode at the Athlone background station (a typical background station located far from local emission sources).

For comparison purposes it is also mentioned that using the criterion that the daily average should be twice the monthly average leads to 20 episode days in the winter period, of which 8 occur in just two stations, 5 in three, 4 in four, 1 in five and 2 in all six.

3. Climate Change

According to the Fourth Assessment report (AR4) of the Intergovernmental Panel on Climate Change (IPCC), an average global warming of 0.74°C ± 0.18°C has been observed in the last 100 years (IPCC, 2007a: 237). It is estimated that by the end of the century, even if global Greenhouse Gas (GHG) concentrations are stabilised at year 2000 levels, the long response time of the climate system will still lead to further global warming of around 0.6°C (IPCC, 2007a: Table TS.6). It is therefore clear that changes to the currently observed climate will occur due to past GHG emissions, even if drastic measures to halt their further increase are immediately taken. Until today the international community has failed to reduce GHG emissions and drastic measures do not seem to be under discussion, so it appears very unlikely that concentrations will be stabilised at year 2000 levels in the immediate future. This means that by the end of the century global warming is expected to be more than 0.6°C.

Although global average temperature is expected to increase, the changes in climate will be different in each region reflecting changes in the atmospheric and oceanic circulation and other components of the climate system. According to the AR4 the whole of Africa is predicted to get warmer during this century and in southern Africa the rainfall is likely to decrease in the western part and in much of the winter rainfall region (IPCC, 2007a: 866). In order to further assess the impact of climate change at the regional scale, the application of regional climate models or empirical downscaling techniques is required (IPCC, 2007a: 852), as the spatial resolution of General Circulation Models (GCM) is too coarse to reveal detailed information.

The insufficient climate data and the restrictions in computational facilities and human resources have lead to very few regional studies being conducted in Africa (IPCC, 2007b: 443). However, in recent years significant efforts have been made to develop the potential to assess regional climate change within Africa (e.g. Hewitson et al, 2006) and important findings have already been published (e.g. New et al, 2003; Tadross et al, 2005; Hewitson & Crane, 2006; Tadross et al, 2006; Tadross et al, 2007).

A study of precipitation changes over South Africa using empirical downscaling indicates an increased summer rainfall over the central and eastern part of the country, whereas little

change is expected in the region of the Western Cape, though an overall drying in summer and a slight decrease in winter frontal rainfall is noted (Hewitson & Crane, 2006).

3.1 General Circulation Models (GCMs)

Climate is defined as the long-term statistics of the weather, i.e. the average of the weather globally or in a particular region over a long period of time. General Circulation Models (GCMs), also referred to as Global Circulation Models, incorporate the fundamental physical laws such as conservation of mass and energy and momentum and consider a series of observations to simulate the overall behaviour of the atmosphere. GCMs are mathematical representations of the climate system, expressed as computer codes and run on powerful computers.

GCMs have shown "significant and increasing skill" (IPCC, 2007a: 600) in representing many important mean climate features, such as the large-scale distributions of atmospheric temperature, precipitation, radiation and wind, and of oceanic temperatures, currents and sea ice cover. They have also been found able to simulate essential aspects of many of the patterns of climate variability observed across different time scales (e.g. advance and retreat of monsoon systems, seasonal shifts of temperatures, the Northern and Southern 'annular modes'). GCMs, or models very closely related to them, have been successfully used to make seasonal forecasts, demonstrating their ability to represent important features of the general circulation across shorter time scales, as well as aspects of seasonal and interannual variability (IPCC, 2007a: 600).

Another very important aspect of GCMs is their ability to reproduce features of past climates and climate changes. They have been found capable of simulating ancient climates, such as the warm mid-Holocene (~6,000 years ago) or the last glacial maximum (~21,000 years ago).

GCMs have also been found to simulate many observed aspects of climate change over the instrumental record. The most important example is global temperature trend over the past century, which can be modelled with high skill when both natural *and* human factors that influence climate are included (IPCC, 2007a: 601). However, this does not directly imply that GCMs can also simulate future climate with a similar degree of accuracy, as it cannot necessarily be assumed that the relationships between circulations and variables used in the various parameterisation schemes remain constant in time.

It remains a fact that many micro-physical processes are still poorly understood, rendering their consideration in GCMs very difficult and resulting in inherent inaccuracies and uncertainties in all GCMs (Peixoto & Oort, 1992, IPCC, 2007a: 601). Moreover, the effect of some large scale circulations on remote areas of the earth are also either not understood or captured in many models.

To assess the differences between GCM outputs, a number of model intercomparison studies have taken place to compare model results under different types of simulations (IPCC, 2007a: 594). In recent years, the Coupled Model Intercomparison Project (CMIP) Phase 3 provided important input to the IPCC AR4 by collecting and archiving GCM output from simulations of the past, present and future climate. This unprecedented collection of recent model output is officially known as the "WCRP CMIP3 multi-model dataset" (CMIP, 2009).

In this study three GCMs were used to acquire an insight in the range of possible climate futures in the region influencing the climate in the GCTA, according to the selected IPCC SRES scenario. The data was obtained from the "WCRP CMIP3 multi-model dataset". A brief description of the three models can be found in the section below.

3.1.1 ECHAM5

The ECHAM5 is the fifth generation most recent version of the Max Planck Institute (MPI) for Meteorology (Germany) GCM. Like its predecessors, ECHAM5 employs a spectral dynamical core. Vorticity, divergence, temperature and the logarithm of surface pressure are represented in the horizontal by a truncated series of spherical harmonics. A transform technique developed in the 1970's (details in Roeckner et al (2003)) is used such that non-linear terms, including parameterizations, are evaluated at a set of almost regularly distributed grid points - the Gaussian grid. The model's horizontal resolution roughly translates to 1.9^{o} x 1.9^{o}. In the vertical, a flexible coordinate is used, enabling the model to use either the usual terrain following sigma coordinate or a hybrid coordinate for which upper-level model surfaces flatten over steep terrain, becoming surfaces of constant pressure in the stratosphere. There are 31 levels in the vertical and the pressure at the top level is 10 hPa. The ocean model has a horizontal resolution of 1.5^{o} x 1.5^{o} and 40 levels in the vertical. A detailed description of the atmospheric model is given in Roeckner et al (2003) and of the ocean model in

Marsland et al (2003) and references therein and a summary of the main characteristics are available through the Coupled Model Intercomparison Project website (CMIP, 2009).

3.1.2 CNRM-CM3

The CM3 is a coupled GCM model developed by the Centre National de Recherches Météorologiques (CNRM) at Météo France. This coupled GCM is based on the ARPEGE-Climat version 3 atmospheric model and the OPA8.1 oceanic model. ARPEGE-Climat is a spectral model with a progressive hybrid sigma-pressure coordinate and a two-time-level semi-Lagrangian semi-implicit integration scheme. All the physics and the treatment of model nonlinear terms require spectral transforms to a Gaussian grid. The model's horizontal resolution roughly translates to 1.9^{o} x 1.9^{o}. The vertical levels are defined with a progressive hybrid sigma-pressure vertical coordinate including 45 layers, in order to correctly represent the atmospheric circulation in the stratosphere. The pressure at the top level is 0.05 hPa. The OPA 8.1 ocean model has a horizontal resolution of 2^{o} in longitude and varies in latitude from 0.5° at the equator to 2° in polar regions and has 31 levels in the vertical. A detailed description of the atmospheric model is given in Salas-Mélia et al (2005) and of the ocean model in Madec et al (1998) and references therein and a summary of the main characteristics are available through the Coupled Model Intercomparison Project website (CMIP, 2009).

3.1.3 CSIRO-MK3.5

The MK3.5 GCM model is one of a series of models developed by the Commonwealth Scientific and Industrial Research Organisation (CSIRO) in Australia. It is based on MK3.0, but includes a number of physical parameterisation and numerical improvements compared to its predecessor. The model's horizontal resolution roughly translates to 1.9^{o} x 1.9^{o} and it has 18 vertical levels with 4.5 hPa pressure at the top level. The dynamical framework of the atmospheric model is based upon the spectral method. The atmospheric model includes a comprehensive cloud microphysical parameterisation and the convection parameterisation is based on that used in the Hadley Centre model. Atmospheric moisture advection is carried out by the semi-Lagrangian method. A simple treatment of the direct radiative effect of sulphate aerosol using a perturbation of the surface albedo is included. The MK3.5 ocean model is based on the Geophysical Fluid Dynamics Laboratory (GFDL) Modular Ocean Model version 2.2 (MOM2.2). It has a horizontal resolution of 0.8^{o} x 1.9^{o} and 31 levels in the vertical. A detailed description of both model components is given in Gordon et al (2002) and

references therein and a summary of the main characteristics are available through the Coupled Model Intercomparison Project website (CMIP, 2009).

3.2 Scenarios and tools for the assessment of climate change

For synthesising and communicating the extensive information produced and used in studies related to CC, a number of tools must be combined. In this study two tools are used. CC scenarios are necessary to contextualise the future and set the range of values for certain variables and SOMs are used to visualise and assess GCM results.

3.2.1 Climate Change scenarios

"Climate scenarios are plausible representations of the future that are consistent with assumptions about future emissions of GHGs and other pollutants and with our understanding of the effect of increased atmospheric concentrations of these gases on global climate" (IPCC-TGICA, 2007). A climate scenario is an indication of what the future could be like depending on assumptions about e.g. economic growth, global population figures, energy demand, emissions of GHGs and aerosols as well as aerosol precursors (which lead to secondary aerosol production), land use changes, which together with the assumptions about the behaviour of the climate system over long time scales lead to an image of the future.

The IPCC Special Report on Emission Scenarios (SRES) groups the IPCC scenarios into four families A1, A2, B1 and B2, which explore alternative development pathways, covering a wide range of demographic, economic and technological driving forces and resulting GHG emissions. The SRES scenarios do not include additional climate policies above current ones.

The current study will make use of the SRES A2 scenario which according to IPCC (2000) "describes a very heterogeneous world. The underlying theme is self-reliance and preservation of local identities. Fertility patterns across regions converge very slowly, which results in continuously increasing global population. Economic development is primarily regionally oriented and per capita economic growth and technological change are more fragmented and slower than in other storylines".

The focus of this study will be on the changes likely to occur in the period 2046-2065. According to the A2 scenario, a global temperature increase of 1.65°C is predicted for the period 2046-2065 relative to the period 1980 to 1999 (IPCC, 2007a: 763). The CO_2

concentrations for the middle of the century are predicted to be ~550 ppm as a result of a steady increase of CO_2 emissions which will reach 18 GtC/yr by the middle of the century (IPCC, 2007a: Figure 10.26).

3.2.2 Self-Organising Maps (SOMs)

A Self-Organising Map (SOM) is part of a large group of techniques known as Artificial Neural Networks (ANNs). It was developed by Kohonen (1997) and is a tool that can be used to cluster, classify and visualize multi-dimensional data sets. SOMs are widely used across a number of disciplines and in recent years have been successfully used in climate applications (Hewitson, 2008).

A SOM is a type of unsupervised ANN that will span the data set and determine nodes (archetypal points) around which the data can be clustered. Unlike other clustering techniques, it does not identify clusters in the multi-dimensional data set, but rather identifies archetypal points that are capable of representing the data around them. An important characteristic, compared to other synoptic classification techniques is that a SOM is capable of representing non-linear relationships, as it makes no assumptions about the properties of the data set (Skupin & Agarwal, 2008). Also, in the atmospheric field the SOM analysis is particularly useful as it preserves the continuous nature of the synoptic states, while allowing their complex distribution to be clearly visualised, as it places the most dissimilar atmospheric states in the most distant nodes of the SOM and the similar states in adjacent nodes (Hewitson, 2008).

A SOM provides the user with a two-dimensional matrix, reflecting the distribution of the input data set. Each element of the matrix is a node (archetypal point) capable of representing the data around it. The SOM (matrix) is trained in an iterative way, with each node being weighted by the input data that most closely match the node. A difference with most cluster algorithms is that during this process the neighbouring nodes are also incrementally adjusted, in accordance with a user defined update kernel (Skupin & Agarwal, 2008).

In atmospheric applications each node is a particular synoptic state for a particular variable. By studying the frequency with which each synoptic state occurs in the initial data set used to train the SOM (i.e. the number of input data that map to each node), the current climate characteristics (synoptic states) for the reference period are determined. New data can then be

introduced and the SOM will map the new data set onto the existing matrix. The changes in the frequency with which the new data maps to each node compared to the initial "training" data set can then easily be visualised and interpreted (Hewitson & Crane, 2002; Hewitson, 2008).

4. Data and Methods

4.1 Radiosonde data and link to air pollution episodes

In section 2.4.3, the criteria for selecting air pollution episode days in 2002 are discussed in detail. These are:

1. The daily average should be at least 1.5 times the monthly average.
2. The above criterion should be met across more than two stations.

These criteria lead to the selection of 49 days between April-September 2002 (see Annex II). In order to link air pollution episodes to temperature inversions, radiosonde data are used. These were provided by the South African Weather Service following a specific formal request (Linnow, 2008). The data are from Cape Town International Airport (World Meteorological Organisation Index number 68816) which is located at 33°58'S 18°36'E and 46 m above sea level. The vertical profile of the atmosphere at this location is registered twice daily, at approximately midday and midnight. As has already been discussed, the wintertime temperature inversions that occur during the night persist into the morning hours and therefore the midnight soundings are considered to be more representative of the conditions that occur in morning hours (when brown haze is most observed) compared to the midday soundings and these will be used in the analysis that follows.

The vertical temperature profile in the boundary layer, which is taken to be between 0 and ~1500 m, for each of the 49 episode days is given in Figures 4-1 to 4-3 separately for each winter month. Temperature inversions in the lower boundary layer (approx. below 200 m) become progressively stronger as one moves towards the coldest winter months (radiative inversions). Temperature inversions are observed to occur on almost all 49 days, with the exception of 10/9. Also, very weak inversions are observed on 26/4 and 10/7.

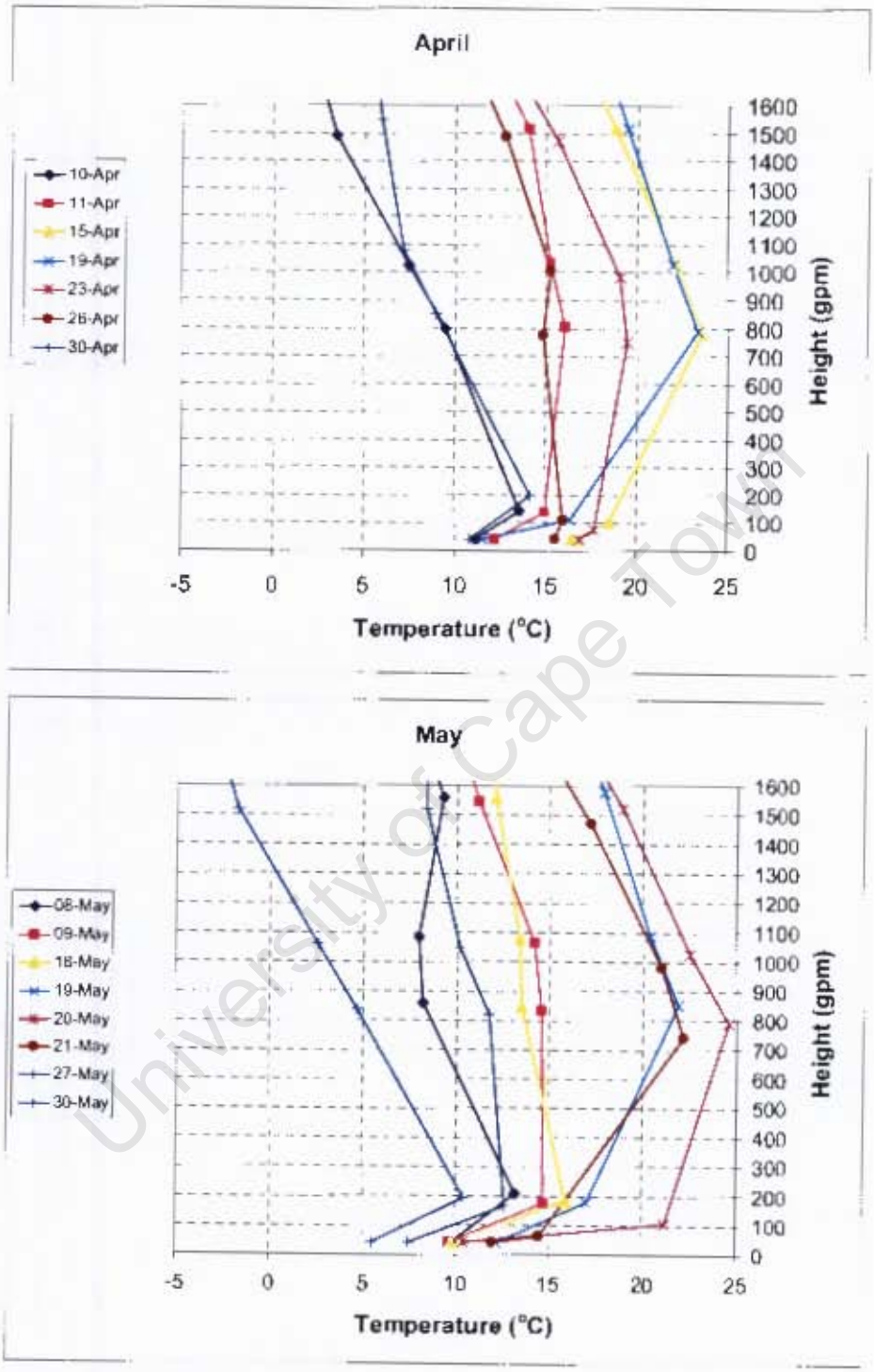

Figure 4-1: Vertical temperature profiles from radiosonde data for the air pollution episodes in April (top) and May (bottom).

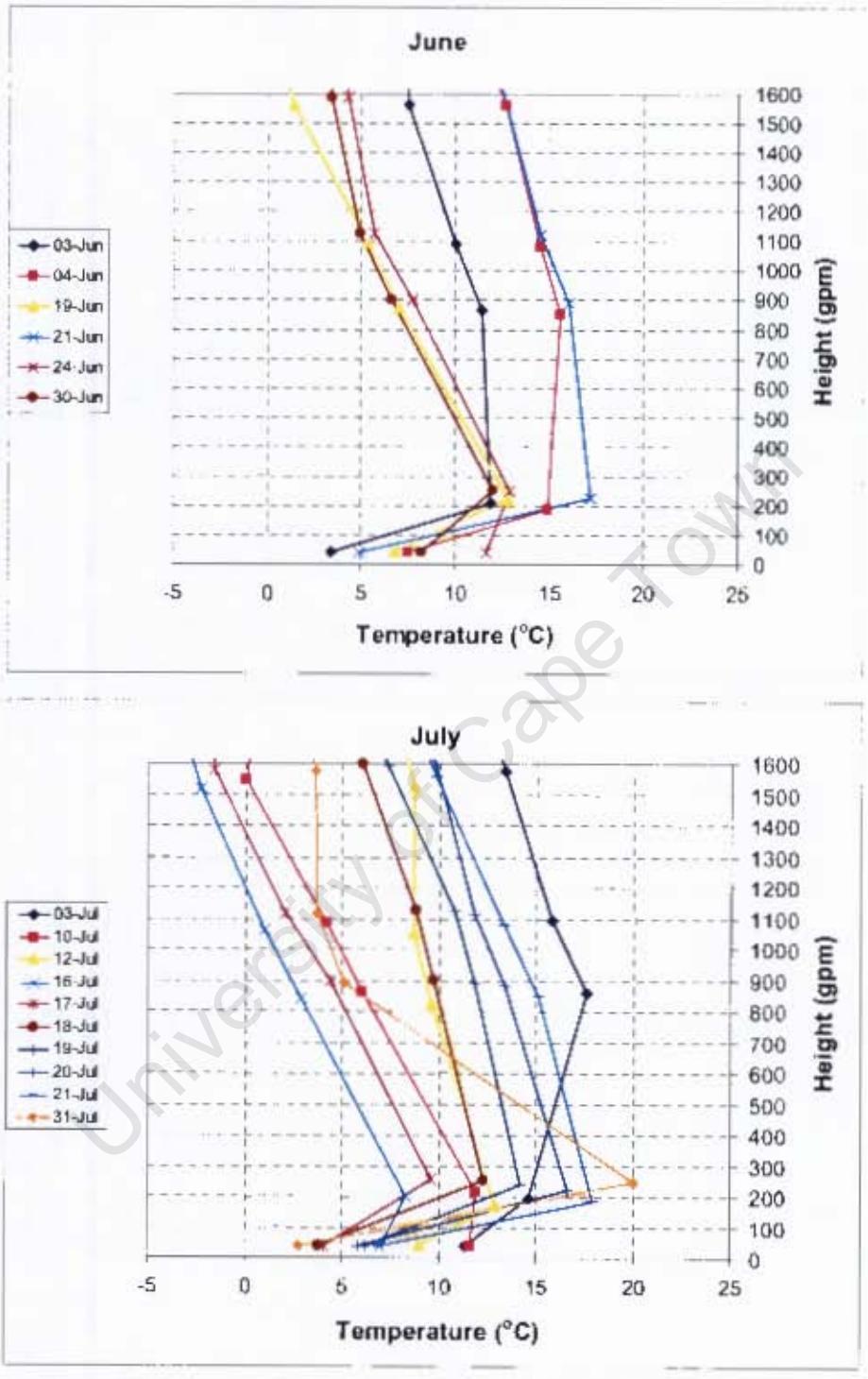

Figure 4-2: Vertical temperature profiles from radiosonde data for the air pollution episodes in June (top) and July (bottom).

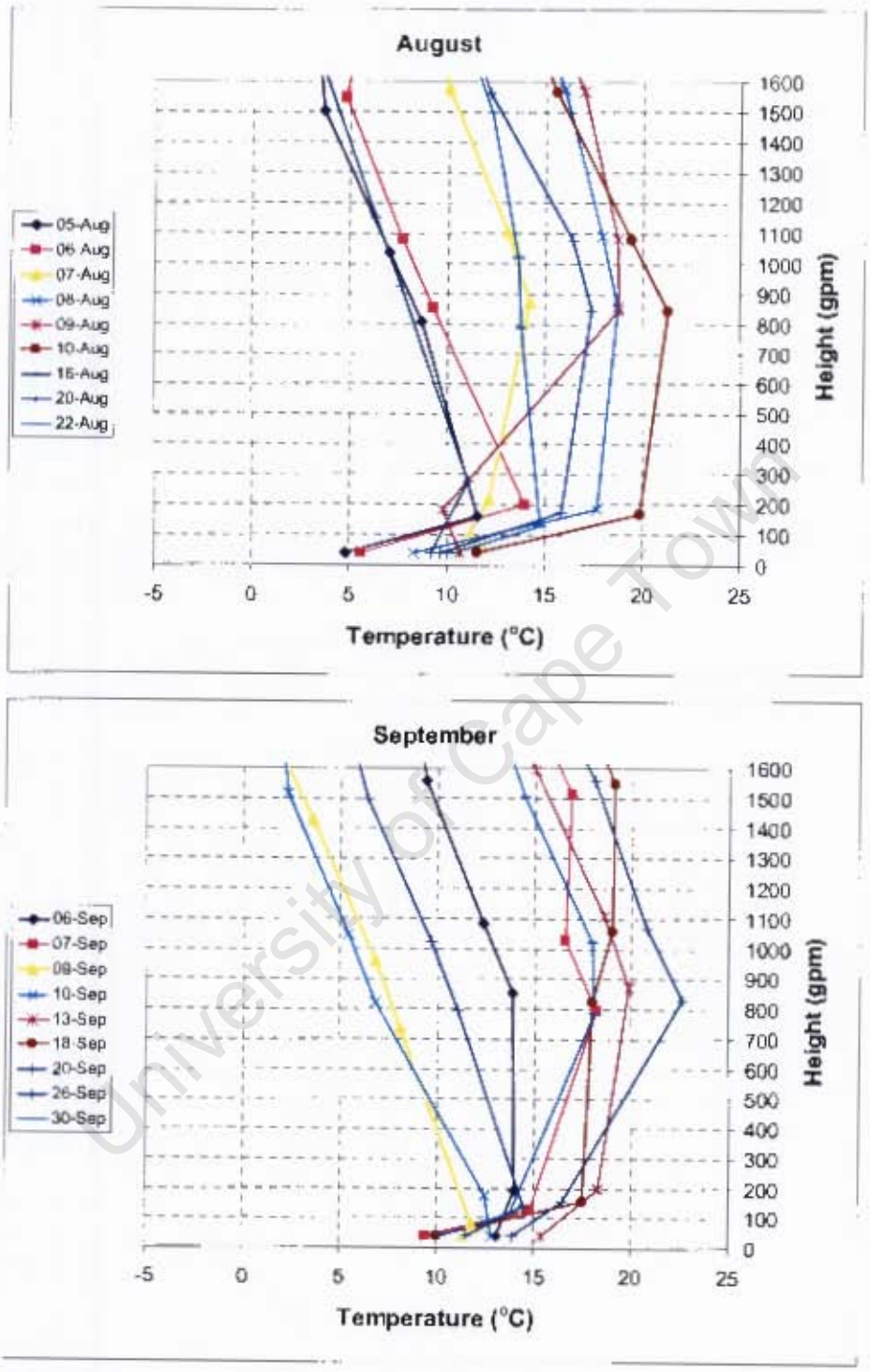

Figure 4-3: Vertical temperature profiles from radiosonde data for the air pollution episodes in August (top) and September (bottom).

4.2 SOMs applied for the analysis of current climate

In this study two variables are selected to apply the SOM technique, (i) Sea Level Pressure (SLP) which is expected to capture the anticyclonic circulation influence on temperature inversions and (ii) humidity at 850 hPa which is expected to reflect the drier conditions associated with the influence of berg winds (see analysis of Figure 1-2).

The software package SOM_PAK version 3.2 (Kohonen et al, 1996) was used to create the SOMs used in this study. The procedure involves firstly a random distribution of nodes, where each node is defined by a reference vector of weighting coefficients and each coefficient is associated with each variable. As the input data are presented to the SOM, the similarity of each data record and each of the node reference vectors is calculated (Hewitson & Crane, 2002). The second round of iterations uses a smaller update radius (number of neighbouring nodes adjusted) and its purpose is to fine tune the values of the reference vectors. The user defines the update radius (radius parameter), the number of iterations (running length parameter) and the degree of similarity between the reference vector and the input vector (learning rate). The latter two should increase and decrease respectively in the second round of iterations. The topology of the map and the neighbourhood function type are also user defined (for details see Kohonen et al, 1996).

The user also defines the size of the SOM at the start of the process, by defining the number of nodes in the x and y direction (e.g. a 4 x 3 SOM matrix has 12 nodes). The definition of the SOM size is mostly arbitrary, but a balance should be sought since the use of too few nodes will not allow for sufficient generalisation and too many will make the analysis overly complex (Crane & Hewitson, 2003). As the number of nodes increases with the use of a larger size SOM array (matrix), the number of input data mapping to each node will decrease and if this results in very few data mapping to each node, this can lead to difficulties in the interpretation. In this study two different size SOMs were tested, 4 x 5 and 4 x 3 and the 4 x 3 SOM was found to be optimal.

4.2.1 NCEP reanalysis data

For the characterisation of present-day/recent climatology in the region of study, climatological data are required for a specific baseline period. In this study the NCEP-DOE Reanalysis 2 data set (NOAA, 2008) for a 29 year winter period (April-September 1979-

2007) is used. The study domain extends from lat 40° to 24°S and lon 10° to 26°E and includes the western part of South Africa and the south part of Namibia, as shown in Figure 4-4.

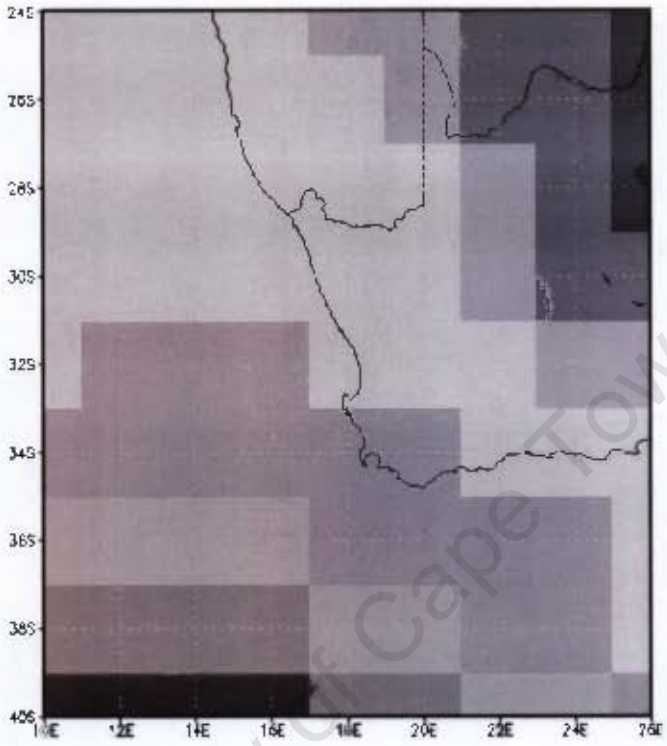

Figure 4-4: The NCEP re-gridded study domain used to analyse the synoptic conditions affecting meteorology in the GCTA.

The NCEP-DOE Reanalysis 2 data set has a spatial resolution of 2.5° x 2.5°. As the results will need to be compared against GCM data, both NCEP and GCM were re-gridded to a common compromise grid of 2.0° x 2.0° using the Bessel interpolation method. It should be recalled that the original spatial resolution of all three GCMs was approximately 1.9° x 1.9°. The NCEP-DOE Reanalysis 2 data are available for four hours a day at 0000, 0600, 1200 and 1800. However, the GCM results are only available as daily averages therefore the daily average of the NCEP-DOE Reanalysis 2 data was used to train the SOM. The re-gridded domain size is 9 x 9 grids and can be seen in Figure 4-4. The data for the two variables chosen (SLP and relative humidity at 850 hPa) were normalised (standardised by subtracting the mean and dividing by the standard deviation) and concatenated into the file format required by the software package. Using standardised data assists in the analysis of the results as the systematic bias is removed, thus enabling the comparison against other data sets (here against the model results) since the data is expressed as a difference from its mean value.

For the creation of the SOM maps, a number of runs with different parameter settings were performed. In the final runs presented in this study random initialisation training was used with a rectangular lattice topology type and a bubble neighbourhood function type. The running length was set initially at 30 000, with a learning rate (alpha) of 0.1 and a radius of 3 and then increased to 50 000, with an alpha of 0.01 and a radius of 1. The size of the SOM was 4 x 3 and therefore consisted of 12 nodes. The results can be found in section 5.1.

4.2.1.1 Comparison between NCEP reanalysis and radiosonde data

In order to test how well the NCEP-DOE Reanalysis 2 data reflect the vertical profile of the atmosphere in the study domain, a comparison between the vertical temperature profiles from the radiosonde data for the 49 air pollution episode days and the NCEP data was performed. There are certain restrictions in performing this comparison. Firstly, the NCEP data set has a spatial resolution of 2.5° x 2.5° and the grid cells where the GCTA is located can be seen in Figure 4-5. A problem that is immediately apparent is that the GCTA is not located in the centre of a grid cell, but rather it is located very close to a grid point. Also the cell in which the GCTA is located contains mostly sea and very little land surface and therefore the NCEP data for this cell are likely to represent the conditions above the ocean better than those over the land surface.

The four cells closest to the GCTA are located at (approximate centre of the grid cells): lat 33°S lon 17.5°E (cell_1), lat 33°S lon 20°E (cell_2), lat 35°S lon 17.5°E (cell_3), lat 35°S lon 20°E (cell_4). The radiosonde data obtained from Cape Town International Airport (located at 33°58'S 18°36'E) were compared against the NCEP data for cell_1 and cell_3. The NCEP data has 10 levels in the lower boundary layer and the vertical temperature profiles are available for the following distances from the surface (m): 200, 250, 300, 400, 500, 600, 700, 850, 925, 1000. Only the first two levels were used for the comparison. The NCEP-DOE Reanalysis 2 data are available 4 times a day (0000, 0600, 1200 and 1800) and the midnight (0000) hour was used and compared against the midnight radiosonde data that were used in other parts of this study (see section 4.1).

As the vertical resolution of the NCEP data is coarse compared to that of the radiosonde data, NCEP data were searched for either temperature inversions or very stable atmospheric

conditions (temperature differences near to constant). The results showed that for grid cell_1 37 days and for grid cell_3 35 days, out of the total 49 episode days, showed temperature inversions or very stable atmospheric conditions. Out of the episode days not found to have a temperature inversion or very stable atmospheric conditions, the three days are those also noted in section 4.1 (10/9, 26/4 and 10/7) for which either a temperature inversion was not observed in the radiosonde data, or a very weak inversion was observed. Overall, the vertical profiles extracted from the NCEP data are found to compare well against the radiosonde data.

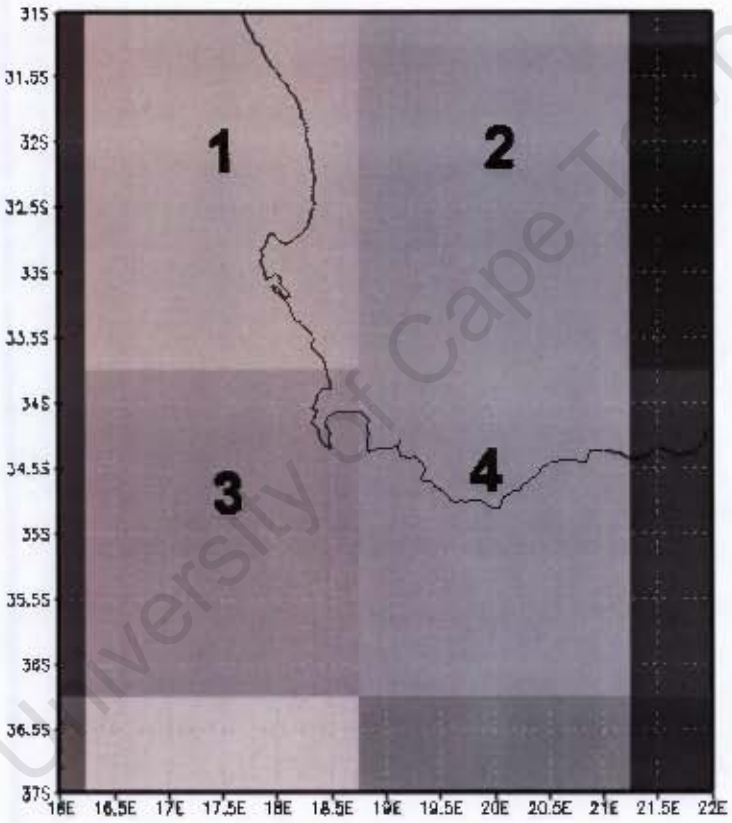

Figure 4-5: The NCEP-DOE Reanalysis 2 grid cell location (prior to the re-gridding) for the area close to the GCTA (spatial resolution 2.5° x 2.5°). Each of the four cells of interest has been numbered for ease-of-use in the analysis.

4.2.2 GCM data

Prior to using GCM results to study the changes likely to occur in the climatology of a region in the future, it is necessary to compare the GCM results for a control period against those obtained using an observational data set. The GCM results used in this study were obtained

from the World Climate Research Programme (WCRP) Coupled Model Intercomparison Project Phase 3 (CMIP3) multi-model database (CMIP, 2009).

For the assessment of the performance of the three GCMs used in this study, a 40 year control (reference) period was chosen (April-September 1961-2000), which was compared against the current climatology projected through the NCEP-DOE Reanalysis 2 data set described in section 4.2.1. The GCM data was available as daily averages at a spatial resolution of approximately 1.9° x 1.9° and was re-gridded to 2.0° x 2.0° using the Bessel interpolation method. The data for the two variables chosen (SLP and relative humidity at 850 hPa) were normalised (standardised by subtracting the mean and dividing by the standard deviation) and concatenated into the file format required by the SOM software package and were then introduced to the SOM trained using the NCEP-DOE Reanalysis 2 data set. The results can be found in section 5.2. Using standardised data assist in the analysis of the results as has already been mention in section 4.2.1.

4.2.3 Means and standard deviations for NCEP and GCM data

The means and standard deviations for each of the three GCMs and the NCEP-DOE Reanalysis 2 data set, which were used to standardise the data and prepare the input data sets to run the SOM, are shown in Table 4-1.

Table 4-1: Mean and standard deviation for the two variables (SLP and relative humidity at 850 hPa) for each of the three GCMs (ECHAM5, CNRM-CM3 and CSIRO0MK3.5) and the NCEP-DOE Reanalysis 2 data set.

Data set	Variable		Control	Future	Difference between model and NCEP	% change between Control and Future
NCEP	SLP (Pa)	mean	101,690	-		
		stdev	552	-		
ECHAM5	SLP (Pa)	mean	101,814	101,825	0.1%	0.0%
		stdev	668	655	21.0%	
CNRM-CM3	SLP (Pa)	mean	102,052	102,097	0.4%	0.0%
		stdev	539	536	-2.2%	
CSIRO-MK3.5	SLP (Pa)	mean	101,653	101,635	0.0%	0.0%
		stdev	651	657	18.0%	
NCEP	Relative Humidity (%)	mean	48.2	-		
		stdev	23.7	-		
ECHAM5	Relative Humidity (%)	mean	59.2	56.4	22.7%	-4.7%
		stdev	24.8	25.7	0.2%	
CNRM-CM3	Relative Humidity (%)	mean	56.0	55.3	16.1%	-1.2%
		stdev	24.7	24.5	0.2%	
CSIRO-MK3.5	Relative Humidity (%)	mean	52.1	50.2	8.1%	-3.7%
		stdev	22.9	23.3	-0.1%	

From the statistics presented in Table 4-1 it is important to note the differences between model and the NCEP-DOE Reanalysis 2 data set for the control simulation, as well as the differences between GCM control and future simulations. For SLP, CNRM-CM3 slightly overestimates (by 0.4 %) the NCEP baseline value but has a standard deviation close to that of NCEP, whereas both ECHAM5 and CSIRO-MK3.5 simulate mean values close to that of NCEP, but with a relatively higher standard deviation. All models simulate very similar SLP in the future compare to the GCM control period.

For relative humidity the results are rather different. In the control simulation ECHAM5 and CNRM-CM3 models overestimate the average value for the study domain (by 22.7 % and 16.1 % respectively) compared to NCEP but have a similar standard deviation. The CSIRO-MK3.5 model also overestimates the relative humidity compared to NCEP but less than the other two models (8.1 %) and also has a similar standard deviation to NCEP. All models project a reduction in the relative humidity in the future compared to the model control period, with models ECHAM5 and CSIRO-MK3 projecting an average reduction of 4.7 % and 3.7 % respectively and CNRM-CM3 only projecting a reduction of 1.2 %.

5. Results

5.1 SOM training using NCEP data

A 4 x 3 sized SOM was selected which lead to 12 nodes, i.e. the categorisation of the input data into 12 synoptic classes. Each synoptic class was determined using two variables, SLP and relative humidity at 850 hPa and the results are shown in Figure 5-1. The use of SLP allows for the surface flow to be visualised, whereas the relative humidity at 850 hPa allows for a characterisation of the properties of the upper air mass.

The Sammon map corresponding to the SOM results presented in Figure 5-1 is shown in Figure 5-2. In reality the nodes are not equally spaced out in the SOM space as shown in Figure 5-1 and the Sammon map is a two dimensional approximation of the Euclidean distance between the nodes (e.g. Hewitson & Crane, 2002). The nodes are found to be very well spaced out i.e. correspond to relatively distinct synoptic classes, and although the Sammon map is tilted to the left it is still apparent that the nodes in the top and bottom left

corner are more similar than the ones in the top and bottom right side of the SOM. This point also becomes clear from the analysis that follows.

The synoptic states in the top right side of the SOM are associated with strong anticyclonic influence over the south western part of South Africa, as a stronger than average SLP associated with the South Atlantic High Pressure (SAHP) system is clearly seen in the west/south-western part of the domain. The relative humidity at 850 hPa for these synoptic states appears to be close to, perhaps even slightly lower than, the average observed for the winter period.

Moving down towards the bottom right side of the SOM, the synoptic conditions are related to a west coast trough. This is also associated with berg winds which bring dry continental air towards the south-western part of the country and the relative humidity at 850 hPa for these synoptic states is clearly lower than the winter period average.

In the top left and bottom left side of the SOM, a cold front is present in the south, south-east or south-west of the continent, causing a lower than average SLP and a higher than average relative humidity in the area of interest (south-western part of the country).

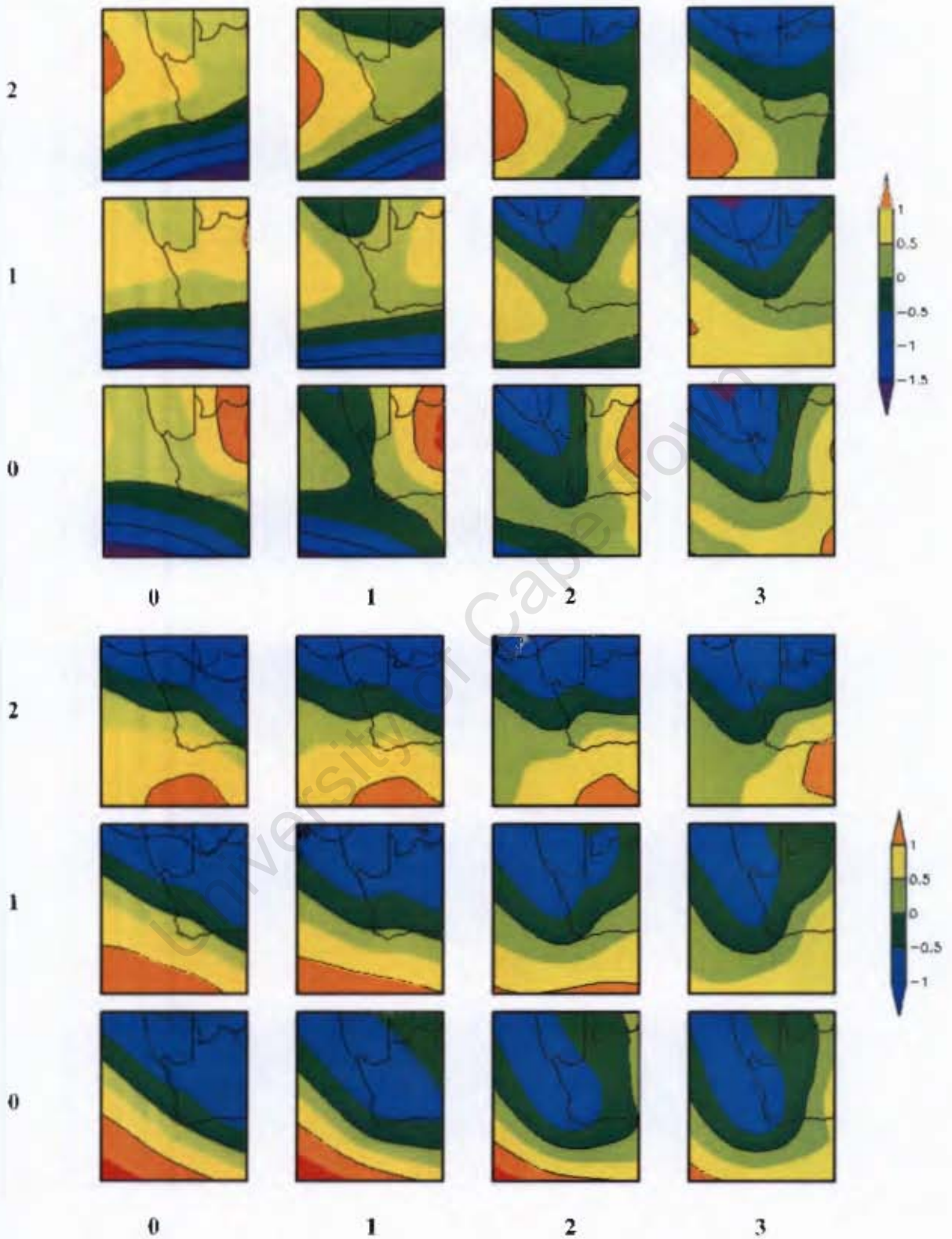

Figure 5-1: A SOM of standardised SLP (top) and relative humidity (bottom) based on NCEP-DOE Reanalysis 2 data for a 29 year winter period (April-September 1979-2007), blue corresponds to lower than average values and red to higher than average.

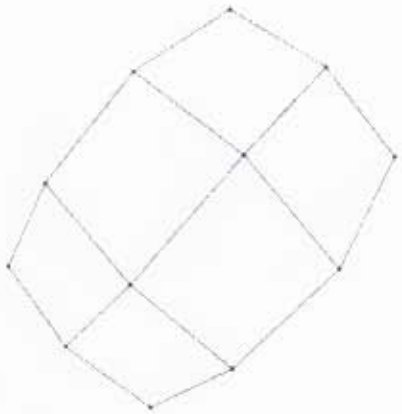

Figure 5-2: Sammon map corresponding to the 4 x 3 SOM of Figure 5-1, where a very good spacing of the nodes in SOM space is noted.

The frequency of days in the NCEP-DOE Reanalysis 2 data that map to each node is shown in Figure 5-3. The distribution of days is fairly uniform, with the frequency for most nodes varying between 7.5 – 10.0 %, though a lower frequency is noted for the central nodes (6.1 and 5 %). The average error associated with each node is shown in Figure 5-4.

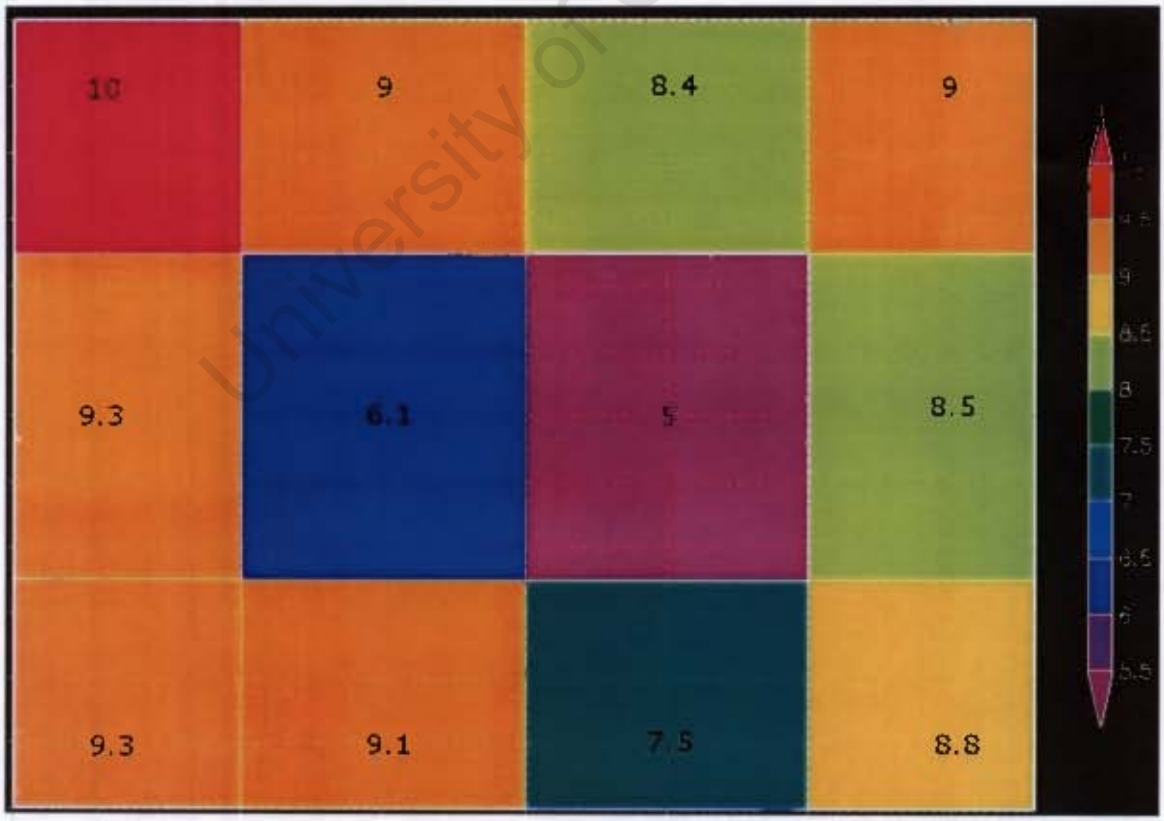

Figure 5-3: The NCEP-DOE Reanalysis 2 frequency of days (% of days) that map to each node in the SOM for the complete set of input data (April-September 1979-2007).

10.0	9.0	8.4	9.0
9.3	6.1	5.0	8.5
9.3	9.1	7.5	8.8

12.6	7.7	6.0	11.5
8.7	6.0	2.2	10.4
8.2	8.7	9.3	8.7

0.0	4.1	6.1	16.3
2.0	6.1	0.0	16.3
0.0	8.2	20.4	20.4

Figure 5-4: Comparison between the NCEP-DOE Reanalysis 2 frequency of days (% of days) that map to each node in the SOM for the whole reference period (1979-2007) on the left, for 2002 in the middle and for the air pollution episode days in 2002 on the right.

6.1	7.2	8.0	8.1
5.6	7.3	8.6	8.5
6.0	7.4	8.6	8.8

6.7	8.3	9.3	8.5
6.0	7.7	10.0	8.6
6.9	9.0	8.7	8.9

	9.0	10.3	9.0
6.5	9.3		8.6
	7.9	8.2	9.0

Figure 5-5: The average error with which the complete set of NCEP input data (April-September 1979-2007) maps to each node on the left, the error for 2002 in the middle and for the air pollution episode days in 2002 on the right.

In Figure 5-4, the frequency of days mapping to each node for the entire baseline period (April-September 1979-2002) from Figure 5-3 is compared against the frequency for April-September 2002 and also against the frequency with which the 49 air pollution episode days map to each node. The results are found to be largely comparable. The NCEP frequency distribution in 2002 is found to have a slightly larger range (8 – 13 %) compared to that of the whole data set, but still comparable thus verifying that the year 2002 climatology does not differ significantly from the average climatology. A low frequency for nodes (2,1) and (1,1) is also noted in 2002, in line with baseline period results where the frequency for these nodes was also found to be low, though for node (2,1) this is found to be lower than in the NCEP results using the whole data set (2 % compared to 5 %).

The average error values for each node shown in Figure 5-5 give an indication of how well the synoptic states reflected by the SOM match the actual data. Each input data (each day of data) is associated with an error value, from which an average error value per node is

determined. The error values are a measure of the average Euclidean distance each data entry has from the node reference vectors. The range of error for the NCEP data for the complete baseline period is 5.6 – 8.8. This range is relatively high, indicating that a detailed analysis using other size SOMs could take place and another size may be found to have a smaller error range. For the 2002 data the range of error is found slightly larger (6.0 – 10.0), which is to be expected since not all the synoptic states over the period 1979-2007 are expected to be observed in one year. However, this error is still comparable to that for the whole baseline period, verifying that overall the synoptic states in the year 2002 are reflected in the SOM. The range of error for the 49 episode days is found to be similar to that for the whole of 2002 (6.5 – 10.3).

The frequency with which the air pollution episode (and hence temperature inversion) days map to each node reveals a clear preference towards the synoptic conditions associated with (a) the South Atlantic High Pressure (SAHP) system off the coast of the south western part of the country (represented by the states in the top right side of the SOM) due to the subsiding air mass linked to this higher pressure system and (b) the west coast trough associated with berg winds bringing dry continental air towards the south western part of the country (bottom right side of the SOM). From the data used in this study it appears that in 2002 more air pollution episode days are associated with west coast troughs than with the influence of the SAHP system, though for a generalisation of this finding a larger data set would be needed. A very low frequency is associated with the synoptic states representing the cold fronts, as the winds and precipitation associated with them break down any chance of temperature inversion and hence the probability of having an air pollution episode is greatly reduced.

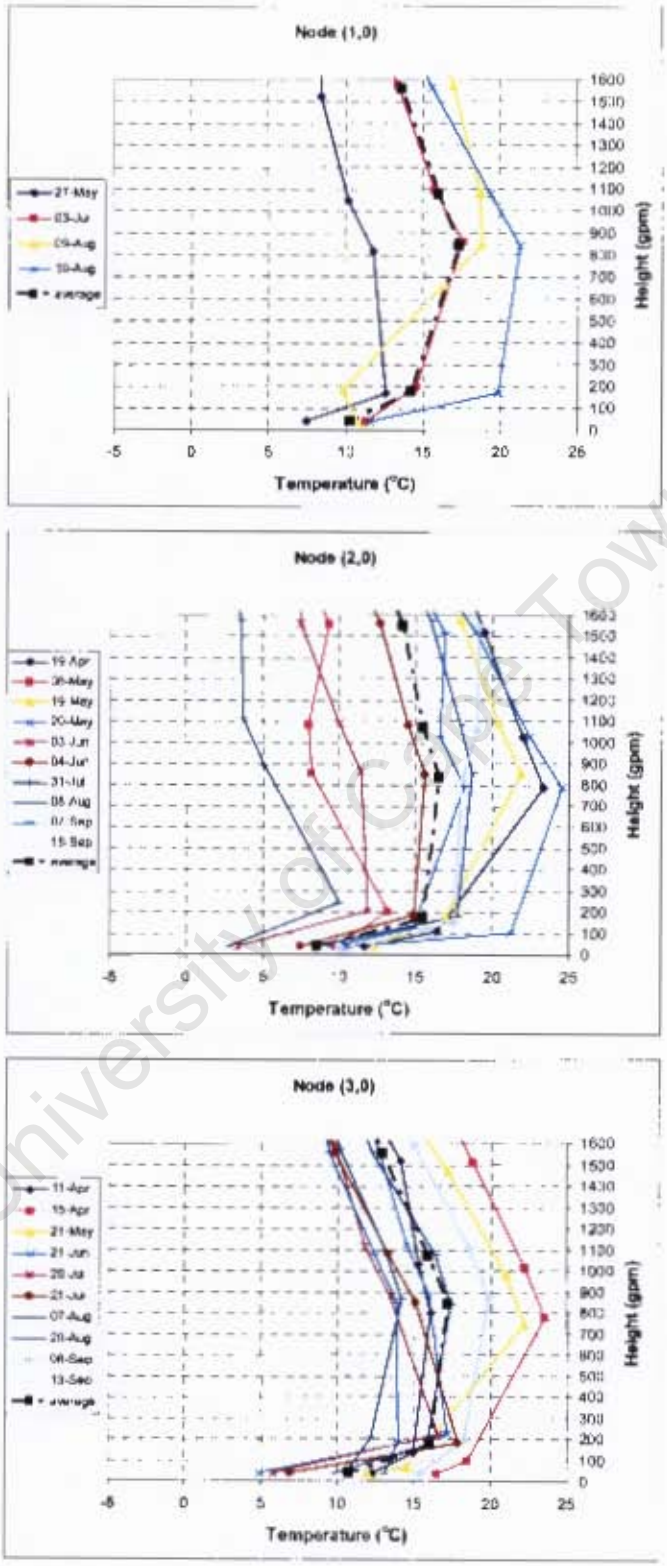

Figure 5-6: Vertical temperature profiles from radiosonde data for the air pollution episodes days that map to nodes (1,0) (top), (2,0) (middle) and (3,0) (bottom). The node co-ordinates correspond to the numbering in Figure 5-1.

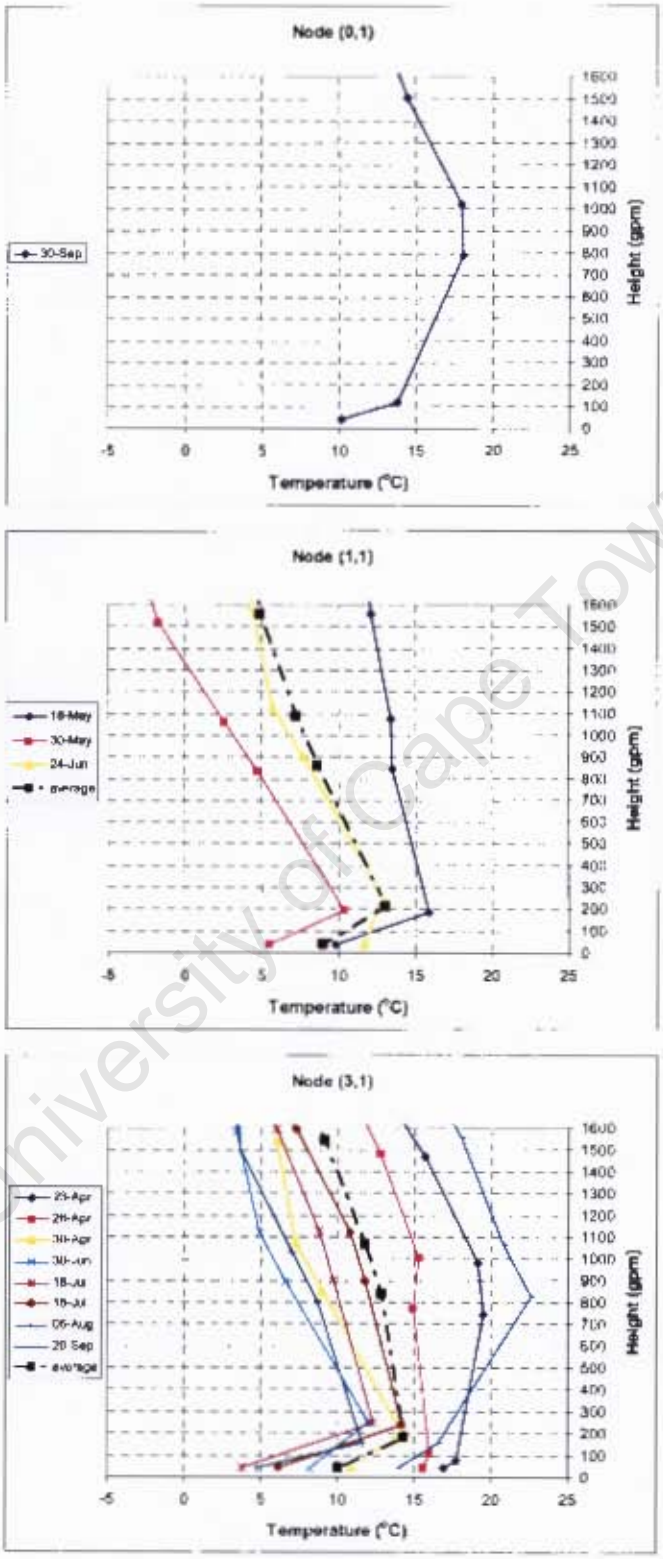

Figure 5-7: Vertical temperature profiles from radiosonde data for the air pollution episodes days that map to nodes (0,1) (top), (1,1) (middle) and (3,1) (bottom). The node co-ordinates correspond to the numbering in Figure 5-1.

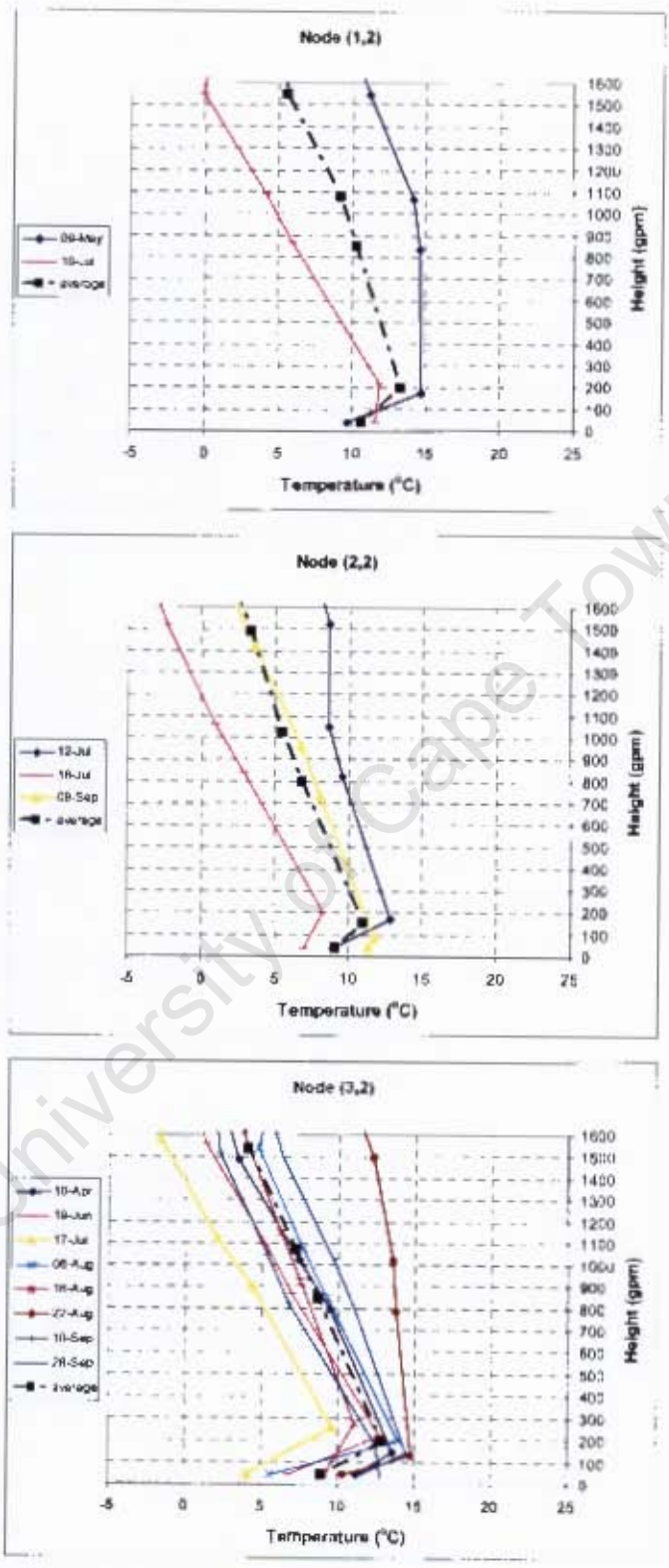

Figure 5-8: Vertical temperature profiles from radiosonde data for the air pollution episodes days that map to nodes (1,2) (top), (2,2) (middle) and (3,2) (bottom). The node co-ordinates correspond to the numbering in Figure 5-1.

In Figures 5-6, 5-7 and 5-8 the temperature inversion profiles of the days mapping to each node in the SOM are presented. As can also been seen from Figure 5-4, most episode days map to the nodes in the bottom right corner (nodes 2,0 and 3,0) associated with a west coast trough and consequent dry berg winds. Interestingly, the average temperature inversion strength at heights below ~200 m associated with these synoptic states (Figure 5-6) is also the highest observed (6.9°C for node 2,0 and 5.3°C for node 3,0). The nodes with the next highest frequency of episode days are nodes (3,1) and (3,2) associated with the anticyclonic circulation off the south western South African coast. The average temperature inversion strength associated with these synoptic states is also high, but lower than for the previous two nodes and is found to be 4.3°C for (3,1) and 3.9°C for (3,2) as shown in Figure 5-7 and Figure 5-8 respectively. Table 5-1 summarises the average temperature inversion strength for the days mapping to each SOM node.

Table 5-1: Average temperature inversion strength (°C) for heights below ~200 m corresponding to each synoptic state of the SOM.

0	2.7	1.9	3.9
3.6	4.1	0	4.3
0	4.0	6.9	5.3

Overall, the strength of the temperature inversions associated with west coast troughs combined with the results of Figure 5-4 where more air pollution episode days are found to be associated with the west coast troughs, may imply that the west coast trough is a stronger driver for air pollution episodes compared to SAHP system. However, this finding still needs to be confirmed using a larger radiosonde and air pollution data set.

5.2 Current climatology using GCMs

The three GCMs were used to simulate the present climate (referred to as control or reference run) using data (daily averages) for the period April-September 1961-2000. The new input data were presented to the SOM, which mapped each sample in the new data set to a node in the two-dimensional node space. The results are presented in terms of the frequency of days mapping to each synoptic state (Figure 5-9 for ECHAM5, Figure 5-11 for CNRM-CM3 and

Figure 5-13 for CSIRO-MK3.5). In Figures 5-10, 5-12 and 5-14 the skill of each model in simulating the current climatology is compared against the results using the NCEP-DOE Reanalysis 2 data set. The error with which each model data set maps to the SOM can be found in Annex III.

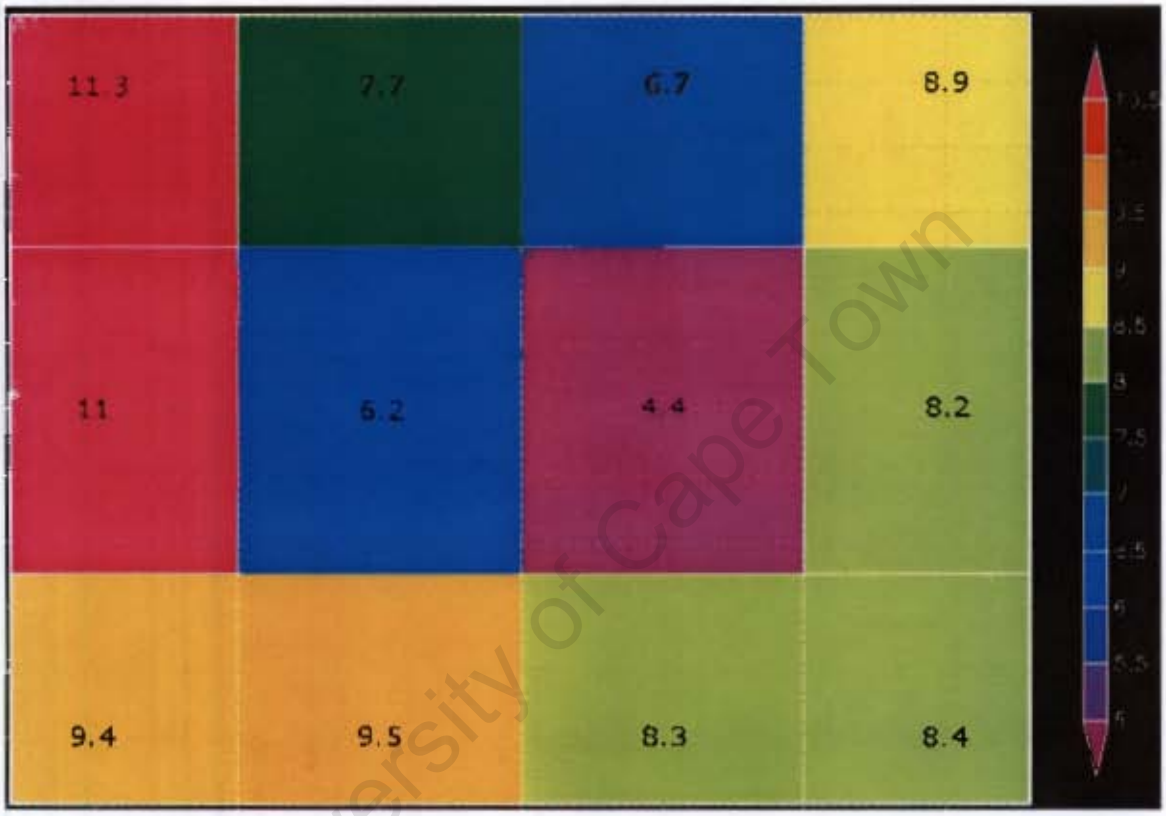

Figure 5-9: The ECHAM5 frequency of days (% of days) that map to each node in the SOM for the control period run (April-September 1961-2000).

11.3	7.7	6.7	8.9
11.0	6.2	4.4	8.2
9.4	9.5	8.3	8.4

10.0	9.0	8.4	9.0
9.3	6.1	5.0	8.5
9.3	9.1	7.5	8.8

Figure 5-10: Comparison between the ECHAM5 frequency of days (% of days) that map to each node in the SOM for the control period run (April-September 1961-2000) on the left and the NCEP-DOE Reanalysis 2 frequency for the baseline period (1979-2007) on the right.

The results of the ECHAM5 model compare well against the results using the NCEP data set. The distribution of days is found to be fairly uniform in the control period, with the frequency for most nodes varying between 7.7 – 11.3 % (compared to 7.5 – 10.0 % for NCEP). A lower frequency is noted for the two central nodes, 6.2 % and 4.4 %, similarly to the NCEP results where these nodes were found to have a frequency of 6.1 and 5.0 % respectively.

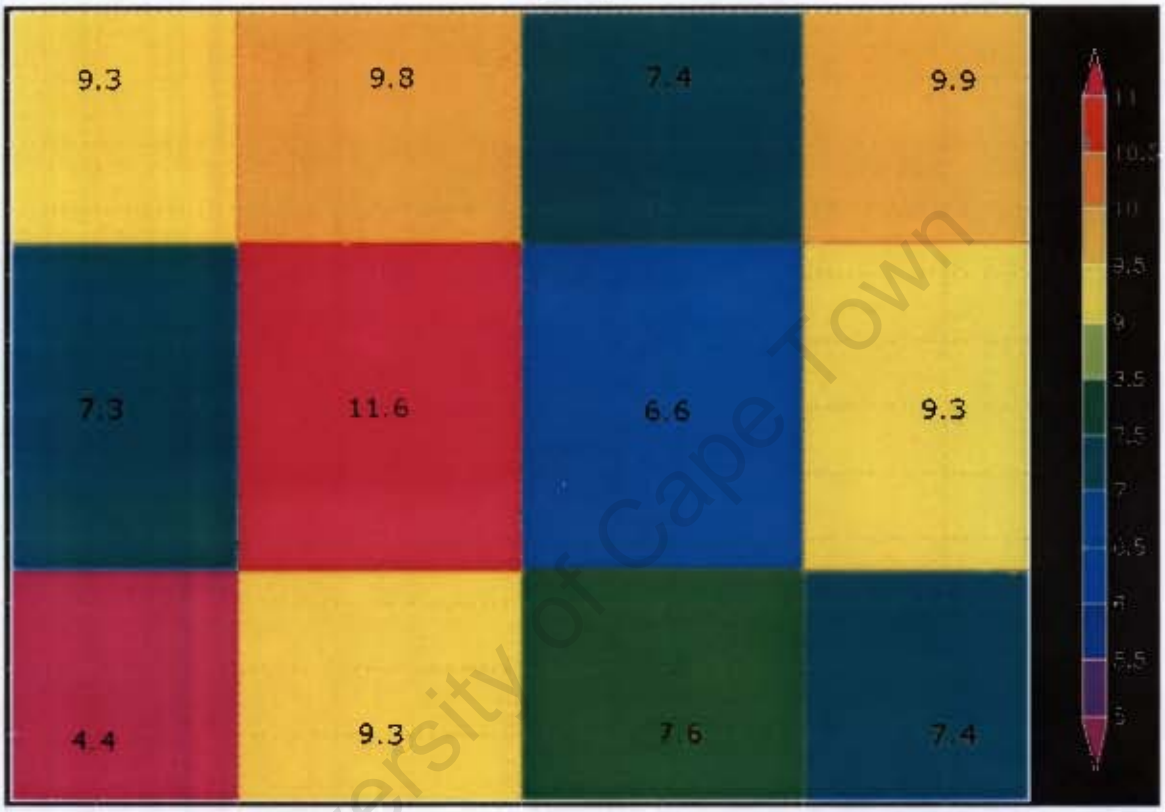

Figure 5-11: The CNRM-CM3 frequency of days (% of days) that map to each node in the SOM for the control period run (April-September 1961-2000).

9.3	9.8	7.4	9.9
7.3	11.6	6.6	9.3
4.4	9.3	7.6	7.4

10.0	9.0	8.4	9.0
9.3	6.1	5.0	8.5
9.3	9.1	7.5	8.8

Figure 5-12: Comparison between the CNRM-CM3 frequency of days (% of days) that map to each node in the SOM for the control period run (April-September 1961-2000) on the left and the NCEP-DOE Reanalysis 2 frequency for the baseline period (1979-2007) on the right.

The frequency with which the CNRM-CM3 model results map to the SOM nodes is slightly different to that of the NCEP baseline in the lower left side of the SOM and for the central nodes. The frequency for the node (1,1) is found to be 11.6 %, whereas for the NCEP data it is considerable lower at 6.1 %, indicating that the model may overestimate this particular state which is associated with cold fronts of a rather lower intensity located at a fair distance from the South African coast (see Figure 5-1). Similarly, in the lower left side of the SOM the frequency of node (0,0) is found to be 4.4 %, which is low compared to the 9.3 % found using the NCEP data set, indicating that the model may underestimate this particular synoptic state associated with a strong cold fronts from the south-east.

Figure 5-13: The CSIRO-MK3.5 frequency of days (% of days) that map to each node in the SOM for the control period run (April-September 1961-2000).

0.5	8.9	7.3	10.8
1.7	15.6	9.5	23.5
4.1	6.0	3.9	8.2

10.0	9.0	8.4	9.0
9.3	6.1	5.0	8.5
9.3	9.1	7.5	8.8

Figure 5-14: Comparison between the CSIRO-MK3.5 frequency of days (% of days) that map to each node in the SOM for the control period run (April-September 1961-2000) on the left and the NCEP-DOE Reanalysis 2 frequency for the baseline period (1979-2007) on the right.

The frequency with which the CSIRO-MK3.5 model results map to the SOM nodes is found to be similar to that of CNRM-CM3 for certain nodes, but generally quite different to the NCEP baseline results. Overall, the difference between areas of highest and lowest frequency is quite large (see Figure 5-13). A low frequency is found for the left column of the SOM (synoptic states associated with cold fronts) indicating that these may be under represented in the model results and, similarly to CNRM-CM3, a high frequency is found for node (1,1) which is also associated with cold fronts but perhaps of a slightly lower intensity and located at a greater distance from the South African coast (see Figure 5-1). The model results also show a preference for node (3,1) which is associated with the west coast trough and the dry berg winds leading to temperature inversions (frequency of 23.5 % compared to 8.5 % for NCEP).

Overall, the ECHAM5 model frequency for the control climate period is found to be the closest to that obtained using the NCEP data set for this particular study, i.e. for the specific study domain and the synoptic states reflected by the 4 x 3 SOM using the variables SLP and relative humidity at 850 hPa. The CNRM-CM3 model also shows results close to those using the NCEP data, though the frequency for two nodes is found to be slightly different. However, the synoptic states reflected by these two nodes are associated with cold fronts and especially for node (0,0), for which the frequency is found to be lower than in NCEP, there are no episode days that map to this synoptic state. Also for node (1,1) for which an overestimation is observed, very few episode days map to this state (see Figure 5-4). Therefore, although differences between the model's control period and that of NCEP are observed, these differences are mainly concentrated in synoptic states that are not primarily

linked with the study's main focus (synoptic states in the top right and bottom right part of the SOM) and the results of CNRM-CM3 can be considered to provide a reasonable approximation of the current climate.

Out of the three model used, the CSIRO-MK3.5 GCM is the one that reveals results most different to those using the NCEP data set. Amongst other, the differences also lie in the synoptic states associated with the occurrence of air pollution episodes (e.g. nodes 3,1 and 2,0), thus making it harder to distinguish between model bias and the changes that will be associated with these states in the future (analysed in chapter 5.3).

5.3 Future predictions

All three models were used to study the future climatology for the period 2046-2065 in the region of interest. In Table 5-2 the results are compared against those obtained for the control period.

Overall, the ECHAM5 model does not show large differences in the frequency with which the SOM derived synoptic states occur in the future, compared to the control period. The largest reduction in the frequency (1.4 %) is found in the top left side of the SOM, in the synoptic state associated with strong cold front influence located in the south-eastern part of the domain. The largest increase in the frequency (1.7 %), a change that is also related to the nodes associated with air pollution episodes, is observed in the top right side of the SOM (node 3,2) where there is an increase in the synoptic states associated with strong anticyclonic influence over the south western part of South Africa. As the control simulation revealed results very close to those observed using the NCEP data set, this change indicates that according to the ECHAM5 model these states will occur slightly more often in the future during the period April-September. A similar increase in frequency, though not as large (0.7 %), is observed for node (2,2) which is also associated with anticyclonic influence over the south western part of South Africa.

Table 5-2: The frequency with which each data set (NCEP, ECHAM5, CNRM-CM3 and CSIRO-MK3.5) maps to each SOM node for the control (April-September 1961-2000) and future (April-September 2046-2065) periods.

	Control				Future			
NCEP	10.0	9.0	8.4	9.0				
	9.3	6.1	5.0	8.5				
	9.3	9.1	7.5	8.8				
ECHAM5	11.3	7.7	6.7	8.9	9.9	7.5	7.4	10.6
	11.0	6.2	4.4	8.2	10.9	6.5	4.5	8.2
	9.4	9.5	8.3	8.4	9.7	8.7	8.2	7.9
CNRM-CM3	9.3	9.8	7.4	9.9	7.0	9.0	7.0	10.7
	7.3	11.6	6.6	9.3	5.7	10.5	6.0	12.2
	4.4	9.3	7.6	7.4	4.6	9.2	8.3	9.8
CSIRO-MK3.5	0.5	8.9	7.3	10.8	10.6	10.2	7.6	9.7
	1.7	15.6	9.5	23.5	7.6	12.0	5.8	8.6
	4.1	6.0	3.9	8.2	4.6	8.9	7.4	7.0

Similarly to ECHAM5, the CNRM-CM3 model also does not show large differences in the frequency with which the SOM derived synoptic states occur in the future, compared to the control period. The largest increase in the future frequency is observed for nodes (3,1) and (3,0) (2.9 % and 2.4 % respectively) located in the right and bottom right side of the SOM.

Both these synoptic states reflect the influence of a west coast trough and consequent berg winds bringing dry continental air towards the south western part of the country and have been strongly associated with the occurrence of air pollution episodes. An increase, though smaller (0.7 %), is observed for node (2,0) which is also associated with this type of synoptic states. A small increase of 0.8 % in the future frequency is also observed for node (3,2), a synoptic state associated with strong anticyclonic influence over the south-western part of the continent, also linked to the occurrence of air pollution episodes. A reduction in the frequency of most of the synoptic states associated with cold fronts is observed (left side of the SOM).

The CSIRO-MK3.5 model frequency shows much larger changes between the control and future periods, compared to the other two models. The differences between the control CSIRO-MK3.5 results and the NCEP baseline results have already been noted in section 5.2. When comparing the control and the future CSIRO-MK3.5 frequency it is noticed that for most states the future frequency resembles closely the NCEP baseline frequency, indicating that the future conditions occupy the SOM space better than the control. An exception is node (1,1) for which a higher frequency is observed in both the control and the future periods compared to the NCEP results. As already discussed in section 5.2, this node is associated with cold fronts of a slightly lower intensity and located at a greater distance from the South African coast see Figure 5-1). The reasons behind the differences observed between the control CSIRO-MK3.5 results and the NCEP baseline results and why the future period closely resembles the NCEP baseline are not clear. Given the large model bias in the simulating current climate in the domain of study, it is difficult to distinguish between model bias and future climate trends and this point needs to be studied further.

6. Conclusions

This study examined the link between air pollution episodes in the GCTA, the occurrence of temperature inversions, the larger scale processes influencing the generation of temperature inversions and the implication of future climate change on air pollution episodes.

The relationship between air pollution episodes and the occurrence of temperature inversions was confirmed and the strongest temperature inversions in the lower boundary layer (less than 200 m) for 2002 were found to occur in July, with average strength of 7°C. The air

pollutant concentrations were found to be closely linked to traffic emissions, with the highest concentrations occurring in the morning hours, when temperature inversions are also most likely to be observed. These findings confirmed that the deteriorating air quality in the GCTA is a combination of high emission rates and meteorological conditions inhibiting adequate pollutant dispersion during particular peak hour emissions.

The observed circulation projected through NCEP data was successfully related to temperature inversions and air pollution episodes using the Self-Organising Maps (SOMs) technique and the synoptic states most associated with temperature inversions are found to be the anticyclonic conditions caused by the South Atlantic High Pressure (SAHP) system and the west coast trough associated with berg winds bringing dry continental air towards the GCTA. These results confirmed the findings of previous studies which used other methods of classifying the synoptic states and relating them to temperature inversions. The data used in this study also showed that in 2002 more air pollution episode days were associated with west coast troughs than with the SAHP system. Moreover, the average strength of the temperature inversions associated with west coast troughs was found to be approximately 50 % higher than that associated with the SAHP system. These findings are important and may imply that the west coast trough is a relatively stronger driver of air pollution episodes compared to the SAHP system, though the use of a larger radiosonde and air pollution data set would confirm these findings.

Following the successful application of SOMs for the baseline climatology, the impact of climate change, as projected through three different GCMs, was studied using the synoptic states defined by the SOM technique. The IPCC SRES A2 climate change scenario and its impacts in 2046-2065 were chosen for this application.

The results showed that for the period April-September, the ECHAM5 model predicts a small increase (of the order of 2 %) in the synoptic state reflecting a strong anticyclonic influence over the south western part of South Africa, which is associated with temperature inversions over the GCTA and a small decrease (around 1.5 %) in the synoptic state associated with strong cold front influence over GCTA, which are not related to temperature inversions and air pollution episodes. For the same period, the CNRM-CM3 model also shows an increase in synoptic states associated with temperature inversions (around 5 % in total), but this is observed in the states corresponding to a west coast trough and the consequent dry berg

winds affecting temperature inversions over the GCTA. A smaller increase (around 0.8 %) is also observed for the synoptic state associated with strong anticyclonic influence, similarly to the results of ECHAM5. CNRM-CM3 also shows a decrease in almost all the synoptic states associated with cold fronts. The results of the third model, CSIRO-MK3.5, were not found to adequately reflect the current climatology in the domain, making it difficult to distinguish between model bias and future climate trends.

Although the increase in the synoptic conditions associated with temperature inversions is projected to be small, it is observed in the results of both ECHAM5 and CNRM-CM3 models. Given the industrial activity in the area, the increase in the number of vehicles circulating in the GCTA and the effects of urban sprawl, such an increase and its link with an increased pollution potential can be significant. Nevertheless, the restrictions in model results should be carefully considered and the application of more GCMs would increase the reliability of these findings.

6.1 Suggestions for future research

The findings of this study can be considered the starting point of a more detailed study for the GCTA, which would mainly focus on climate change and its impacts on the region of interest. Some important points to consider are the following:

- The air pollution and radiosonde data sets should be extended to include a larger number of years and as many stations as possible, as this would considerably strengthen the statistical reliability of the results, confirming the synoptic states that were linked to air pollution episodes in this study.
- Different size SOMs should be considered as it is likely that some synoptic states may not be adequately reflected is the SOM used in this study.
- For the SOM analysis, a smaller domain size should also be studied and combined with the use of different variables. The use of lower atmospheric winds at the surface and a higher level (700 hPa or 850 hPa) and possibly 850 hPa geopotential heights may be found more capable of reflecting the synoptic conditions associated with temperature inversions.
- In the analysis of the SOM results, the error with which the input data match each node should be considered in more detail and compared against the NCEP input data error.

Finally, the use of a larger number of models to study a greater range of possible future changes in climate under a given scenario is particularly important, as no single model can be considered accurate in its predictive capabilities. It should however be noted that the performance of GCMs can depend critically on the size of the region (i.e. small regions are less likely to be well described than large regions) and a balance should be sought in this respect. The choice of variables also needs to be carefully considered as some variables are more difficult to model than others. As is also mentioned in IPCC-TGICA (2007), the reliability in model results should be studied in terms of the features of the climate that are of critical importance for the impact application, bearing in mind that the models representing most accurately the current climate may not necessarily be the models providing the most reliable predictions.

References

AIRBASE 2008. Internet: http://air-climate.eionet.europa.eu/databases/airbase/aggregation_statistics.html. December 2008.

Anderson, H R, Derwent, R G & Stedman, J 2001. Air Pollution and Climate Change. *The Health Effects of Climate Change in the UK.*

Barry, R G & Perry, A H 1973. *Synoptic Climatology: Methods and Applications*. London: Methuen.

Bell, M L & Davis, D L 2001. Reassessment of the Lethal London Fog of 1952: Novel Indicators of Acute and Chronic Consequences of Acute Exposure to Air Pollution. *Environmental Health Perspectives*, 109 (3): 389-394.

CapeTown 2008a. Internet: http://www.capetown.gov.za/en/CityHealth/AirQualityManagement/Pages/KhayelitshaAirPollutionStrategy.aspx. November 2008.

CapeTown 2008b. Internet: http://web1.capetown.gov.za/web1/NewCityAirpol/monitoringlist.asp. December 2008.

Cavazos, T 1999. Large-Scale Circulation Anomalies Conducive to Extreme Precipitation Events and Derivation of Daily Rainfall in Northeastern Mexico and Southeastern Texas. *Journal of Climate*, 12 (2): 1506-1523.

Cavazos, T 2000. Using Self-Organizing Maps to Investigate Extreme Climate Events: An Application to Wintertime Precipitation in the Balkans. *Journal of Climate*, 13 (10): 1718-1732.

City Health Department 2005. Air Quality Management Plan for the City of Cape Town. Report AQM 20050823 - 001, Cape Town.

City of Cape Town (2001) Air pollution control by-law. PN [number]/ 2001 of [date] 2001.

CMIP 2009. Internet: http://www-pcmdi.llnl.gov/ipcc/model_documentation/ipcc_model_documentation.php. January 2009.

Crane, R G & Hewitson, B C 2003. Clustering and upscaling of station precipitation records to regional patterns using self-organizing maps (SOMs). *Climate Research*, 25 (2): 95-107.

Dracoulides, D A 1994. Air Pollution Modelling for the Greater Cape Town Region. MSc Thesis, Faculty of Engineering, Energy Research Institute, University of Cape Town.

EEA 2008a. Exceedances of air quality objectives due to traffic. TERM04 factsheet produced under the Transport and Environment Reporting Mechanism (TERM) task, European Environment Agency, Copenhagen.

EEA 2008b. Use of cleaner and alternative fuels. CSI 037 factsheet produced under the Transport and Environment Reporting Mechanism (TERM) task, European Environment Agency, Copenhagen.

EEA 2008c. Air pollution by ozone across Europe during summer 2007. Technical report 5/2008, European Environment Agency, Copenhagen.

European Commission 2001. Amending the Annexes to Council Decision 97/101/EC establishing a reciprocal exchange of information and data from networks and individual stations measuring ambient air pollution within the Member States. Commission Decision 2001/752/EC, European Commission.

Gordon, H B, Rotstayn, L D, McGregor, J L, Dix, M R, Kowalczyk, E A, O'Farrell, S P, Waterman, L J, Hirst, A C, Wilson, S G, Collier, M A, Watterson, I G & Elliott, T I 2002. The CSIRO Mk3 Climate System Model. Atmospheric Research technical paper no. 60, CSIRO, Victoria.

Griffin, R D 2007. *Principles of Air Quality Management.* Boca Raton: CRC Press.

Hewitson, B C 2003. Developing Perturbations for Climate Change Impact Assessments. *Eos*, 84 (35): 337–348.

Hewitson, B C 2008. Climate Analysis, Modelling, and Regional Downscaling Using Self-Organizing Maps. In Agarwal, P & Skupin, A (Eds.) *Self-Organising Maps: Applications in Geographic Information Science.* Chichester: John Wiley & Sons.

Hewitson, B C & Crane, R G 2002. Self-organizing maps: applications to synoptic climatology. *Climate Research*, 22 (1): 13-26.

Hewitson, B C & Crane, R G 2006. Consensus between GCM climate change projections with empirical downscaling: precipitation downscaling over South Africa. *International Journal of Climatology*, 26 (10): 1315-1337.

Hewitson, B C, Tadross, M A, Sarr, A, Jain, S, Mdoka, M, Jack, C, McKellar, N, Walawege, R, Intsiful, J, Gutowski, W J J, Crane, R G & Stendel, M 2006. *The Development of Regional Climate Change Scenarios for Sub-Saharan Africa.* Washington DC: START secretariat.

IPCC 2000. Summary for Policymakers. In Nakicenovic, N & Swart, R (Eds.) *IPCC Special Report on Emissions Scenarios*. Geneva: Intergovernmetal Panel on Climate Change.

IPCC 2007a. *Climate Change 2007: The Physical Science Basis.* Cambridge: Cambridge University Press.

IPCC 2007b. *Climate Change 2007: Impacts, Adaptation and Vulnerability.* Cambridge: Cambridge University Press.

IPCC-TGICA 2007. General Guidelines on the Use of Scenario Data for Climate Impact and Adaptation Assessment. Version 2. Prepared by T.R. Carter on behalf of the Intergovernmental Panel on Climate Change, Task Group on Data and Scenario Support for Impact and Climate Assessment.

Jury, M R & Barclay, J J 1992 Air Pollution Meteorology: An episode in Cape Town 12 May 1992. *Photochemical smog/brown haze in Cape Town: one day seminar 12 August 1992.* Oude Libertas, Stellenbosch, National Association for Clean Air Western Cape.

Jury, M, Tegen, A, Ngeleza, E & Du Toit, M 1989. Meteorological aspects of winter air pollution episodes in the Cape Town area. *Clean air journal*, 7 (8): 19-24.

Jury, M, Tegen, A, Ngeleza, E & Dutoit, M 1990. Winter Air-Pollution Episodes Over Cape-Town. *Boundary-Layer Meteorology*, 53 (1-2): 1-20.

Katsouyanni, K 2003. Ambient air pollution and health. *British Medical Bulletin*, 68: 143-156.

Keen, C S 1979. Meteorological aspects of pollution transport over the South-Western Cape. Department of Geography, University of Cape Town, Cape Town.

Kohonen, T 1997. *Self-Organizing Maps*. Second Edition, Berlin: Springer.

Kohonen, T, Hynninen, J, Kangas, J & Laaksonen, J 1996. SOM_PAK: The Self-Organizing Map Program Package. Report A31, Helsinki University of Technology, Faculty of Information Technology, Laboratory of Computer and Information Science, Espoo.

Kruger, A C 2002. Climate of South Africa: Surface Winds. WS43, South African Weather Service, Pretoria.

Linnow, G 2008. Private communication.

Loewenheim, L 1988. Smog in the Cape Town Area. M.Sc. Thesis, Department of Environmental and Geographical Science, University of Cape Town.

Madec, G, Delecluse, P, Imbard, M & Lévy, C 1998. OPA version 8.1 Ocean General Circulation Model Reference Manual. Notes du Pôle de Modélisation no 11, Institut Pierre-Simon Laplace, Paris.

Magill, P L 1949. The Los Angeles Smog Problem. *Industrial and Engineering Chemistry*, 41 (11): 2476-2486.

Marsland, S J, Haak, H, Jungclaus, J H, Latif, M & Roske, F 2003. The Max-Planck-Institute global ocean/sea ice model with orthogonal curvilinear coordinates. *Ocean Modelling*, 5 (2): 91-127.

Mauderly, J L & Samet, J M 2009. Is There Evidence for Synergy Among Air Pollutants in Causing Health Effects? *Environmental Health Perspectives*, 117 (1): 1-6.

Michaelides, S C, Liassidou, F & Schizas, C N 2007. Synoptic classification and establishment of analogues with artificial neural networks. *Pure and Applied Geophysics*, 164 (6-7): 1347-1364.

Medina, S, Plasència, A, Artazcoz, L, Quénel, P, Katsouyanni, K, Mücke, H-G, De Saeger, E, Krzyzanowsky, M, Schwartz, J & and the contributing members of the APHEIS group 2002. APHEIS Health Impact Assessment of Air Pollution in 26 European Cities. Second year report 2000-2001, Institut de Veille Sanitaire, Saint-Maurice.

Mickley, L J, Jacob, D J, Field, B D & Rind, D 2004. Effects of future climate change on regional air pollution episodes in the United States. *Geophysical Research Letters*, 31 (L24): L24103.1-L24103.4.

Moussiopoulos, N, Sahm, P, Tourlou, P M, Friedrich, R, Simpson, D & Lutz, M 2000. Assessing ozone abatement strategies in terms of their effectiveness on the regional and urban scales. *Atmospheric Environment*, 34: 4691-4699.

NEM-AQA 2004 National Environment Management: Air Quality Act 39 of 2004.

New, M, Hewitson, B C, Jack, C & Washington, R 2003. Sensitivity of southern African rainfall to soil moisture. *CLIVAR Exchanges*, 27: 45-47.

Ngeleza, E 1989. The Synoptic Meteorologicl Aspects of Winter NOx Episodes in Cape Town. Honours Dissertation, Department of Environmental and Geographical Science, University of Cape Town.

NOAA 2008. Internet: http://www.cdc.noaa.gov/cdc/data.ncep.reanalysis2.html.

Norman, R, Cairncross, E, Witi, J, Bradshaw, D & Group, the South African Comparative Risk Assessment Collaborating Group 2007. Estimating the burden of disease attributable to urban outdoor air pollution in South Africa in 2000. *South African Medical Journal*, 97: 782-790.

NRC 1991. *Rethinking the Ozone Problem in Urban and Regional Air Pollution*. Washington D.C.: National Academy Press.

Peixoto, P J & Oort, H A 1992. *Physics of Climate*. New York: American Institute of Physics.

Piketh, S J, Otter, L B, Burger, R P, Walton, N, van Nierop, M A, Bigala, T, Chiloane, K E & Gwaze, P 2004. Brown Haze II. Cape Town.

Pope, C A 3rd, Burnett, R T, Thun, M J, Calle, E E, Krewski, D, Ito, K & Thurston, G D 2002. Lung cancer, cardiopulmonary mortality, and long-term exposure to fine particulate air pollution. *The Journal of the American Medical Association*, 287 (9): 1132-1141.

Roeckner, E, Bäuml, G, Bonaventura, L, Brokopf, R, Esch, M, Giorgetta, M, Hagemann, S, Kirchner, I, Kornblueh, L, Manzini, E, Rhodin, A, Schlese, U, Schulzweida, U & Tompkins, A 2003. The atmospheric general circulation model ECHAM5. Part I: Model description. Rep. 349, Max Planck Institute for Meteorology, Hamburg.

Salas-Mélia, D, Chauvin, F, Déqué, M, Douville, H, Guérémy, J, Marquet, P, Planton, S, Royer, J & Tyteca, S 2005. Description and validation of the CNRM-CM3 global coupled model. Note de Centre n 103, CNRM, Paris.

SANS 2004. Framework for setting and implementing national ambient air quality standards. SANS 69:2004, Standards South Africa.

SANS 2005. Ambient air quality - Limits for common pollutants. SANS 1929:2005, Standards South Africa.

SAWB 1996. Regional Description of the Weather and Climate of South Africa: The Weather and Climate of the Extreme South-western Cape. Department of Environmental Affairs and Tourism, Pretoria.

Schwartz, J & Hayward, S F 2004. Emissions Down, Smog Up. Say What? AEI Environmental Policy Outlook, January-February 2004

Shannon, D A & Hewitson, B C 1996. Cross-scale relationships regarding local temperature inversions at Cape Town and global climate change implications. *South African Journal Of Science*, 92 (4): 213-216.

Skupin, A & Agarwal, P 2008. Introduction: What is a Self-Organizing Map? In Agarwal, P & Skupin, A (Eds.) *Self-Organising Maps: Applications in Geographic Information Science*. Chichester: John Wiley & Sons.

Tadross, M A, Gutowski, W J J, Hewitson, B C, Jack, C J & New, M 2006. MM5 simulations of interannual change and the diurnal cycle of southern African regional climate. *Theoretical and Applied Climatology*, 86: 63-80.

Tadross, M A, Jack, C & Hewitson, B C 2005. On RCM-based projections of change in southern African summer climate. *Geophysical Research Letters*, 32 (L23): L23713.1-L23713.4.

Tadross, M, Suarez, P, Lotsch, A, Hachigonta, S, Mdoka, M, Unganai, L, Lucio, F, Kamdonyo, D & Muchinda, M 2007. Changes in growing-season rainfall characteristics and downscaled scenarios of change over southern Africa: implications for growing maize. *IPCC regional Expert Meeting on Regional Impacts, Adaptation, Vulnerability, and Mitigation.* Nadi, Fiji, 20-22 June, 193-204.

Tyson, P D, Preston-Whyte, R A & Diab, R D 1976. Towards an inversion climatology of southern Africa: Part 1, surface inversions. *The South African Geographical Journal*, 58 (2): 151-163.

Tyson, P D & Preston-Whyte, R A 2000. *The weather and climate of southern Africa.* Second edition, Cape Town: Oxford University Press.

Waggie, F 2008. Private communication.

WHO 2003. Health aspects of air pollution with particulate matter, ozone and nitrogen dioxide. World Health Organization, Regional Office for Europe, Bonn.

Wicking-Baird, M C, de Villiers, M G & Dutkiewicz, R K 1997. Cape Town Brown Haze study. GEN 182, Energy Research Institute, University of Cape Town, Cape Town.

Glossary and Acronyms

CO	Carbon monoxide
DEAT	Department of Environmental Affairs and Tourism
CC	Climate Change
GCM	General or Global Circulation Model
GCTA	Greater Cape Town Area
GHG	Greenhouse Gas
H_2S	Hydrogen Sulfide,
IPCC	Intergovernmental Panel on Climate Change
NO	Nitric oxide
NO_2	Nitrogen dioxide
NO_x	Nitrogen oxides
O_3	Ozone
PM_{10}	Particulate matter which passes through a size-selective inlet with a 50 % efficiency cut-off at 10 μm aerodynamic diameter
$PM_{2.5}$	Particulate matter which passes through a size-selective inlet with a 50 % efficiency cut-off at 2.5 μm aerodynamic diameter (therefore included in PM_{10} measurements).
SAHP	South Atlantic High Pressure
SANS	South African National Standard
SAWS	South African Weather Service
SO_2	Sulphur dioxide
SOMs	Self-Organizing Maps
Traffic	Pollution levels for roadside locations - within around 5m of the roadside.
TRS	Total Reduced Sulphur Compounds
Urban background	Background pollution levels for urban areas, representative for a large area, far from point sources
VOC	Volatile Organic Coumpound

Annex I: Data availability

The data availability percentage refers to the hourly data available for the indicated time period.

		Air Quality data							Meteorological data	
Station name	Code		PM10	NO2	NOx	SO2	CO	O3	Wind speed	Wind direction
Athlone	cc3									
		from 1-8-1998 to 31-12-1998	45%	-	-	-				
		1999	92%	-	-	-				
		2000	36%	81%	80%	70%				
		2001	-	88%	88%	91%				
		2002	53%	90%	90%	97%				
		from 1-1-2003 to 31-7-2003	88%	97%	97%	98%				
		2004								
		2005								
		2006								
		2007								
Bothasig	bm3									
		from 1-8-1998 to 31-12-1998	98%	74%	74%	100%				
		1999	54%	68%	68%	70%				
		2000	-	46%	46%	84%				
		2001	93%	99%	99%	95%				
		2002	83%	88%	88%	81%				
		2003	85%*	99%		100%				
		2004		79%		89%				
		2005		66%		85%				
		2006		12%		74%				
		2007		99%		92%				
City Hall	cc1									
		from 1-8-1998 to 31-12-1998		100%	100%	76%				
		1999		98%	97%	98%	35%			
		2000		98%	98%	99%	83%			
		2001		96%	97%	96%	96%			
		2002		97%	97%	98%	97%			
		2003		99%	-	99%	99%*			
		2004								
		2005								
		2006								
		2007								

* Data only available from 1-1-2003 to 31-7-2003

		Air Quality data							Meteorological data	
Station name	Code		PM10	NO2	NOx	SO2	CO	O3	Wind speed	Wind direction
Drill Hall	cc6									
		from 1-8-1998 to 31-12-1998	100%							
		1999	99%							
		2000	100%							
		2001	100%							
		2002	99%							
		2003	100%							
		2004	99%							
		2005	77%							
		2006	98%							
		2007	16%							
Goodwood	dd7									
		from 1-8-1998 to 31-12-1998	93%	38%	-	35%	-	-	-	-
		1999	99%	90%	90%	80%	39%	85%	21%	21%
		2000	99%	98%	98%	98%	99%	99%	99%	99%
		2001	100%	100%	100%	100%	100%	99%	100%	100%
		2002	97%	98%	98%	98%	95%	99%	99%	99%
		from 1-1-2003 to 31-7-2003	98%	99%	99%	99%	99%	96%	99%	99%
		2004	99%	99%	98%	99%	96%	95%	100%	100%
		2005								
		2006								
		2007								
Khayelitsha	cc4									
		1998	-							
		1999	51%							
		2000	85%							
		2001	21%							
		2002	58%							
		2003	97%							
		2004	96%							
		2005	94%							
		2006	86%							
		2007	93%							

		Air Quality data						Meteorological data	
Station name	Code	PM10	NO2	NOx	SO2	CO	O3	Wind speed	Wind direction
Killarney	zd7								
	1998								
	1999								
	2000								
	2001								
	2002	88%	88%	88%	88%				
	2003								
	2004								
	2005								
	2006								
	2007								
Molteno	cc2								
	from 1-8-1998 to 31-12-1998						57%		
	1999						91%		
	2000						97%		
	2001						94%		
	2002						98%		
	from 1-1-2003 to 31-7-2003						99%		
	2004								
	2005								
	2006								
	2007								
Plattekloof	dd8								
	1998								
	1999								
	2000	47%	48%	48%	49%				
	2001	38%	39%	39%	39%				
	2002								
	from 1-1-2003 to 31-7-2003	-	39%	39%	39%				
	2004								
	2005								
	2006								
	2007								

		Air Quality data							Meteorological data	
Station name	Code		PM10	NO2	NOx	SO2	CO	O3	Wind speed	Wind direction
Tableview	tm1									
		from 1-8-1998 to 31-12-1998	100%	100%	-	100%			100%	100%
		1999	91%	68%	67%	90%			61%	72%
		2000	91%	75%	77%	94%			53%	66%
		2001	97%	88%	89%	93%			80%	93%
		2002	97%	96%	98%	98%			75%	83%
		from 1-1-2003 to 31-7-2003	99%	98%	98%	97%			99%	99%
		2004								
		2005								
		2006								
		2007								

South African Weather Service stations

									Meteorological data	
Station name	Code								Wind speed	Wind direction
Capt Town - Portnet	PORT	2002							70%	70%
Cape Town - WO	WO-AIR	2002							100%	100%
Molteno reservoir	RES	2002							99%	99%

Annex II: Episode days

Episode days between April-September 2002, according to the criteria defined in chapter 2, section 2.4.3. Daily average NO_x concentrations are given in $\mu g/m^3$.

	Station Code						
Date	BOTH	CH	ATHL	GOOD	TBLV	KILL	Number of stations that exceeded criterion
10.04.2002	63	274	114	122	40	164	4
11.04.2002	71	421	102	117	52	116	6
15.04.2002	100	390	99	164	43	139	5
19.04.2002	107	458	158	222	44	110	6
23.04.2002	81	290	132	143	56	109	5
26.04.2002	67	338	45	69	62	110	4
30.04.2002	80	254	62	100	80	151	4
08.05.2002	152	383	.	211	62	167	5
09.05.2002	163	278	.	175	71	139	4
18.05.2002	102	303	.	187	52	106	2
19.05.2002	93	355	.	107	88	112	2
20.05.2002	94	314	.	215	63	157	4
21.05.2002	177	484	.	199	72	195	5
27.05.2002	90	361	.	144	73	153	4
30.05.2002	112	249	220	206	18	97	3
03.06.2002	92	394	318	149	59	164	5
04.06.2002	228	484	340	258	88	376	6
19.06.2002	97	293	239	229	38	152	3
21.06.2002	212	585	383	434	59	355	6
24.06.2002	95	334	245	296	41	133	4
30.06.2002	92	166	136	167	61	124	2
03.07.2002	102	509	162	153	71	131	5
10.07.2002	90	222	198	151	32	112	3
12.07.2002	135	423	217	201	61	158	6
16.07.2002	92	132	.	148	50	147	2
17.07.2002	106	137	68	133	77	162	3
18.07.2002	93	347	100	180	83	151	5
19.07.2002	106	461	302	222	88	213	6
20.07.2002	82	422	166	184	58	147	4
21.07.2002	157	410	359	226	24	149	5
31.07.2002	104	339	248	245	63	224	5
05.08.2002	.	420	302	.	42	145	3
06.08.2002	.	176	158	113	50	105	3
07.08.2002	.	344	79	86	62	134	3
08.08.2002	.	572	209	191	89	165	5
09.08.2002	.	329	68	156	41	100	2
10.08.2002	.	360	107	142	64	129	4
16.08.2002	.	92	32	82	55	136	2
20.08.2002	.	337	194	207	42	222	4
22.08.2002	.	329	210	.	78	189	4
06.09.2002	40	282	37	46	39	93	2
07.09.2002	53	220	65	77	27	118	3
09.09.2002	55	187	68	63	29	83	2
10.09.2002	37	149	44	62	38	75	2
13.09.2002	74	246	116	133	37	186	5
18.09.2002	38	243	70	.	44	103	2
20.09.2002	28	307	37	31	39	89	2
26.09.2002	51	219	98	74	41	76	4
30.09.2002	38	232	120	86	14	43	2

Annex III: GCM model results

GCM model results for the control period (1961-2007) and future period (2046-2065) compared against the NCEP baseline period results (1979-2007).

Table AIII.1: Number of days attributed to each SOM node.

	BASELINE	CONTROL			FUTURE		
Node	NCEP	ECHAM5	CNRM-CM3	CSIRO-MK3.5	ECHAM5	CNRM-CM3	CSIRO-MK3.5
X=0, Y=0	491	691	325	302	354	168	170
X=1,Y=0	482	692	682	439	319	336	325
X=2,Y=0	398	606	557	286	299	302	270
X=3,Y=0	465	616	543	597	288	360	256
X=0,Y=1	496	803	531	123	399	208	278
X=1,Y=1	325	455	848	1140	239	386	439
X=2,Y=1	267	320	483	695	163	221	214
X=3,Y=1	449	597	678	1722	301	445	314
X=0,Y=2	533	829	681	40	364	257	388
X=1,Y=2	478	565	721	655	273	328	372
X=2,Y=2	444	492	545	531	272	257	279
X=3,Y=2	479	654	726	790	389	392	355

Table AIII.2: The error (Euclidean distance) with which each data set (NCEP, ECHAM5, CNRM-CM3 and CSIRO-MK3.5) maps to each SOM node.

	Control				Future			
NCEP	6.1	7.2	8.0	8.1				
	5.6	7.3	8.6	8.5				
	6.0	7.4	8.6	8.8				
ECHAM5	6.6	7.8	8.2	8.6	6.2	7.4	7.9	8.4
	6.2	7.7	9.0	8.8	6.1	7.8	8.6	8.7
	6.5	7.8	9.3	9.3	6.2	7.6	9.2	9.2
CNRM-CM3	7.1	8.3	8.7	8.7	6.9	8.1	8.4	8.4
	6.3	8.2	9.4	9.3	6.3	8.2	9.3	9.2
	6.4	8.1	9.6	9.6	6.3	8.3	9.9	9.5
CSIRO-MK3.5	14.5	14.2	14.0	13.2	7.1	8.3	8.8	8.6
	14.2	14.0	13.9	12.3	6.4	8.1	9.1	9.1
	13.8	13.5	13.3	12.0	6.4	8.1	9.5	9.5